AFRL-VS-TR-
2001-1083

HIGHLY DAMPED LIGHTWEIGHT WAVY COMPOSITE

William F. Pratt, Matthew S. Allen, Troy J. Skousen

Patterned Fiber Composites Inc.
923 West 500 North
Lindon, UT 84042

July 2001

Final Report

AIR FORCE RESEARCH LABORATORY
Space Vehicles Directorate
3550 Aberdeen Ave SE
AIR FORCE MATERIEL COMMAND
KIRTLAND AIR FORCE BASE, NM 87117-5776

AFRL-VS-TR-2001-1083

Using Government drawings, specifications, or other data included in this document for any purpose other than Government procurement does not in any way obligate the U.S. Government. The fact that the Government formulated or supplied the drawings, specifications, or other data, does not license the holder or any other person or corporation; or convey any rights or permission to manufacture, use, or sell any patented invention that may relate to them.

This report has been reviewed by the Public Affairs Office and is releasable to the National Technical Information Service (NTIS). At NTIS, it will be available to the general public, including foreign nationals.

If you change your address, wish to be removed from this mailing list, or your organization no longer employs the addressee, please notify AFRL/VSSV, 3550 Aberdeen Ave SE, Kirtland AFB, NM 87117-5776.

Do not return copies of this report unless contractual obligations or notice on a specific document requires its return.

This report has been approved for publication.

Tang-Tat Ng
Project Manager

FOR THE COMMANDER

KIRT S. MOSER, DR-IV
Chief, Spacecraft Technology Division

REPORT DOCUMENTATION PAGE

Form Approved
OMB No. 0704-0188

1. REPORT DATE *(DD-MM-YYYY)*	2. REPORT TYPE	3. DATES COVERED *(From - To)*
18/07/2001	Final Report	9 Feb 1999 - 9 Feb 2001

4. TITLE AND SUBTITLE
Highly Damped Lightweight Wavy Composite

5a. CONTRACT NUMBER
F29601-98-C-0217

5b. GRANT NUMBER

5c. PROGRAM ELEMENT NUMBER
65502F

6. AUTHOR(S)

William F. Pratt, Matthew S. Allen, Troy J. Skousen

5d. PROJECT NUMBER
3005

5e. TASK NUMBER
V0

5f. WORK UNIT NUMBER
BS

7. PERFORMING ORGANIZATION NAME(S) AND ADDRESS(ES)

Patterned Fiber Composites, Inc.
923 West 500 North
Lindon, UT 84042

8. PERFORMING ORGANIZATION REPORT NUMBER

9. SPONSORING / MONITORING AGENCY NAME(S) AND ADDRESS(ES)

AFRL/VSSV
3550 Aberdeen Ave., SE
Kirtland AFB, NM 87117-5776

10. SPONSOR/MONITOR'S ACRONYM(S)

11. SPONSOR/MONITOR'S REPORT NUMBER(S)
AFRL-VS-TR-2001-1083

12. DISTRIBUTION / AVAILABILITY STATEMENT
Approved for public release; distribution is unlimited.

13. SUPPLEMENTARY NOTES

14. ABSTRACT

Wavy composite had its origin in the Star Wars programs of the late 1980s as part of a space-based laser anti-missile program and is a new material that exhibits both high stiffness and damping when combined with capable viscoelastic materials. If high modulus fibers are used in the production of the wavy composite, it is possible to attain the stiffness of steel, thousands of times the damping, with the lightweight advantages of graphite-based composite. Prior to this effort, wavy composite had never been modeled accurately, tested comprehensively, or adequately characterized, and there was no capability to produce commercial grade wavy composite. This contract focused on creating and characterizing this new material system. Comparisons with test data have shown that the finite element code developed for this contract accurately models this new material. The FEA code has been shown to be accurate to 5% when predicting stiffness in tubes tested in the axial mode. The damping results are even more reliable, typically accurate to within 2%. This material has been shown to reduce vibrations at resonance by a minimum of 96% and as much as 99% over a broad band of frequencies.

15. SUBJECT TERMS
composites, damping, wavy composite, patterned fiber composites, acoustics, finite element analysis

16. SECURITY CLASSIFICATION OF:			17. LIMITATION OF ABSTRACT	18. NUMBER OF PAGES	19a. NAME OF RESPONSIBLE PERSON
U					Tang-Tat Ng
a. REPORT	b. ABSTRACT	c. THIS PAGE	Unlimited	148	19b. TELEPHONE NUMBER *(include area code)*
U	U	U			505 846-5123

Standard Form 298 (Rev. 8-98)
Prescribed by ANSI Std. 239.18

Table of Contents

CHAPTER 1: SUMMARY 1
1.1. Objectives 1
1.2. Accomplishments 1
1.3. Developments 1
1.4. Discoveries 2
CHAPTER 2: INTRODUCTION 3
2.1. Objectives 3
2.2. Background Information 3
2.3. The value of damping in aerospace structures 6
2.4. Damped wavy composite concept 9
2.5. Experimental Approach 9
2.6. Commercialization 11
2.7. Summary 12
CHAPTER 3: FINITE ELEMENT ANALYSIS 13
3.1. General 13
3.2. Important concepts 14
3.3. Model size and performance 18
CHAPTER 4: TESTING 20
4.1. General 20
4.1.1. Introduction 20
4.1.2. Process unknowns and limitations 21
4.2. Test setup 21
4.2.1. Axial test stand 22
4.2.2. Derivation of test algorithm for axial test stand 23
4.2.3. Axial test performance 25
4.2.4. Sensitivity Analysis 29
4.3. Time-temperature Superposition 35
4.3.1. Background 36
4.3.2. Arrhenius Constant Determination 39
4.3.3. WLF Constant Determination 44
4.3.4. Experimental Shift Constants vs. Viscoelastic Only Constants 46
4.3.5. Time-Temperature Superposition Sensitivity Analysis 52
4.4. Torsion & Bending 56
4.4.1. Panel testing 56
4.4.2. Tubes in Bending 59
4.4.3. Derivation of Torsional Test Algorithm 61
4.4.4. Torsional Test Stand Performance 62
4.5. Conclusions 64
CHAPTER 5: DOE AND MODEL CORRELATION 66
5.1. General 66
5.2. Material Properties 66
5.3. Test and evaluation of Wavy Composite Tubes 70
5.4. Summary 84

CHAPTER 6: DESIGNING PRACTICAL STRUCTURES 85
6.1. The Value of material damping 85
6.1.1. A new material paradigm 85
6.1.2. Settling times and space structures 86
6.1.3. Vibration control and the pogo effect 88
6.1.4. Sound attenuation 89
6.2. Designing with wavy composites, basic concepts 92
6.2.1. Assumptions 93
6.2.2. Basic Concepts 93
6.2.2.1. Characteristics of wavy composites 94
6.2.2.2. The effect of wavelength 95
6.2.2.3. The effect of waveform angle 97
6.2.2.4. Temperature shift and time-temperature superposition 98
6.2.2.5. Thickness ratio effects 99
6.2.2.6. High modulus fibers and increasing performance in wavy composites 101
6.3. Crossply wavy composites 103
6.3.1. Wavy crossply structures 105
6.3.2. Detailed description 106
6.4. Advanced wavy composite designs 109
6.5. Design considerations 111
6.5.1. Operational temperature range 112
6.5.2. Frequency range and important modes 112
6.6. Aerospace structural concepts 113
6.6.1. Dynamically stiff space based lasers (STAR WARS) 113
6.6.2. Launch shrouds and payload containers 114
6.6.3. Missile bodies and dynamic stiffness 118
6.7. Summary 119
CHAPTER 7: CONCLUSIONS 122
7.1. Objectives: 122
7.2. Accomplishments 122
7.2.1. Production: 122
7.2.2. Wavy Composite Testing: 123
7.2.3. Finite Element Modeling and Model Correlation: 123
7.2.4. Design Expertise and Experience: 124
CHAPTER 8: RECOMMENDATIONS 126
8.1. Recommended future research 126
8.1.1. Use the material 126
8.1.2. Material research 127
8.1.3. Testing of torsion, bending, acoustic, strength, and fatigue 127
8.1.4. Finite Element Analysis code improvements 128
8.2. Summary 129
REFERENCES 130
APPENDIX A: Additional test data and FEA predictions 132

List of Figures

Figure 1: Viscoelastic layer shown between two layers of wavy composite of opposite patterns. 3
Figure 2: The origin of wavy composite was as a structural damping concept for space-based lasers used in anti-missile defense. 4
Figure 3: Actual settling time of two tubular beams, damped wavy vs. undamped 7
Figure 4: Viscoelastic layer shown between two layers of wavy composite of opposite patterns. 9
Figure 5: Constructed nodes (side view of laminate) 15
Figure 6: Foam core of a wavy laminate model showing the first bending mode shape 17
Figure 7: Foam core of a wavy laminate model showing the third bending mode shape 17
Figure 8: Interlaminar shear stresses in a viscoelastic layer 18
Figure 9: Photo of Axial Test Stand. 22
Figure 10: Magnitude, phase, and coherence plots for a wavy composite tube at 36°C 27
Figure 11: Actual axial stiffness and damping results for a wavy composite tube at 36°C 28
Figure 12: Stiffness and damping predictions with ±5% error in tube mass 31
Figure 13: Stiffness and damping with ±5% error in End Mass 32
Figure 14: Converged stiffness and damping with ±5% error in magnitude. 33
Figure 15: Stiffness and damping results with 5% change in phase angle. 34
Figure 16: Measured elastic stiffness of composite tube at various temperatures. 36
Figure 17: Stiffness and damping vs. reduced frequency referenced to 25° C 38
Figure 18: Stiffness and damping at various temperatures. 40
Figure 19: Linear fits of damping data at various temperatures. 41
Figure 20: Linear fit used to determine arrhenius shift constants. (42.0° C ref. temp.) 42
Figure 21: Shifted stiffness & damping curves 43
Figure 22: Linear curve fit used to determine WLF constants. 44
Figure 23: Data for 3"22° tube shifted by three methods. 45
Figure 24: Curve fits used for damping data TR16 47
Figure 25: Linear fit used to find Arrhenius constants 47
Figure 26: TR16 Data shifted according to Arrhenius and Avery-Dennison constants 48
Figure 27: Curve fits through damping data at discrete temperatures—TR17 49
Figure 28: Linear fit used to find Arrhenius shift constants for TR17 49
Figure 29: Data for TR17 shifted according to Arrhenius and Avery-Dennison 50
Figure 30: Curve fits on segments of simulated data with 1% error 52
Figure 31: Arrhenius Fit on Simulated Data with 1% Error. 53
Figure 32: Resulting Shifted Curves with +/- 1% Error in Transfer Function 54
Figure 33: Beam Test Apparatus 57
Figure 34: Magnitude response of Damped and Undamped Panels 57
Figure 35: Panel master curves. Damped and Undamped 58
Figure 36: Bending results for Wavy Composite Tube 60
Figure 37: Magnitude and Phase results for torsion tester 62
Figure 38: Shear Stiffness and Damping for Aluminum Test Specimen 63
Figure 39: VEM Test Data vs. Avery-Dennison and WLF Curve Fits 68
Figure 40: Basic Tube Design 71
Figure 41: FEA prediction vs. test results for 3.75 cm (1.5 in.) 30° tubes 73
Figure 42: FEA prediction vs. test data for 7.5 cm (3.0 in.) 30° tubes. 74

Figure 43: FEA prediction vs. test data for 15 cm (6.0 in.) 30° tubes. 75
Figure 44: FEA prediction vs. test data for 5.0 cm (2.0 in.) 22° tubes. 77
Figure 45: FEA prediction vs. test data for double-thick composite tubes..... 79
Figure 46: FEA prediction vs. test data with 0.56 mm (0.022 in.) thick viscoelastic layer..... 80
Figure 47: FEA prediction vs. test data for 0.15 mm (0.006 in.) thick viscoelastic layer. 81
Figure 48: Optical microscope image of viscoelastic-composite interface. 82
Figure 49: Stiffness and Damping results for +3/+80/11m/-80/-3 tubes. 83
Figure 50: Actual settling time of two tubular beams, damped wavy vs. undamped 87
Figure 51: Actual vibration magnification or "Pogo effect" in wavy damped vs. undamped tubes excited in the axial mode. 89
Figure 52: Test data showing damping measurements of wavy damped panel vs. equivalent undamped panel. 90
Figure 53: Amplification of vibrations, wavy damped vs. undamped foam core panels. 91
Figure 54: Projected transmission loss comparison, undamped vs. damped foam core panels made with standard graphite pre-preg and projections for high modulus wavy composite. 92
Figure 55: Modulus and damping of wavy composite tube made with FT1190 VEM (upper chart) compared with FT1190 series viscoelastic properties at 25° C (lower chart). 94
Figure 56: Equivalent axial modulus for carbon fiber wavy composite – viscoelastic tube. 95
Figure 57: Damping (%) performance for carbon fiber wavy composite – viscoelastic tube. 96
Figure 58: Effects of a change in angle for a sinusoidal waveform of a 7.6 cm wavelength. 97
Figure 59: Frequency shift of the stiffness curve due to temperature..... 98
Figure 60: Shift in damping peak due to changes in temperature..... 99
Figure 61: Effects of changing thickness of composite or viscoelastic layers on stiffness. 100
Figure 62: Effects of changing thickness of composite or viscoelastic layers on damping. 101
Figure 63: High modulus fiber based wavy composite tube axial modulus and damping performance at different maximum angles, wavelength 7.6 cm..... 102
Figure 64: Comparison between high modulus fiber (K13710) and standard carbon fibers..... 103
Figure 65: Typical crossply composite structural concept 104
Figure 66: Wavy crossply (3) fabricated from two pairs of wavy composite (1 & 2)..... 105
Figure 67: Several examples of wavy crossply tubular structures..... 108
Figure 68: Damped wavy laminate with unidirectional crossplies..... 109
Figure 69: Damping vs. percent fill (cross plies)..... 110
Figure 70: Stiffness vs. percent fill (cross plies)..... 110
Figure 71: Damped wavy laminate with targeted VEM layers..... 111
Figure 72: Space-based laser anti-missile concept which inspired the wavy composite concept 114
Figure 73: Payload container concept..... 115
Figure 74: Characteristic transmission loss of a panel (Norton 1996)..... 116
Figure 75: Launch shroud concept 118
Figure 76: Actual vibration magnification or "Pogo effect" in wavy damped vs. undamped tubes excited in the axial mode. 119
Figure 77: Space-based laser anti-missile system (SBL-IFX), a candidate for wavy composite 121

Figure 78: Test Data vs. FEA prediction for 5.0 cm (2.0 in.) 30° +3/11m/-3 tubes 132
Figure 79: Test Data vs. FEA prediction for 10.0 cm (4.0 in.) 30° +3/11m/-3 tubes 133
Figure 80: Test Data vs. FEA prediction for 12.5 cm (5.0 in.) 30° +3/11m/-3 tubes 134
Figure 81: Test Data vs. FEA prediction for 3.75 cm (1.5 in.) 22° +3/11m/-3 tubes 135
Figure 82: Test Data vs. FEA prediction for a 7.5 cm (3.0 in.) 22° +3/11m/-3 tube 136

List of Tables

Table 1: Wavy composite performance comparisons 6
Table 2: Temperature and Shift Factor Data 42
Table 3: Test Results for Unidirectional Tubes 67
Table 4: Values used in analysis and correlation 67
Table 5: Avery-Dennison and WLF curve fit equation constants 70
Table 6: Properties Varied and Levels 72
Table 7: Tubes Properties and Names 72
Table 8: Performance comparisons 86
Table 9: Performance comparisons of wavy and conventional crossply laminates 107

CHAPTER 1: SUMMARY

1.1. OBJECTIVES

Wavy composite is a new material with stiffness that can rival steel with thousands of times the damping. Prior to this contract, wavy composite had never been modeled accurately or tested comprehensively, and the only existing manufacturing processes were rudimentary at best. This development work has focused on characterizing the performance of this remarkable new material.

Specifically, the objectives of this Phase II work were to

1) Develop a wavy composite pre-preg manufacturing capability,
2) Develop a Finite Element Analysis code that would accurately predict the performance of wavy composite,
3) Test and characterize wavy composite damping and correlate results to the FEA code.

1.2. ACCOMPLISHMENTS

These efforts have provided the capability to design aerospace structures with stiffness and weight that rival the best conventional composites but with unprecedented damping. Use of this material will reduce stresses and strains at resonance by up to two orders of magnitude, dampen structural vibrations hundreds of times faster, reduce acoustic transmission, and solve most structural vibration problems.

1.3. DEVELOPMENTS

Major developments are summarized as follows:

- Successful development of a wavy pre-preg machine capable of producing 25 kilotons of wavy composite annually with quality rivaling conventional processes.
- A finite element modeling capability that predicts stiffness and damping within 5% hundreds of times faster than the best commercial codes. (See Chapters 3 & 5)
- A test system capable of determining broadband stiffness and damping. Over 100 tube samples were tested. (See Chapter 4)

- Expertise gained in the performance of this contract has been successfully applied to design basic structural elements, foam-core panels, skis and golf club shafts with high stiffness and exceptional damping performance.

1.4. DISCOVERIES

- Stiffness and damping in wavy composite are frequency-temperature dependent with properties that mirror the viscoelastic material used to provide damping.
- The performance of wavy composites can be accurately modeled using classical linear elastic and viscoelastic principles. Therefore the finite element code developed as part of this contract can be used to quickly predict the performance for any fiber, resin, or viscoelastic system.
- Stiffer fibers used in the fabrication of wavy pre-preg will increase both stiffness and damping.
- Stiffness, damping, and strength can be increased using 90° unidirectional fill fibers.
- Viscoelastic can be applied in patches to enhance bending and torsional performance with no reduction in damping.
- Measured performance of this material has shown a 96% reduction of vibration amplitudes and settling times using standard modulus graphite fibers. With the use of high modulus fibers vibrations and settling time can be reduced by 99% or better over a broad frequency range.

CHAPTER 2: INTRODUCTION

This report describes and details work accomplished under contract F29601-98-C-0217 a Phase II Small Business Innovative Research effort with the objective of developing a new composite material system that exhibits both high damping and stiffness.

2.1. OBJECTIVES

The objective of this Phase II work was to

1) Develop a wavy composite pre-preg manufacturing capability,
2) Develop a Finite Element Analysis code that would accurately predict performance of wavy composite,
3) Test and characterize wavy composite damping and correlate results to the FEA code,
4) And develop a demonstration project that would evaluate this new material.

2.2. BACKGROUND INFORMATION

Wavy composite damping had its origin in the Star Wars programs of the late 1980's as part of a space-based laser anti-missile program called "Asterix"; the NASA concept is shown in Figure 1 (Dolgin 1990).

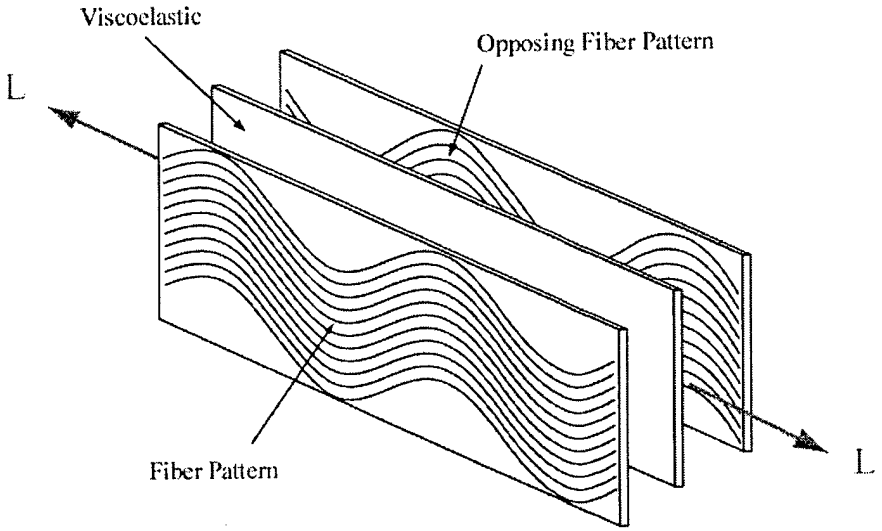

Figure 1: Viscoelastic layer shown between two layers of wavy composite of opposite patterns.

The Asterix program involved a space-based laser mounted on a composite truss structure. In order to focus enough energy on an incoming missile from a geo-synchronous orbit,

the structure had to be *dynamically* stiff so that vibrations in the structure would be dissipated rapidly. The use of wavy composite for construction of the truss members was proposed and prototypes built (using cut-segmented chevron patterns), but were never tested by NASA (Olcott 1992). Instead an active control system consisting of piezoelectric patches controlled by a multi-input multi-output computer was used to provide dynamic stability to the satellite's structure; the working model can be seen at AFRL's Kirtland AFB facility.

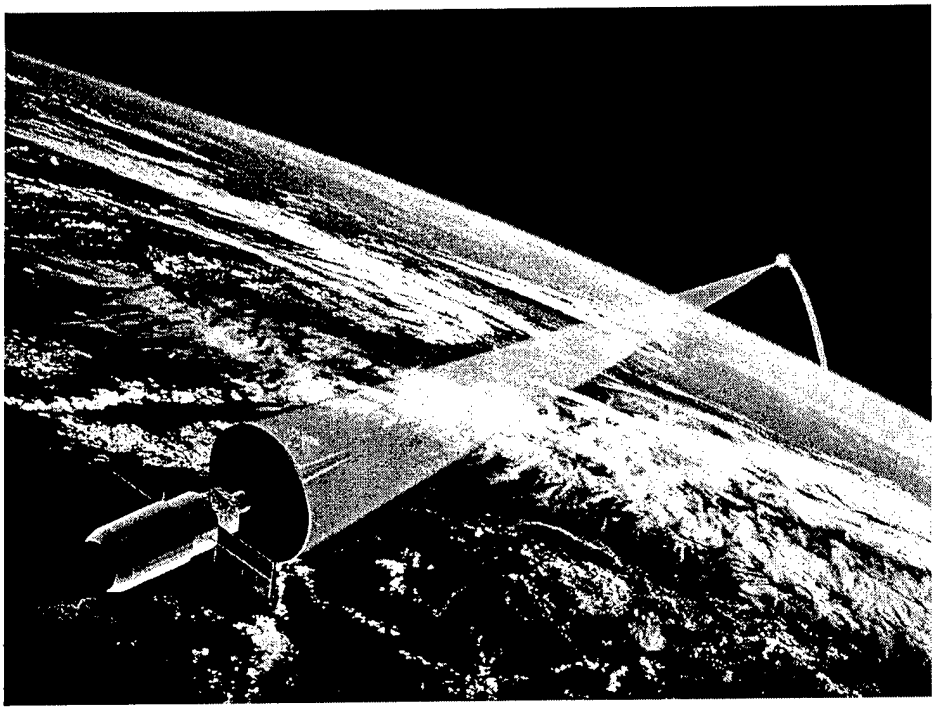

Figure 2: The origin of wavy composite was as a structural damping concept for space-based lasers used in anti-missile defense.

An audiovisual presentation entitled "Spacecraft Launch Protection" on AFRL's web site states "...the isolation system...reduced critical vibrations by 86%..." If the structure of the launch vehicle was made from wavy composite, vibrations in the structure (and settling times for satellites) would be reduced by a minimum of 96% and as much as 99% over a broad band of frequencies, not just the narrow band of frequencies of an isolation system. An isolation system represents a band-aid solution. Wavy composites represent the solution to the root problem.

A practical way of increasing the damping in mechanical structures has been a subject of continuing research and development. Methods used to control vibration in structures have taken

many forms, from passive treatments to extensive redesign of structures. More recent methods integrate computer technology in active control schemes.

There are three traditional methods used in the past to control vibration problems in structures. The oldest method is to change the dynamics of the structure by changing the mass or stiffness which changes the natural frequency of the structure. Since traditional structural materials have no inherent damping (Lazan 1968), the typical response to a dynamic problem has usually been to "make it stiffer". If this solution is possible and there is design latitude, it may in fact solve the immediate single frequency problem. Suppose the problem is more complex, i.e. the offending frequencies are broadband, or the dynamics of the structure change over time? In this case, simply modifying the stiffness (or mass) of the structure may not provide either a practical or a robust solution to the problem.

The other methods involve the addition of damping to the structure through either passive material methods or active control.

In the early 1990's "active control" of vibration (and noise) attracted great interest in the engineering community because it represented a new high tech solution that promised to solve many vexing and persistent vibration problems that state-of-the-art passive methods could not. In theory the adaptability of a computer controlled system promised to solve even the most sophisticated problems. In reality the complexity of the system, cost, weight and a host of reliability issues have prevented wider use in practical applications (von Flotow and Mercadal 1995). The original objective of active control of vibration was to add damping to the structure but it is the lack of inherent damping in the structure that makes active control difficult to accomplish *and* maintain (von Flotow and Mercadal 1995).

Regardless of the nature of the problem or the form of the solution, vibration damping is an area that should be handled in the least costly, least intrusive, and simplest way. Bluntly put, no company will opt for expensive solutions for the control of noise and vibration in a structure if an inexpensive, reliable, passive method exists. Many methods have been investigated, but past experience has shown that adding damping to a structure represents a compromise between stiffness, weight, strength, and performance... until now.

A new material paradigm: High damping and high stiffness

Wavy composites exhibit both high inherent damping *and* stiffness while preserving the lightweight advantages of composites. This new technology has the potential of advancing the state-of-the-art in passive dynamic structural control and serving as a capable replacement for conventional composites. Because the cost of wavy composite is comparable with standard composite materials, this new technology represents an inexpensive, unobtrusive, simple, and practical material for building the high performance structures of the future.

The performance of wavy composite made with *standard* modulus fibers is comparable in stiffness to aluminum or conventional composite structures but damping can be as high as 30%. Using a stiffer fiber increases both stiffness and damping.

Table 1: Wavy composite performance comparisons

Material (waveform)	Stiffness (GPa)	Damping (%)	Density (g/cc)
Std Graphite (3" 15° wave)	108*	15*	1.1
Std Graphite (3" 20° wave)	92*	21*	1.1
Std Graphite (3" 25° wave)	72*	25*	1.1
HiMod Graphite (3" 14° wave)	229*	32*	1.1
HiMod Graphite (3" 18° wave)	175*	38*	1.1
HiMod Graphite (3" 22° wave)	133*	42*	1.1
Aluminum	68	.1-.2	2.7
Titanium	110	.1-.2	4.5
Steel	203	.001-.01	7.4

* Stiffness at peak damping shown

Using damped wavy composites, it is now possible to fabricate structures with the stiffness of steel, the weight of graphite composite, and thousands of times the damping. Unlike low performing, conventional constrained layer damping, wavy composites exhibit their exceptional damping qualities when excited by longitudinal, shear, and bending loads.

2.3. THE VALUE OF DAMPING IN AEROSPACE STRUCTURES

The most efficient solution to a dynamic structural problem is to use a material that provides high damping.

- Damping limits amplification of vibrations, stress, and strain at resonance
- Damping dramatically improves settling time of free vibrating structures
- Damping improves transmission loss in panels

- Damping improves the performance of isolation mounts and active control methods

Damping limits the amplification of vibrations at resonance, and thus limits the amplification of stress and strain in aerospace structures. Unchecked by damping, resonance in aerospace structures can cause dangerously high dynamic loads on payloads and guidance systems and can amplify stress and strain levels that can either accelerate fatigue or in extreme cases, can cause catastrophic failure.

Damping dramatically improves settling times in aerospace structures. The lack of inherent damping in conventional composites means that space-based structures will tend to vibrate for long periods after some pertubation; this will adversely affect the accuracy of sensors and weapon systems. While adding stiffness or reducing mass can improve settling time, this approach is most often impractical if not impossible to achieve. To get the same performance out of an undamped composite as can be obtained from highly damped wavy composites, the designer would have to increase stiffness or decrease mass by hundreds and even thousands of times. It is much more efficient to add damping to the structure to reduce settling times.

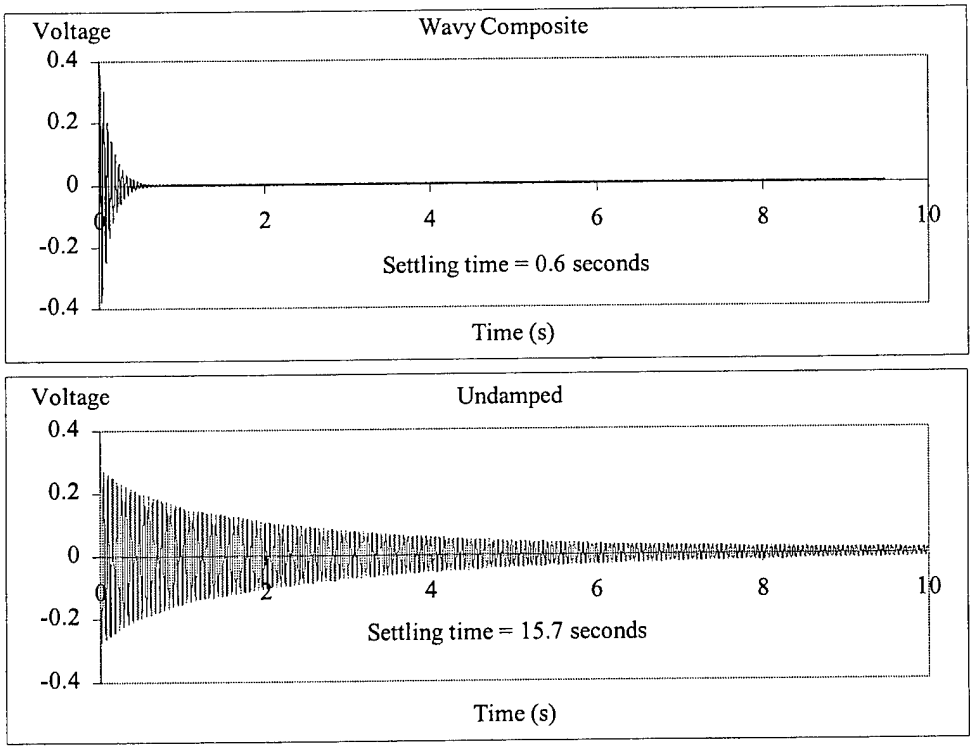

Figure 3: Actual settling time of two tubular beams, damped wavy vs. undamped

Figure 3 shows the effect of damping on settling time for two cantilevered tubular composite beams, one made from wavy composite with approximately 12% damping, and an undamped tube of equivalent mass and stiffness with less than 1% damping. The advantage of wavy composite in space applications is apparent from this test data. In space, the undamped tube would likely ring much longer than is shown here since there is no air damping to help with the structural dynamics. Damping in the wavy tubular beam is unaffected by a change in environment since its damping properties are a characteristic of the material and air damping represents only a very small fraction of the system damping.

Half of all launch failures in recent years have been attributed to excessive noise and vibration in the launch vehicle that damaged or destroyed either the payload or the guidance system (Bicos et al. 1997). Wavy composite, used in the construction of launch shrouds or containers can provide protection from low frequency rumble and structural borne vibrations from the amplified motor fluctuations that can damage or destroy sensitive guidance control systems or payloads. Acoustic excitations caused by non-diffuse, acoustic standing waves, and mechanically excited vibrations of the launch vehicle couple efficiently to the air surrounding the payload. In this case, added stiffness *and* damping are appropriate solution methods for attenuating the sound pressures on the payload (Norton 1996).

Finally, inherent structural damping improves the performance of both isolation mounts and active control because it improves the dynamic impedance of the structure. Without damping, the stiffness of isolation mounts can be greater than the stiffness of the airframes to which they are attached, negating the advantage of the mount. Likewise, structural damping greatly improves the performance of active control and can simplify the magnitude of the control system, reduce the control effort, increase systems robustness, and provide an inherent fail-safe mode (von Flotow and Mercadal 1995).

2.4. DAMPED WAVY COMPOSITE CONCEPT

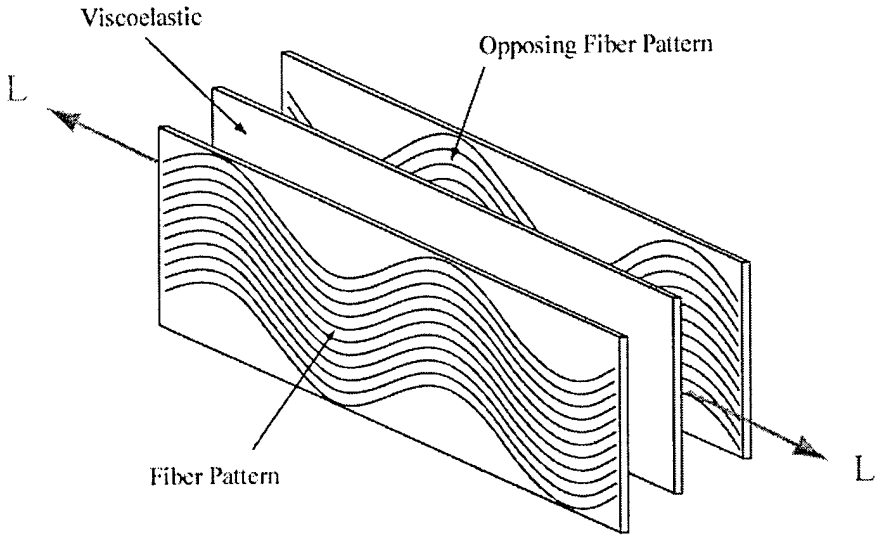

Figure 4: Viscoelastic layer shown between two layers of wavy composite of opposite patterns.

Figure 4 shows two laminates with opposing wavy fiber patterns with a viscoelastic layer sandwiched between them. When this combination is placed under a load (L) the fibers tend to straighten and will cause differential shearing in the sandwiched viscoelastic layer. This shearing action causes stretching of the long chain polymers in the viscoelastic and in turn generates heat, dissipates energy, and causes damping to occur in the structure.

The fiber reinforced resin pre-impregnated composite (or "pre-preg") used in the structure shown in Figure 4 is similar in every respect to standard materials commercially available with the sole distinction of having a wavy fiber lay in the plane of the laminate. As a result, this new material can be used interchangeably with standard pre-preg materials in most composite designs with little or no modification to existing procedures or automation equipment. Bridges, beams, concrete columns, aerospace structures, arrow shafts, golf club shafts, skis, snowboards, panels and machine tool components, can all potentially benefit from these developments.

2.5. EXPERIMENTAL APPROACH

The following section briefly details the experimental approach taken in the development of wavy composite technology. The specific objectives of the phase II work were:

- Develop analysis software that will accurately predict damping, stiffness, stress and strain
- Develop a machine to manufacture wavy composite

- Design and build wavy composite components for testing and correlation to the FEA model
- Design and build equipment that will test and analyze wavy composite materials
- Design and build a damped payload adapter

Prior to this effort, wavy composite was only imperfectly understood. There were no modeling tools, only a rudimentary production capability, and no viable test methods that could be used to characterize this new material. Therefore, the questions that were to be answered by this Phase II effort were:

- What are the characteristics of wavy composite and can these characteristics be accurately predicted?
- How should wavy composites be tested and what are the test limitations?
- Are these materials suitable for use in aerospace applications based upon the performance measures of strength, stiffness, damping, cost, and weight?

To accomplish the requirements of this contract we put together a team of specialist with qualifications in FEA modeling, testing, and manufacturing. The accomplishments are listed below and detailed in this and other reports.

- A 2d generation wavy pre-preg machine was built during the first year of the contract. The machine is capable of producing 25 kilotons of wavy composite annually and has successfully produced waveforms from 152 mm to as small as 25 mm in length with angles from 15 to 35 degrees. The machine is also capable of producing conventional unidirectional pre-preg as well. Details are contained in a separate report and drawings of the as-built configuration are provided separately. Additionally, patents for the US and Europe have been submitted and will issue in Europe; as of this date, the first office action in the US has not been received.
- A discrete layer Finite Element Analysis model was created that has demonstrated both accuracy and exceptional speed in analysis. In "pre-Beta" version as of this report, the code, written in "C" requires the use of a preprocessor and model input in Patran format. The user manual, design, and code are contained in a separate report. The program has been found to be hundreds of times faster that the best commercial codes

and is capable of correctly analyzing tubes, plates, and other simple structures. Additional details on the performance of the FEA program can be found in Chapter 3 of this report.

- A design-of-experiments was conducted to analyze and characterize this material. Tubes were chosen as the basic shape for these experiments since they were easy to build and test. Approximately 100 tubes of various waveforms (wave length and angle), lengths, and layer thickness, were built to test the effects of changes in wave and layer characteristics. Additionally, about a dozen foam-core panels have been constructed and shown to exhibit similar properties. The analysis program predicted the performance of the composite accurately over the entire range of design parameters, and the test data was found to agree with the model prediction to within 5% in both stiffness and damping. (See Chapter 5)

- A test apparatus and analysis software have also been produced since no existing equipment was capable of testing damping materials as stiff as these. The test outputs axial stiffness and damping as a function of frequency from 1000 to 2000 Hz. Test results at various temperatures can be combined to create material master curves of stiffness and damping from 1 Hz to 10,000 Hz. (See Chapter 4)

- The combination of the efforts listed above has produced a firm understanding of wavy composite design principles. The capability now exists for optimizing structures using various damping materials, fiber/resin systems, waveforms and layer configurations. These principles have been successfully applied to design basic structural elements, foam-core panels, skis and golf club shafts with high stiffness and unprecedented damping performance. (See Chapter 6)

2.6. COMMERCIALIZATION

This new material has been successfully applied to the production of golf club shafts and has resulted in the creation of a new commercial company charged with the further development and commercialization. The name of the company is New Revolution Golf, Inc.; details are reported in a separate commercialization report. Other efforts are underway to attract funding for development of products as diverse as tail rotor drive shafts, aircraft interior panels, boring bars for machine tools, skis, snowboards, and snowmobile runners, civil infrastructure, and many

more applications. Additionally, we intend to seek funding for R&D efforts necessary to obtain FAA certification of this new material concept for aerospace applications, and certification of the material for civil infrastructure applications.

2.7. SUMMARY

This new material concept was invented by NASA to solve structural dynamic problems in space-based lasers but was never put into practice. In that early period, NASA estimated that peak damping would be approximately 30%. This research indicates that much higher damping *and* stiffness are possible. Overcoming inertia in the engineering community has been our greatest challenge, not the performance of the material. Where companies have been willing to work with us in the development of their damped wavy composite based application, we have been able to provide a solution that is light years ahead of their existing designs. We seek similar opportunities with the Air Force Research Laboratory and the aerospace community.

CHAPTER 3: FINITE ELEMENT ANALYSIS

3.1. GENERAL

After searching for a way to analyze wavy composite materials in existing Finite Element Analysis (FEA) packages, it was determined that none of the existing codes could perform the analysis correctly (Pratt 1999). Therefore, Patterned Fiber Composites, Inc. developed a FEA code, primarily to analyze damped wavy composite structures.

The main features of the FEA program are shown below.

- Shell based model geometry, meshed with serendipity-8 elements.
- Discrete layer laminate configuration, superimposed on shell geometry inside the FEA program.
- No shear-locking with large, thin elements due to quadratic-linear interpolation.
- Material Properties
    - All materials are modeled with linear properties
    - Viscoelastic materials are modeled with temperature and frequency dependence.
    - Wavy composite is accurately modeled for plates and prismatic shapes.
- Frequency and temperature dependent outputs.

The program is designed to build a discrete layer finite element laminate model from a shell model meshed with serendipity-8 elements, imported from a standard finite element preprocessor. Face pressures and constraints applied inside the preprocessor on the shell are applied to appropriate discrete layers.

The discrete laminate model is defined by the laminate configuration. The number of layers is specified with the material, material waveform, thickness, and loading condition for each layer. With this information, the FEA program converts the serendipity-8 shell model into a "brick-16" based three-dimensional model. The use of "brick-16" elements prevents shear locking by using quadratic interpolation in the plane of the laminate and linear interpolation through the thickness. Not only does this correctly model the material, but it also allows the use

of large thin elements, which reduces model size and reduces analysis time. Boundary conditions (e.g. constraints, loads, and "welds") are converted from the shell model to the three-dimensional model in similar fashion.

The program design allows a number of different material types including isotropic, viscoelastic, unidirectional (transversely isotropic), orthotropic, and wavy composites. Standard linear elastic material properties are used to represent all material properties, such as Young's modulus, Poisson's ratio, and Shear modulus. Damping properties for load-bearing materials are assumed independent of temperature and frequency. Viscoelastic temperature and frequency dependency can be modeled using either WLF or Arrhenius methods (Sperling 1989).

The FEA program allows the operator to accomplishes two types of analyses. Single frequency analysis calculates stress, strain, and displacement values for a given temperature. Multiple frequency analysis produces a swept frequency analysis, which can include or exclude mass effects. Excluding mass effects produces results of damping, stiffness, and compliance (material characteristics). Including mass effects produces results of displacement, phase angle, impedance, and admittance. All swept frequency analyses show results at one node, in one direction, over the several frequencies.

Current limitations of the FEA program are:

- Model geometry is limited to simple structures with the strong composite direction in line with the first parametric direction and the global x-direction. This is because fiber angle and layer thickness can only be varied as a function of the global x-position. Thus, the program works best with structures such as flat plates and tubes.
- The coefficient of thermal expansion (CTE) is not currently enabled.
- Cylindrical coordinate systems are not currently supported, but tubular structures can be correctly modeled in Cartesian coordinates.

3.2. IMPORTANT CONCEPTS

There are two major features of this FEA program that make it a very useful tool for analyzing and characterizing wavy composite. First, the geometric model used as the basis of an analysis is derived from a shell model without thickness or definition of the layer configuration.

In conventional three-dimensional models, the number of layers, and layer thickness are set at the moment the model is created. If the designer wishes to change either of these configurations, a new model must be created or the old model must be modified. Smeared laminate models, like Patterned Fiber Composites, Inc.'s FEA code, use a shell and define the layer configuration separately from the geometric model and thus provide a great deal of flexibility to the designer. The use of a shell model allows the designer to change the layer configuration quickly without the necessity of creating a new discrete layer model for every new configuration. The problem with smeared laminate models is that they do not allow movement of the various layers and thus cannot analyze wavy composite (Zapfe and Lesieutre 1995).

Secondly, the use of complex numbers to represent displacements allows Patterned Fiber Composites, Inc.'s FEA code to correctly calculates vibration mode shapes as well as the standard expected outputs of stress, strain, displacement, compliance, damping, impedance, etc. and display damping and stiffness information in useful nomographs.

Figure 5 shows nodes, layers, and elements created by the program that are associated with the original shell model.

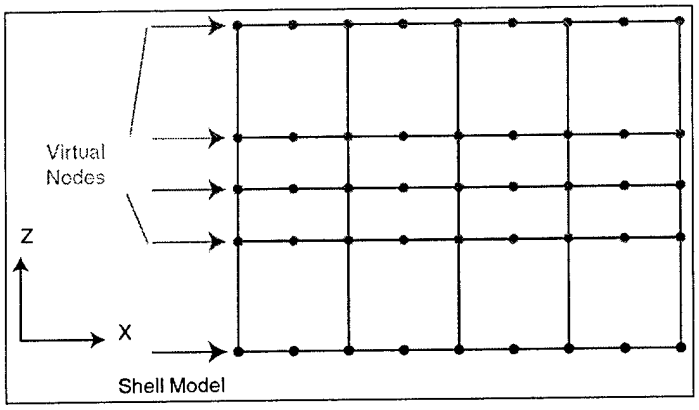

Figure 5: Constructed nodes (side view of laminate)

The vertical line of nodes that define the different layers and thicknesses of the laminate are extensions or "Virtual Nodes" of the original nodes of the shell model as seen in Figure 5. The details of the FEA code are contained in a separate report. The use of a shell model to define the laminate provides tremendous flexibility to pursue optimal designs without the necessity of creating multiple geometric models.

An important idea to understand when performing an analysis in the FEA program is the concept of mass effects. The following equations describe the solution model with and without mass effects.

$$x = \frac{F}{(K + jK\eta)} \qquad \text{Equation 1}$$

$$x = \frac{F}{(K + jK\eta) - \varpi^2 M} \qquad \text{Equation 2}$$

Analyses using Equation 1 do not include mass effects. Without mass effects, the solution characterizes the material. Results of analyses without mass effects are stiffness, compliance, and damping. These are the material characteristics independent of the structure. This is helpful in testing and designing different laminate configurations. When information from several analyses are performed, the results can be used to display damping and stiffness as a function of frequency and temperature in a nomogram format.

Analyses using Equation 2 include mass effects, which show system characteristics. Results from this type of analysis are impedance, admittance, displacement and phase angle results for the model. Additionally, the use of the consistent mass matrix in the calculation of displacements results in the ability to correctly calculate and display mode shapes for the various vibration modes of the structure.

Figure 6 shows the displaced shear stress plot of the core of a foam cored wavy composite laminate, with a face pressure on the bottom of the panel. Note that in addition to the regions of peak stress associated with the interlaminar shearing of the wavy composites (between face sheets) the correct shape of the first bending mode is displayed for the applied load. As the model frequency approaches the first resonant frequency, the displacement will increase as would be expected. Figure 7 shows the third bending mode shapes of the same panel. In this model, the even numbered mode shapes could not be displayed since the loading was not consistent with those modes. To display the even mode shapes (e.g. 2^d, 4^{th}, etc.) the applied force would have to be a point force offset from the center of the panel similar to a hammer test. The interesting fact was that actual testing of the panel behaved in the same manner. If the force was applied to the center of the panel, the even numbered mode shapes could not be displayed since the manner of activation was unable to excite these modes.

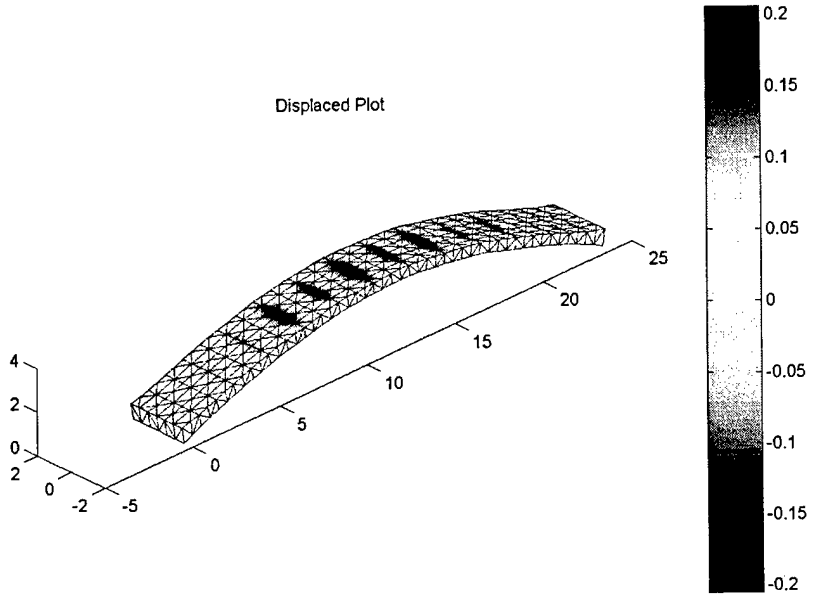

Figure 6: Foam core of a wavy laminate model showing the first bending mode shape

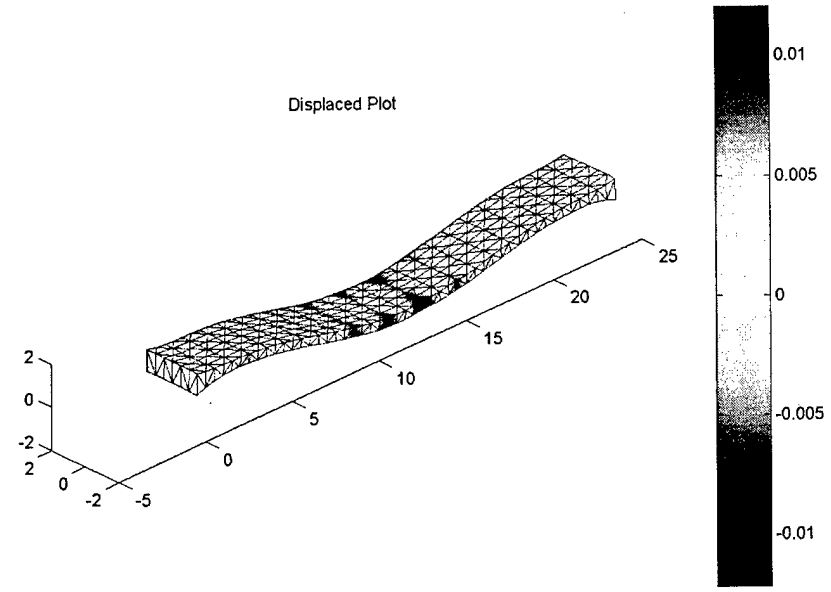

Figure 7: Foam core of a wavy laminate model showing the third bending mode shape

Finally, the structure of the code provides the designer with the ability to analyze any particular layer desired in addition to displays and analysis of "system" level performance. Figure 8 shows a typical displaced plot of a viscoelastic layer used in a damped wavy tube model. As can be seen the interlaminar stresses are fairly low even considering the magnitude of the axial force placed on the structure. This is typical of wavy composites and this figure serves to illustrate some of the information available from the code.

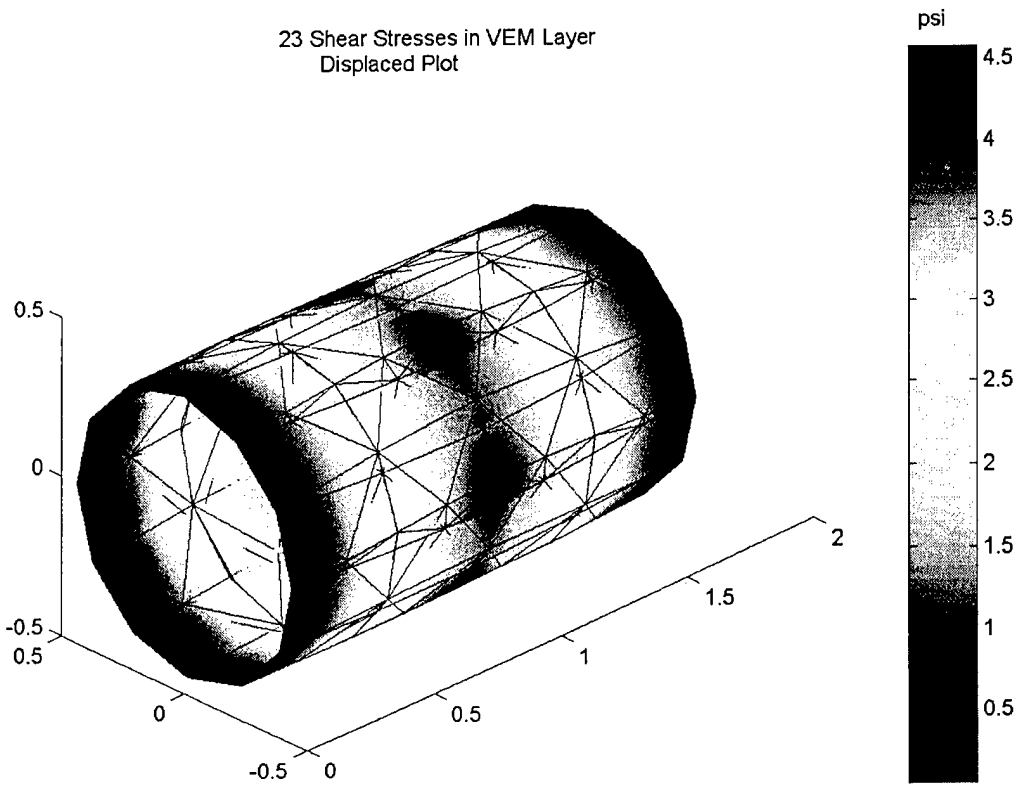

Figure 8: Interlaminar shear stresses in a viscoelastic layer

3.3. MODEL SIZE AND PERFORMANCE

Many conventional FEA composite models use smeared laminate properties. Compared to smeared laminate models, the model size of the discrete layer analysis is large, because smeared laminate models only analyze the shell elements each of which has 24 degrees of freedom regardless of the number of layers represented. A corresponding discrete layer model would have 48 degrees of freedom for each element for the first layer plus an additional 24 degrees of freedom for each subsequent layer. At first glance, the conclusion would be that the discrete layer model is too expensive in terms of degrees of freedom. However, the inability of existing smeared laminate models to calculate interlaminar shear results excludes it from analyzing damped wavy composite, because it is the interlaminar shear strains of the various wavy layers that determine the damping (Zapfe 1995).

Purely linear brick-8 three-dimensional elements are not efficient elements for wavy composites. The element size would need to be small to accurately model the thin layers of the composite without exceeding the limitations imposed by aspect ratios. An analysis was done in

PATRAN using the ABACUS analysis engine, of a wavy composite plate that had three layers, configured as two opposing wavy composite layers with a viscoelastic layer in between them. The physical dimensions of the sample being modeled were 50 mm by 25 mm using 1485 linear brick-8 elements (Pratt 1999). Each analysis took 15 minutes to complete. A comparable analysis can be done using the PFC FEA code with a shell model of only two elements. The shell model is expanded to a discrete laminate model with three layers or in total six brick-16 elements. The analysis of the model takes seconds and gives more accurate results than the PATRAN model. If a linear element is used, care must be taken to prevent shear locking from high aspect ratios, because the thickness of the composite tends to be small relative to other dimensions (Pratt 1999). With the brick-16 elements of the Patterned Fiber Composites, Inc. FEA code aspect ratios as high as 1:1000 have given accurate results, thus fewer elements are needed.

Performance of the code is covered in detail in Chapter 5 and the operator manual and the code description are covered in a separate report.

CHAPTER 4: TESTING

4.1. GENERAL

The purpose of this chapter is to present the major achievements made in testing wavy composite. First, the axial test stand is introduced, its dynamic model derived and it's strengths discussed. Next, the time-temperature superposition principle is introduced. Finally, the extension of these testing methods in bending and torsion will be explored.

4.1.1. Introduction

Characterizing the dynamic performance of damped composite materials presents a number of challenges. First, wavy composites exhibit frequency and temperature dependence in their stiffness and damping properties. Therefore, the material properties must be described as a function of frequency and temperature. Second, no test method exists capable of testing over a range of frequency broad enough to capture the entire material master curve, so it is difficult to characterize the performance of the composite with a single test apparatus. Third, most dynamic test methods don't allow testing of the material properties directly. Typically, a test material is combined with one or more other materials in some "structure" which is then tested. Pure material properties can be difficult to extract from test results for the structure (Sperling 1989).

The axial test apparatus described herein overcomes most if not all of these challenges. Individual tests characterize the material performance from 1000 Hz to 2000 Hz. The test specimens are tested over this same frequency range, at a number of temperatures, and the time-temperature superposition principle is applied to generate a master curve of the material performance at any single temperature over a very broad range of frequencies (approximately 1 Hz to 10^4 Hz or greater). Because the specimens are tested axially, the test algorithm determines axial stiffness and damping independent of the area moment of inertia, cross section shape, or other structural properties. Wavy composite can be rolled onto a mandrel without cutting fibers along the length of the tube, so edge and cut fiber effects associated with flat samples are eliminated.

Testing in bending and torsion is more problematic and will be described in the end of this chapter. Nevertheless, the test concepts described in this chapter are robust and accurate, as

will be shown in the comparison between test results and the Patterned Fiber Composites Inc. FEA program results in Chapter 5.

4.1.2. Process unknowns and limitations

Application of time temperature superposition requires one major assumption. It must be assumed that there is some interdependence of frequency and temperature in the material. Temperature is, in essence, a measure of the kinetic energy of atoms, which is proportional to their velocity. When vibrations are excited in a structure, the frequency of oscillation is also essentially a measure of the velocity of the particles in the material, so in a broad sense frequency and temperature will always be interconnected (Sperling 1989). Obviously, the properties of materials such as metals and ceramics do not change appreciably in the range of temperatures and frequencies in which we commonly use them. The same is true for composites, which typically exhibit properties that are essentially constant over their useful frequency and temperature range.

However, the properties of many polymers, such as viscoelastic, change dramatically with relatively small changes in temperature and/or frequency. Wavy composites are then a combination of a viscoelastic that is strongly frequency and temperature dependent, and a carbon fiber composite that is not. It will be assumed that the overall composite structure will take on the properties of the polymer and exhibit material properties that depend strongly on frequency and temperature. The smoothness of the resulting stiffness and damping curves after applying time-temperature superposition confirms the validity of this assumption. In fact, test data presented herein will show that the properties of wavy composite are indeed dependent on frequency and temperature, with a frequency-temperature dependence very similar to that for the viscoelastic alone.

4.2. TEST SETUP

The test method is generally based on a concept proposed in the testing of viscoelastic samples (Nielsen et al. 2000). Since wavy composites are many orders of magnitude stiffer than viscoelastic materials, several modifications and improvements were necessary in order to obtain accurate results.

Nielsen et al used an accelerometer and a load cell to measure axial displacement and force applied to the driven end of their sample. They assumed displacement at the stationary end would be exactly zero or small enough as to be insignificant (Nielsen et al. 2000). Because the sample stiffness was insignificant relative to the base structure, their assumption was reasonable and simplified the analysis. Such is not the case with a stiffer material.

4.2.1. Axial test stand

Since wavy composites can exhibit stiffness as high as that of steel, the dynamics of a steel or concrete test structure cannot be ignored. Instead of using an accelerometer and load cell on the driven end of the sample and driving it against an immovable base as Nielsen did, the method presented here used two accelerometers, one at each end, to measure the transfer function. The tube is then driven under one of the accelerometers in a driven-free mode.

The wavy composite test tube is mounted between two test fixtures, which also provided a mount for the accelerometers. The tube is excited axially by a piezoceramic actuator driven by an amplifier using white noise. The actual experimental apparatus can be seen in Figure 9.

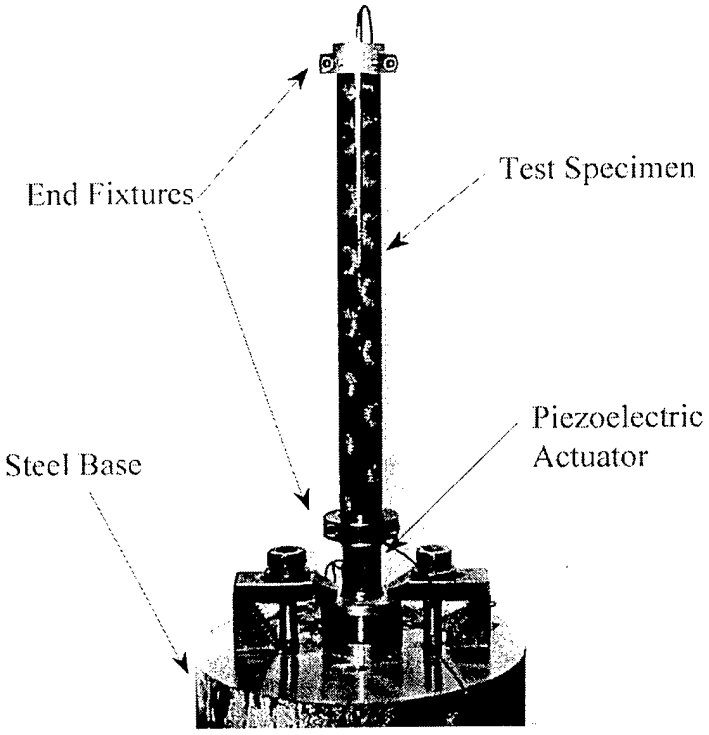

Figure 9: Photo of Axial Test Stand.

Figure 9 shows a photograph of the axial test stand. The tube is well isolated from spurious vibrations, since it is only attached through the actuator. Since the mass of the end fixtures, and the mass and the dimensions of the tube can be accurately measured, the only unknowns are the stiffness and damping of the tube material. These can be determined from the transfer function of the two accelerometers with very good accuracy.

4.2.2. Derivation of test algorithm for axial test stand

Axial excitation of the test specimen was chosen because the material properties can be determined directly. Since the structure of the tube is composed of two or more dissimilar materials (in this case wavy composite and viscoelastic), the material properties derived represent the average or "smear" properties. If it is assumed that the primary load resistance is provided by the composite constraining layers, the equivalent material properties of the composite can be determined by multiplying the stiffness by the cross sectional area of the tube divided by the cross sectional area of the composite only. This provides a relative measure of the stiffness of an equivalent "composite only" sample.

Because the test method is robust enough to measure a stiff structural material it is also capable of determining the properties of conventional composites without viscoelastic layers. This provided a very convenient method of testing and verifying the composite constants used in finite element analysis comparisons in Chapter 5.

The model of the tube-test setup used to determine the material properties of a given sample is derived from the solution to the partial differential equation for longitudinal vibrations shown in Equation 3:

$$\frac{\partial^2 u}{\partial x^2} = \frac{1}{c^2}\frac{\partial^2 u}{\partial t^2} \qquad \text{Equation 3}$$

Subject to the boundary condition:

$$EA\frac{\partial u}{\partial x}(L,t) = -m\frac{\partial^2 u}{\partial t^2}(L,t) \qquad \text{Equation 4}$$

Where "c" is the speed of sound in the material. c and ω are defined as follows:

$$c = \sqrt{\frac{E^*}{\rho}} \text{ and } \omega = c\lambda \qquad \text{Equation 5}$$

The solution to Equation 3 is given by the following:

$$U(x,t) = X(t)T(t) \qquad \text{Equation 6}$$

$$X(x) = c_1 \cos\lambda x + c_2 \sin\lambda x \qquad \text{Equation 7}$$

$$T(t) = c_3 \cos\lambda ct + c_4 \sin\lambda ct \qquad \text{Equation 8}$$

Applying Equation 7 and Equation 8 to Equation 4, and simplifying gives the following:

$$EA \cdot X'(L)T = m\lambda^2 c^2 \cdot X(L)T \qquad \text{Equation 9}$$

Dividing through by T,

$$EA \cdot X'(L) = m\lambda^2 c^2 \cdot X(L) \qquad \text{Equation 10}$$

The use of Equation 8 is no longer needed and combination of Equation 5, Equation 7 and Equation 9 results in the determination of the ratio of the c_1 and c_2 constants:

$$\frac{c_2}{c_1} = \frac{m\omega^2 \cos\lambda L + EA\lambda \sin\lambda L}{EA\lambda \cos\lambda L - m\omega^2 \sin\lambda L} \qquad \text{Equation 11}$$

The "compliance" version of the transfer function for the two accelerometers is:

$$\frac{U(L,t)}{U(0,t)} = \frac{c_1 \cos\lambda L + c_2 \sin\lambda L}{c_1} = \cos\lambda L + \frac{c_2}{c_1}\sin\lambda L \qquad \text{Equation 12}$$

Substituting Equation 11 into Equation 12, simplifying and then inverting the result gives:

$$\frac{U(0,t)}{U(L,t)} = \cos\beta - \frac{Mass_L}{Mass_{tube}}\beta \sin\beta \qquad \text{Equation 13}$$

Where the mass at the free end ($Mass_L$) is m in Equation 11, and the mass of the tube is the product of the density, cross sectional area, and the length of the tube. β is a function of the length L, the frequency, the density of the test specimen, and the complex stiffness E^*:

$$\beta = \lambda L = \sqrt{\frac{L^2\omega^2\rho}{E^*}} \qquad \text{Equation 14}$$

By applying Equation 13 and Equation 14 to the transfer data at each measurement frequency, iterative solutions will converge on a β (and therefore a complex modulus E^*) that will satisfy the Equations. The method converges rapidly using Newton's method where:

$$y = \frac{U(0,t)}{U(L,t)} - \cos\beta + \frac{Mass_L}{Mass_{tube}}\beta\sin\beta \qquad \text{Equation 15}$$

$$\frac{\partial y}{\partial \beta} = \sin\beta + \frac{Mass_L}{Mass_{tube}}\sin\beta + \frac{Mass_L}{Mass_{tube}}\beta\cos\beta \qquad \text{Equation 16}$$

$$\beta_{i+1} = \beta_i - \frac{y}{\frac{\partial y}{\partial \beta}} \qquad \text{Equation 17}$$

The ratio shown in the second term of Equation 17 represents "delta β" and is driven towards zero as β converges on a solution. An initial guess is made for the complex modulus E^*. Equation 14 through Equation 17 are placed in a while loop and solved in the order shown until the absolute value of "delta β" is below an acceptable value. The complex modulus is then solved using an appropriate form of Equation 14. This occurs for each frequency measurement of the transfer function. The result is a table or plot of the real component of the modulus and the damping constant given in the following:

$$E^* = E' + E'' = E + j\eta E = E\cdot(1 + j\eta) \qquad \text{Equation 18}$$

Internal studies have shown that the method is quite robust and is very forgiving of initial guesses that are off by as much as 50% or more on both modulus and damping. Convergence is rapid and the whole process takes less time to solve and plot than it takes to obtain the data.

4.2.3. Axial test performance

This method works best for structural materials over a frequency range centered on the first axial resonance. Considerable error can occur if the frequency range is extended too far from the first axial resonance. This appears to be associated with a number of causes including: spurious resonance associated with the test structure (e.g. bending modes not accounted for in the model or vibrations of the base), sensor noise, and phase angle measurement error or noise. Error associated with the test structure was minimized by using a solid cylindrical steel base 20 cm (8-in.) in diameter by 20 cm (8-in.) high. The dimensions of the base were chosen so that its first

axial and bending modes were well above the test range of interest. The entire structure was then isolated from the building dynamics by laying it on a 1.3 cm (0.5-in.) thick sheet of vibration damping material. Other spurious structural modes were most likely due to bending of the tubes. These errors were minimized by co-axially mounting the accelerometers with the centerline of the tube and by designing the actuator mounts to minimize bending of the actuator.

Sensor noise was the biggest contributor to error in the measurements of magnitude and phase once these other problems were solved. Sensor noise was associated with the sensitivity floors of the accelerometers, especially at frequencies removed from the primary resonance. This is due primarily to two causes. First, not enough energy is applied to the structure at low frequencies. With a conventional white noise generator, the energy imparted to the structure is spread across the frequency spectrum. The accelerometer measures acceleration, which is proportional to the frequency squared (ω^2). At frequencies well below the first resonant mode, the force imparted to the structure is too low to measure accurately. Attempts were made using a digital low pass filter to increase the power input at lower frequencies, though there was little or no improvement in the data. Even with increased power, the piezoceramic actuator wasn't capable of delivering sufficient power at low frequencies to compensate for the reduced sensitivity of the accelerometers.

Second, at anti-resonance and frequencies well away from resonance modes (especially for low damped composites) phase angles are very close to zero. Noise in the phase angle can be greater than the value of the phase angle being measured. This is less problematic for tubes with greater damping. Even so, undamped tubes of conventional unidirectional composite have been successfully tested and exhibit both stiffness and damping accurately. In fact, testing of 90° unidirectional composite tubes (used to determine the E_{22}, E_{33} modulus) produced excellent results, and the tube samples were easier to make than standard ASTM test samples.

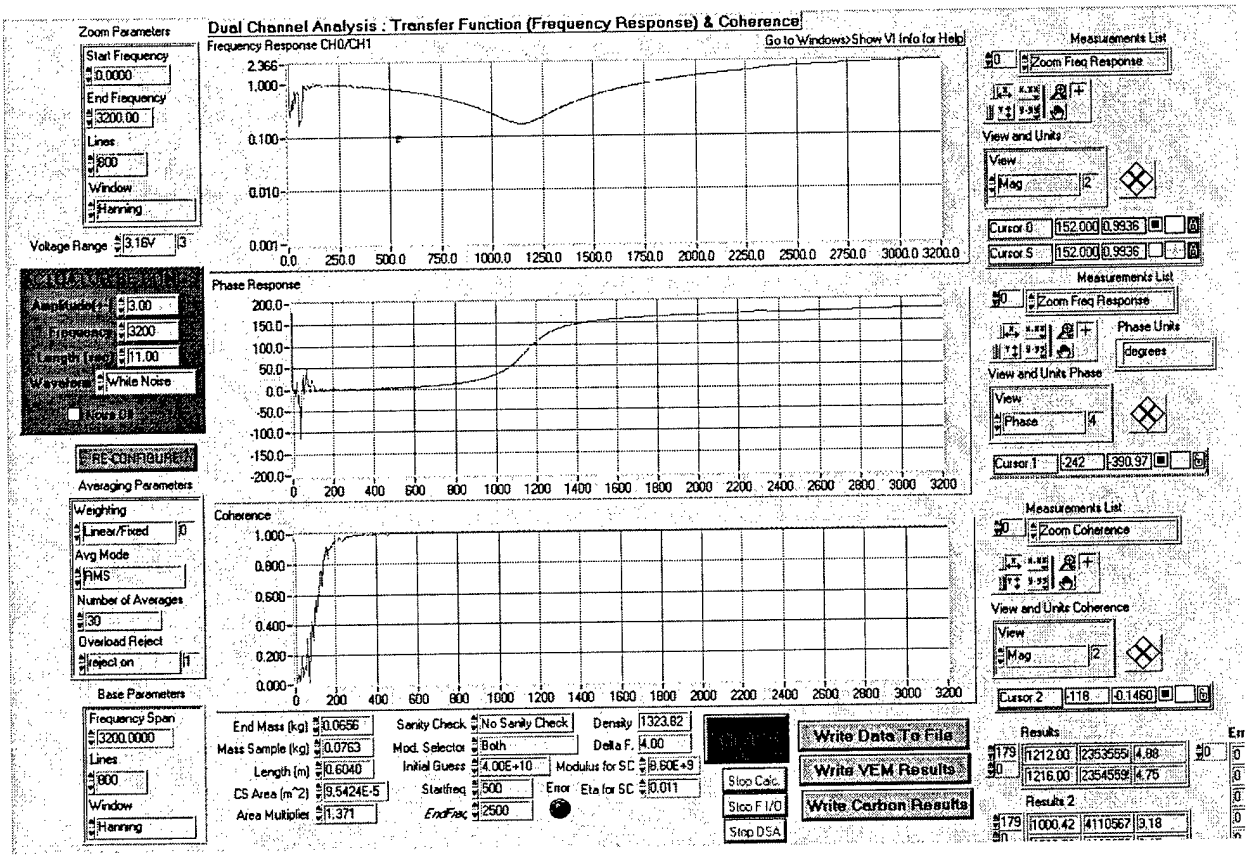

Figure 10: Magnitude, phase, and coherence plots for a wavy composite tube at 36°C

Figure 10 shows a screen capture of the graphical interface of the testing program. The three test windows show typical magnitude, phase and coherence test results of tubes made with wavy composite. The analysis shown was obtained from a tube made using wavy material with a 3.75 cm (1.5 in.) wave period and 30° maximum angle. Results from 0 to 3200 hertz are shown but as can be seen in Figure 10, noise in the measurement below 400 hertz made the data meaningless. The resonant frequency (f_r) is at about 1150 Hz.

The method used to analyze this and other tubes decouples the mass from the system and allows accurate measurement of damping and stiffness over a frequency band of $0.3f_r$ to $1.7f_r$. The main source of error in determining damping and stiffness stems from noise in the measurement of magnitude and phase angle at frequencies lower than $0.3f_r$ or above $1.7f_r$ where the phase angle is close to 0° or 180°.

As shown in Figure 10, the magnitude drops off (probably due to insufficient activation and the sensitivity floor of the accelerometers) and noise in the phase angle becomes pronounced

between 0 and 250 hertz. This is reflected in the measurement of coherence shown in Figure 10. As shown, coherence is at or close to 100% for frequencies between 400 and 3200 hertz.

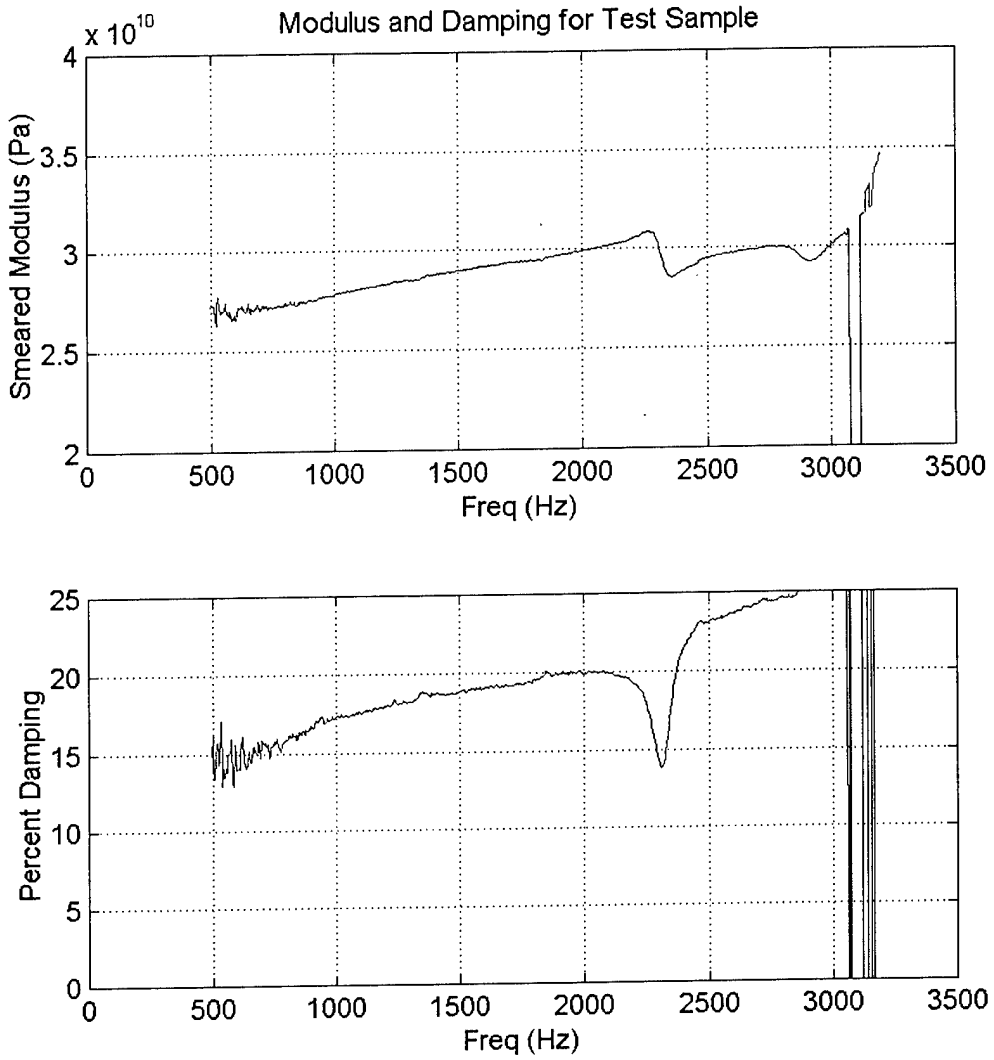

Figure 11: Actual axial stiffness and damping results for a wavy composite tube at 36°C

Using the algorithm discussed previously, the damping and stiffness for the tube over the range of 500 to 3200 hertz can be determined. Figure 11 shows the decoupled stiffness and damping results calculated from the magnitude and phase information shown in Figure 10. The results show that noise trends in the damping strongly mirror the noise in the measurement of phase angle, as would be expected. Despite the noise, the low frequency trend in damping is still apparent, starting at 15% and moving generally upward to 20% at about 2000 Hz.

The stiffness prediction does not seem to be as sensitive to noise in the measurement of magnitude or phase angle. Figure 11 also shows a relatively clean stiffness prediction between 500 and 2200 hertz. As expected for a material with viscoelastic properties, the stiffness increases steadily from about 27 GPa to a peak of 31 GPa at 2200 hertz. The low stiffness in this sample is a result of a very thick viscoelastic layer and large maximum angle used in this sample. Most samples had stiffness between 50-100 GPa. The term stiffness is used here to represent a "smeared" property averaged over the composite layers. Note that the stiffness and damping data become very noisy above about 2200 Hz. In this region far from resonance, very small spurious vibrations in the test setup cause large deviations in the measured values of stiffness and damping.

With this test setup, it is difficult to obtain reliable data at frequencies well above or below the resonance of the tube, and so it is difficult to obtain test data at much lower or higher frequencies. Although the resonant frequency can be altered by building test specimens of different length or thickness or by varying the mass placed on the end, it is best to test over a frequency range of high accuracy for the sensors used. Additionally vibrations in the test structure can be reduced but not eliminated. Even structures as massive as the steel base used in this instrument will resonate at high frequencies, so the test structure must be designed to resonate at frequencies well above the range of interest. This test fixture was optimized by placing the resonance of a specimen of typical stiffness at a high enough frequency to avoid the noise floor of the accelerometers, while low enough to avoid the most serious resonance in the test stand. To overcome this frequency band limitation, time-temperature superposition will be applied to extrapolate to higher and lower frequencies.

4.2.4. Sensitivity Analysis

A sensitivity analysis was performed to determine the effect of inaccuracies in measuring tube properties on the accuracy of the test algorithm. The analysis program requires that the tube cross sectional area, mass, and length be input, as well as the mass of the end piece attached to the free end. To evaluate sensitivity, one set of data was re-analyzed a number of times while one of the properties mentioned above were increased or decreased by five percent. The percent change in stiffness and damping were then recorded.

The effect was essentially one to one for cross sectional area and tube length. Five percent error in either parameter results in five percent error in stiffness. Damping was unaffected. A five percent increase in cross sectional area results in a 5% decrease in stiffness, where a 5% increase in length results in a 5% increase in stiffness. This also held true for 1% error or 10% error.

There is some uncertainty as to whether the actual length of the tube should be used, or if the length between the center of mass of the end pieces should be used. In the results presented here, the actual length has always been used. If some effective length actually results in a more accurate stiffness measurement, then based on this sensitivity analysis, the stiffness results presented here would be off by 2-3% for the worst case.

The cross sectional area of many of the thin-walled tubes could be in error by as much as 5%, since the digital calipers used to measure the tube diameter are only accurate to ± 0.05 mm (0.001-0.002 in.). The mass of the tube and end piece are easier to measure and should be accurate to within about 0.2%, based on the accuracy of the scale used. However, some may argue that some of the mass of the accelerometer cable should also be included in the end mass, or that the tube mass should be reduced to reflect the mass of an effective length of tube. Even a large portion of the accelerometer cable only weighs 2-3 grams and would increase the end mass by only 3-5%. (A 65.6 g end mass was typically used.) The tube mass would be decreased by 1-2% if the mass of the effective length was used. For illustration purposes, the effect of a 5% error in tube mass and end mass will be studied to assess the impact of these possible errors, though errors of this magnitude are highly improbable.

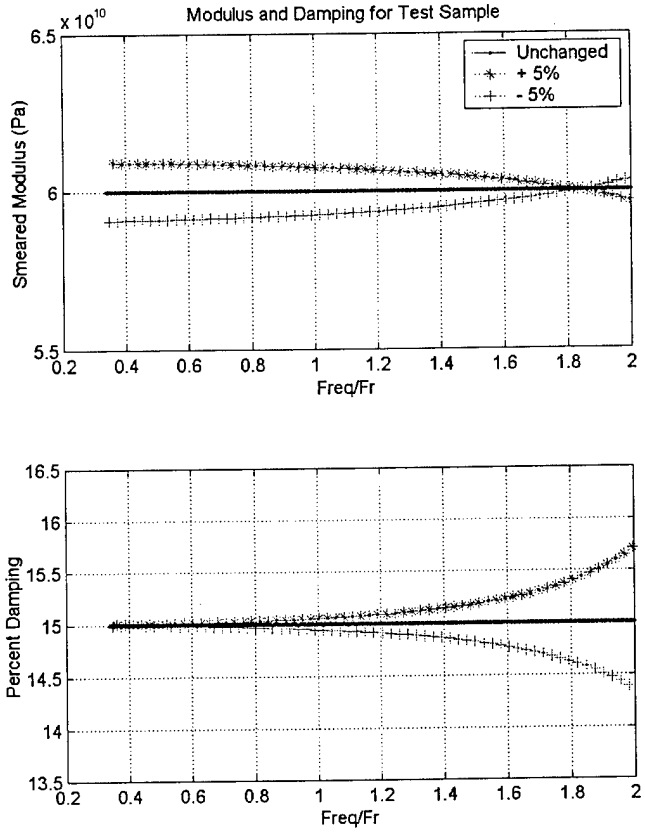

Figure 12: Stiffness and damping predictions with ±5% error in tube mass

Figure 12 shows the resulting stiffness and damping curves when the tube mass is increased or decreased by 5%. A simulated transfer function was constructed for a tube of similar dimensions and weight with a constant 15% damping and a constant stiffness of 60 GPa. This resulted in a resonant peak at 1610 Hz. The results were then nondimensionalized by dividing the actual frequency by the resonant frequency. Figure 12 shows that the error caused by 5% error in the tube mass can become quite large at frequencies well removed from the resonant frequency, however, over most of the $0.2*f_r$ to $2*f_r$ range, the error is attenuated. (5% error in tube mass results in only 1.6% error in stiffness over this frequency range.) The error in the damping prediction begins to increase after the resonant frequency and reaches 5% (loss factor of .1575) at about $2*f_r$. Over most of the test range the stiffness and damping are less sensitive to errors in tube mass, though it is important to remember that error in the tube mass may change the slope of the stiffness and damping versus frequency curves.

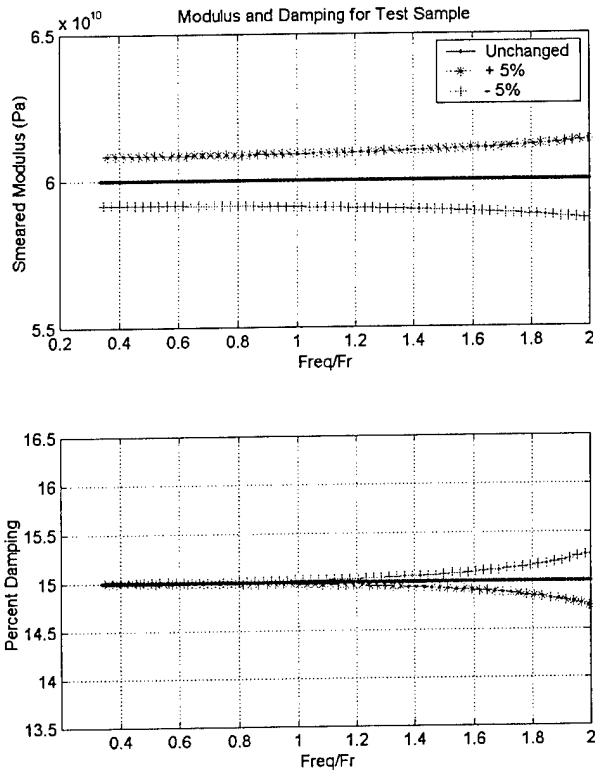

Figure 13: Stiffness and damping with ±5% error in End Mass

Figure 13 shows the stiffness and damping results when the end mass is varied. The trend is similar to that for tube mass, but the error increases at frequencies above the resonance instead of decreasing. Five percent error in end mass resulted in only 1.4% error in stiffness. Studies have shown that the ratio between the masses is really the governing factor. The thin walled tubes weighed 60.9 grams on average, and a 65.6 gram end mass was used, so the mass ratio was nearly 1:1. Since the mass ratio is near unity, the errors due to inaccuracy in either of these parameters have effects of similar magnitude. It should be noted that the test stand may be insensitive to one parameter and highly sensitive to the other for other mass ratios. This has not been tested.

A sensitivity analysis was also performed to determine the sensitivity of the complex stiffness to errors in the transfer function (magnitude and phase). The magnitude and phase may be in error due to spurious vibrations in the test stand or sensor noise. The effect of a constant 5% error in the magnitude was evaluated by multiplying the magnitude of the simulated transfer function by 1.05 and then passing it through the analysis routine. In reality, it is very unlikely that the error in the transfer function would be this high over the whole range of frequencies,

though this analysis will serve to illustrate the effect of error in the transfer function. This was repeated with the magnitude multiplied by 0.95.

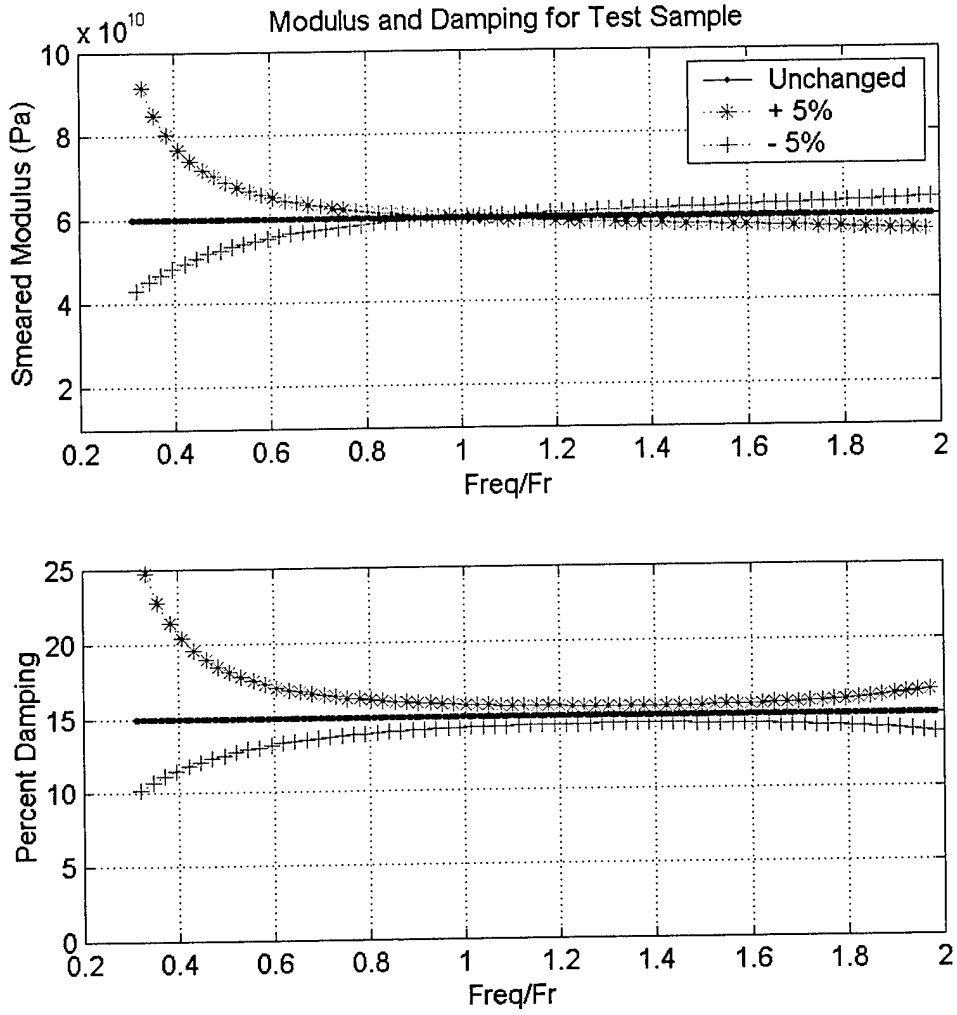

Figure 14: Converged stiffness and damping with ±5% error in magnitude.

Figure 14 shows the results of the analysis when the magnitude of the transfer function is artificially increased or decreased by 5%. The horizontal scale has been normalized by dividing the frequency by the resonant frequency (f_r). Note that the +5% and –5% curves are not symmetrical. Positive error in the magnitude has a more severe effect than negative error at low frequencies. Figure 14 suggests that the most reliable data will be found from $0.8*f_r$ to $1.6*f_r$. The effect of error in the phase angle will be examined next.

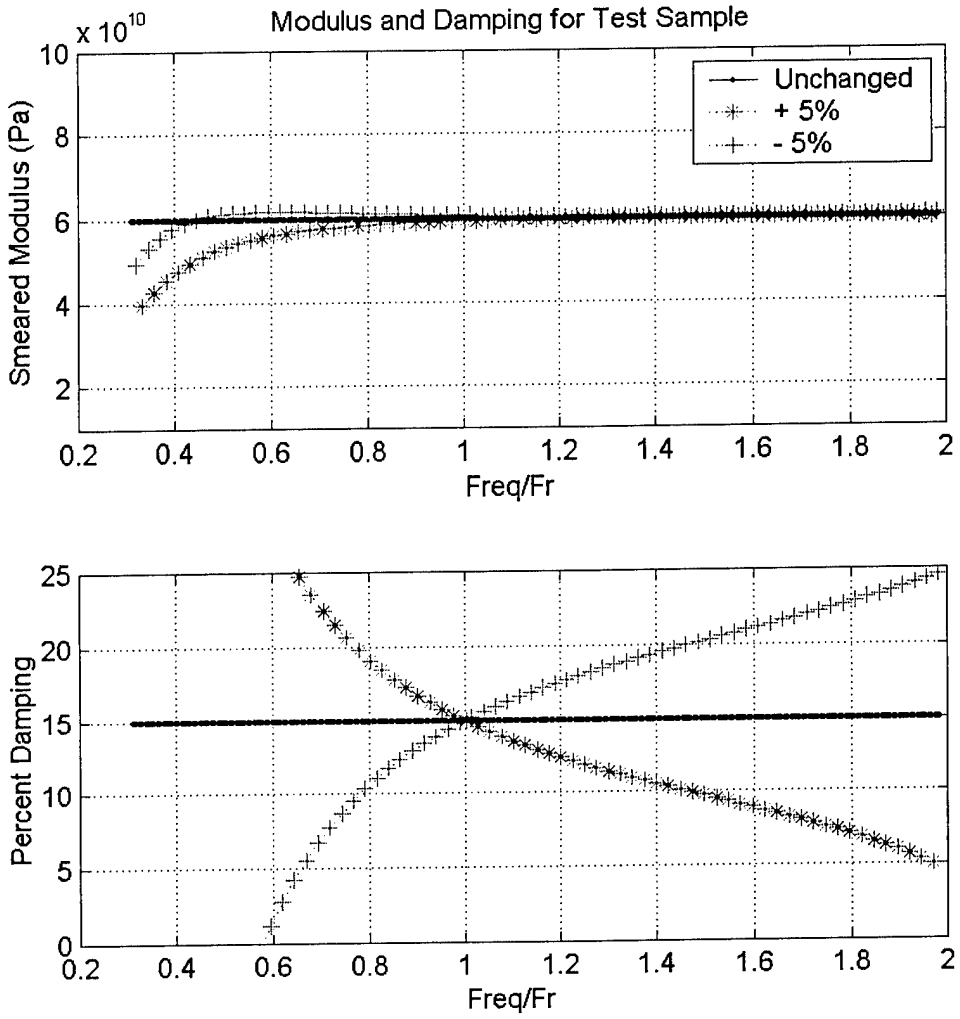

Figure 15: Stiffness and damping results with 5% change in phase angle.

Figure 15 shows the result when 4.5° is added to or subtracted from the phase angle. Since the phase angle starts at 0°, multiplying the phase by 1.05 has a greater effect at higher frequencies where the phase angle approaches 180°. A more fair approach is to add 4.5°, 5% of the phase at the middle value, though this represents a larger error percentage at frequencies well above or below the resonance. The effect of the phase angle on damping is very dramatic, though the data is almost unaffected at the resonance. Once again, phase errors as large as those shown above are very unlikely, though Figure 15 is useful to help in understanding performance of the test stand. It would appear that the stiffness data would be more reliable than the damping data, since the damping data is seen to diverge wildly with errors in the phase angle. However, the spurious vibrations that appear as noise in the test data usually consist of a magnitude

disturbance that covers a large frequency range and a phase disturbance that appears as a peak, which usually only affects the data over a small range of frequency. For this reason the phase and thus damping results may actually be more accurate over a large frequency range.

The results are concluded as follows. The numbers in parenthesis represent the approximate error seen in testing due to each specific source.

Damping is subject to the following errors:

- At Resonance:
  - Damping is completely unaffected by errors in any of the tube properties. (0%)
  - Damping is mostly unaffected by errors in the transfer function. (<1%)
- Away from Resonance:
  - Damping is completely unaffected by errors in cross sectional area or length.
  - Errors in tube mass and end mass are attenuated, but become significant above two times the resonant frequency.
  - Errors in the phase angle have a significant effect.

The stiffness measurement is subject to the following errors:

- At Resonance:
  - Errors in cross sectional area and length have a one to one effect. (5%)
  - Errors in the end mass or tube mass are attenuated. (<1%)
  - The stiffness is sensitive to errors in the transfer function.
- Away from Resonance:
  - Errors in cross sectional area and length have a one to one effect.
  - Errors in the end mass or tube mass become more significant, but are still attenuated below two times the resonant frequency.
  - Error in the stiffness due to error in the transfer function increases away from resonance.

It is evident that the axial test stand is very accurate at resonance. Most of the possible sources of error have no effect on the data at resonance. Errors in the tube mass, end mass, or transfer function can result in small errors in the data away from resonance, though the data at resonance is very reliable.

4.3. TIME-TEMPERATURE SUPERPOSITION

This section discusses the concept of time-temperature superposition in wavy composite-viscoelastic structures. The principle of polymer frequency-temperature superposition states that a shift in frequency is equivalent to a shift in temperature and is the method by which a master curve or nomograph is obtained (Ferry 1980). This principle is true for wavy composites made with polymer viscoelastic layers. This section presents the background necessary to understand

this principle in relation to wavy composite performance, shows examples of how master performance curves can be generated using two methods (WLF and Arrhenius), and discusses the implications of errors in data presented in the preceding section.

4.3.1. Background

Figure 11 shows the axial damping and stiffness results for a tube at a single temperature. If data for the same test specimen is collected over an extended temperature range, the results of each test can be combined using time-temperature superposition to create a "master" damping and stiffness versus frequency curve over a broad frequency range. This master curve can be displayed on a "Nomogram," a simple graph that shows the performance of the composite material over a large range of temperatures and frequencies.

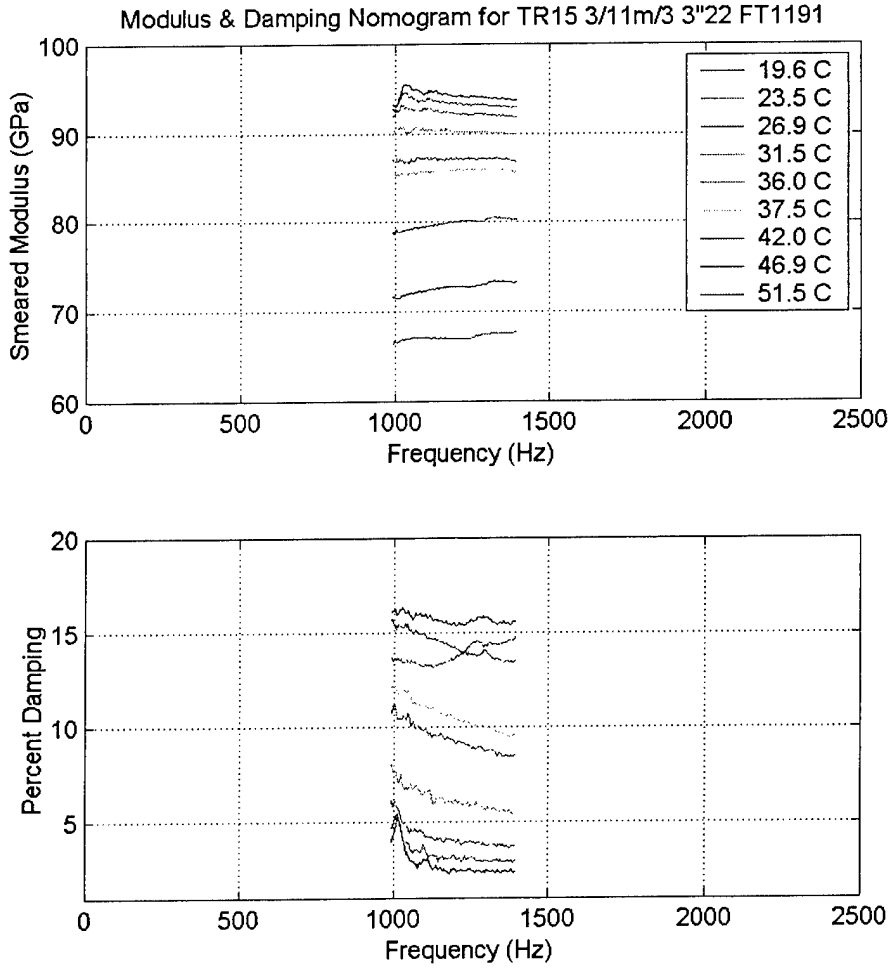

Figure 16: Measured elastic stiffness of composite tube at various temperatures.

The noise in the stiffness and damping results limits the range of reliable test data to approximately 500-2500 Hz. Therefore, without using a different experimental setup it is impossible to collect low frequency data directly with this test equipment. However, it is not difficult to collect data over the 500-2500 Hz frequency range at a wide range of temperatures. Figure 16 shows the experimentally measured stiffness of a composite tube from 1000-1400 Hz at a number of temperatures. For this tube, the most reliable data was found in this range.

Figure 16 shows the effects of temperature or frequency. Increasing the temperature of the composite tube lowers the stiffness curve over the testable freqency range. Also note that at higher temperatures the stiffness generally increases with increasing frequency. This behavior agrees with the expected performance of a viscoelastic material. The time-temperature superposition principle states that a material will behave identically to changes in temperature or frequency. Increasing temperature is identical to decreasing frequency and visa versa. The curves in Figure 16 represent the performance of the material over the same *frequency* range but different temperatures. If the results are normalized for the same *temperature*, the result will be to shift the frequency of each curve.

Equation 19 describes this behavior mathematically, where f_2 is a shifted frequency, f_1 is the original frequency and $\alpha(T)$ is the shift factor. The shift factor is a function of temperature, and quantifies the relationship between frequency and temperature for the given material.

$$f_2 = f_1(\alpha(T)) \qquad \text{Equation 19}$$

A good equation for $\alpha(T)$ is the Arrhenius temperature dependence, Equation 20 (Sperling 1989).

$$\log_{10}[\alpha(T)] = q * \left(\frac{1}{T} - \frac{1}{T_0}\right) \qquad \text{Equation 20}$$

T_0 is the reference temperature and q is the shift constant. The term q may also be expressed as the ratio between the apparent energy of activation for the molecular relaxation process and the gas constant (Sperling 1989).

The Williams Landel Ferry equation or WLF equation has also been used extensively. The WLF equation prescribes the frequency temperature interdependence as follows:

$$\log_{10}[\alpha(T)] = \frac{-c_1(T - T_0)}{c_2 + T - T_0} \qquad \text{Equation 21}$$

The WLF equation is most accurate when testing between the glass transition temperature (T_g) and T_g + 50 (Sperling 1989). This corresponds to 30-100°C for most of our damped composite test specimens. Since many of our tests are performed at much lower temperatures, the Arrhenius temperature dependence was used primarily.

If Equation 20 is substituted into Equation 19, the result is Equation 22. In this equation the shifted frequency is replaced by "reduced frequency" FR. Through the use of this equation, time temperature superposition can be used to construct a single master curve over a broad frequency range. The determination of the time-temperature-superposition shift constants (T_0 and q) is discussed in Sections 4.3.2 and 4.3.3.

$$FR = F * 10\text{^}\left\{q * \left(\frac{1}{T} - \frac{1}{T_0}\right)\right\} \qquad \text{Equation 22}$$

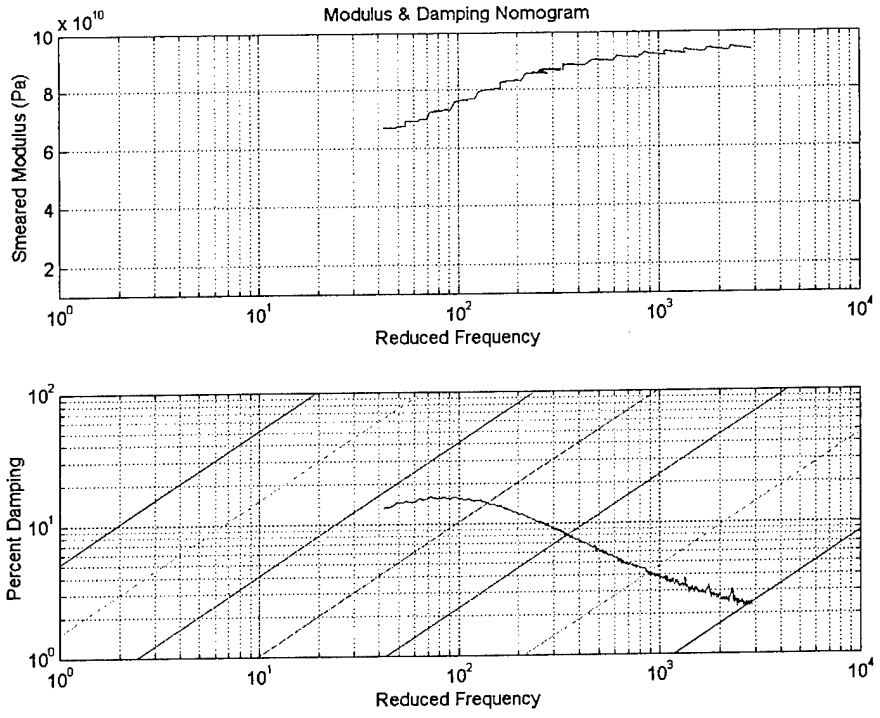

Figure 17: Stiffness and damping vs. reduced frequency referenced to 25° C

Figure 17 shows the data from Figure 16 shifted to a reference temperature of 25° C where the x-axis represents reduced frequency. (The following values were used in the shift equation: q = 5147 K, T_0 = 25° C.)

If we let T= T_0 = 25° C, Equation 22 reduces to F = FR. Thus Figure 17 also represents the dynamic performance of the composite tube at 25° C from 40 to 3,000 Hz. In this example application of the time-temperature superposition principle created the "master" stiffness and damping curves for the sample. The data have been shifted to produce a continuous line covering a larger range of frequency. This allows characterization of the sample for much lower or higher frequencies than is physically possible with test equipment by simply changing the temperature of the test specimen. Because of the temperature limitations of the accelerometers and piezoelectric actuator, test data could be obtained from -5°C to 80°C. This temperature range results in a master curve from 5 Hz to 50,000 Hz for these materials. The data can be easily shifted to any reference temperature by replacing T_0 with the desired reference temperature.

4.3.2. Arrhenius Constant Determination

As mentioned previously, frequency and temperature are merely two different measures of atomic motion. To understand the frequency-temperature dependence of a material, the shift constant q must be determined. The q constant prescribes how many degrees celsius of temperature shift is equivalent to a given frequency shift in Hertz. Thus the shift constants tell us everything we need to know to understand the performance of the composite over a broad range of frequencies and temperatures, given a dataset at a known frequency and temperature. Once the shift constants are obtained, a material nomograph can be created or the test data can be shifted to any temperature of interest.

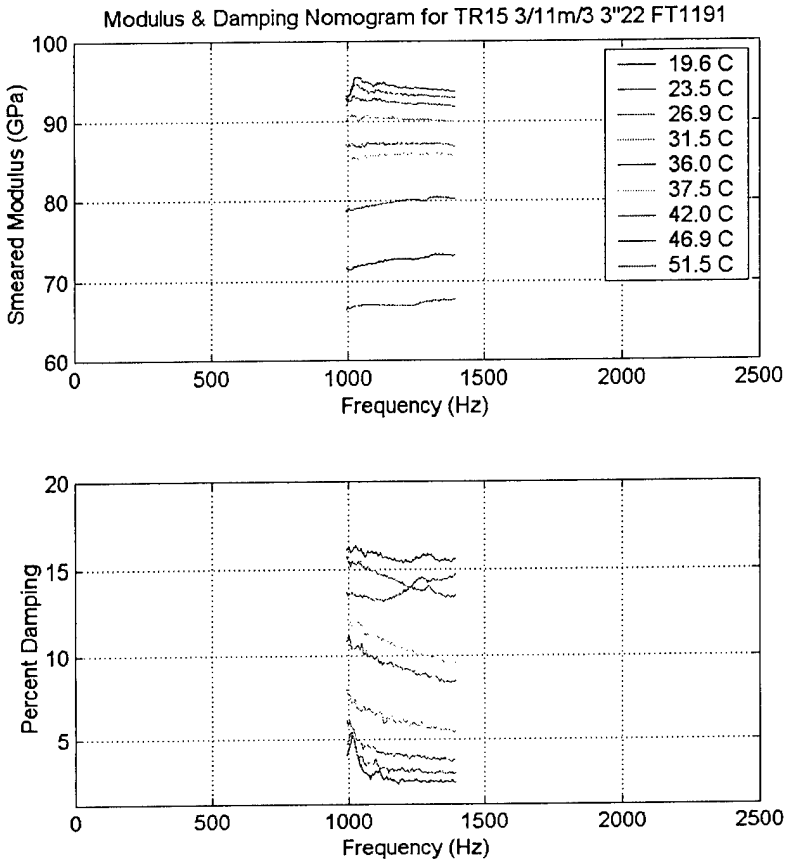

Figure 18: Stiffness and damping at various temperatures.

Figure 18 shows test data collected at various temperatures. For convenience the highest test temperature is taken as the reference temperature. In this case, since the damping data will be used for superposition, only data to the right of the damping peak (42°C and lower) will be used. In this case the reference temperature is 42.0°C. A line is fit to each segment of test data on a log-log plot using a least squares fit.

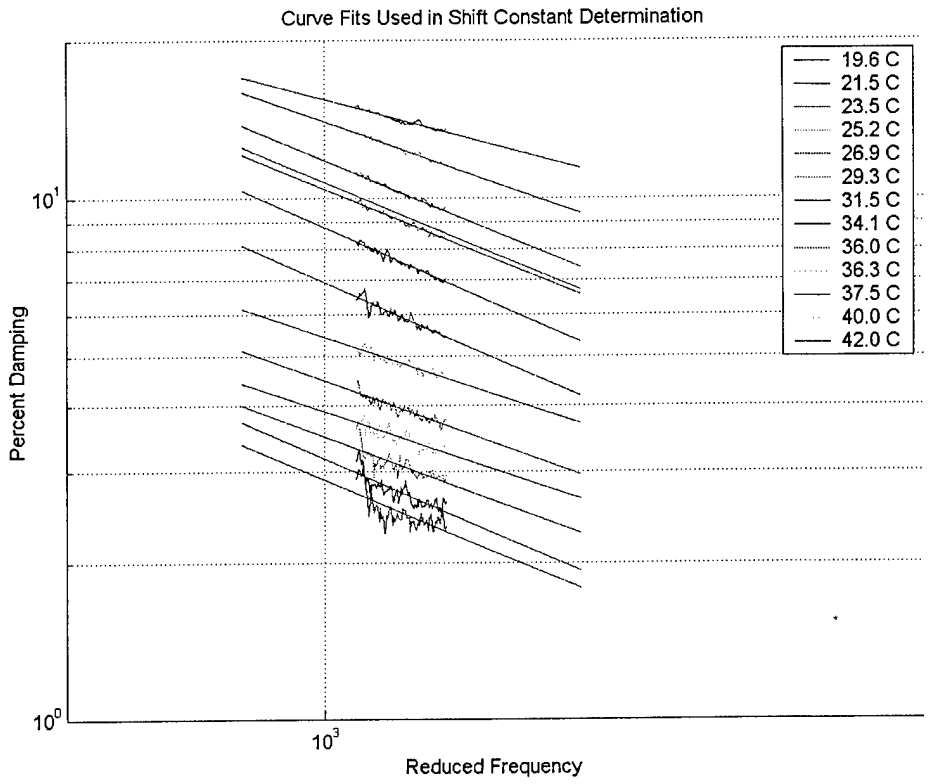

Figure 19: Linear fits of damping data at various temperatures.

Figure 19 shows the least squares linear fits through the damping data from 19.6°C to 42.0°C. At higher temperatures the data is clean and the fit is excellent. At low temperatures (19-23°C) the data is noisy and the curve fit shows noticeable error.

The shift factor $\delta\alpha_t$ is defined as the ratio of shifted frequency to the reference frequency. From the slope and intercept for each set of lines at sequential frequencies a computer algorithm determines the shift factor ($\delta\alpha_t$) which would cause any two curves at sequential temperatures to intersect at certain points along the curve. For each set of data at distinct temperatures a shift factor is recorded. For example, note that the damping is 10% at about 1080 Hz and 36.0°C and also at 1290 Hz and 37.5°C. Thus in order to shift the data at 36.0°C so that it lies on the curve at the next hightest temperature 37.5°C, it would have to be multiplied by the shift factor $\delta\alpha_t$ = (1290/1080). The $\log_{10}$ of the shift factors is taken, and the $\log_{10}(\delta\alpha_t)$ are added beginning at the reference temperature resulting in a value of the log shift factor $\log_{10}(\alpha_t)$ for each temperature tested. Table 2 illustrats this.

Table 2: Temperature and Shift Factor Data.

Temperature C	Log Delta A(T)	Log A(T)
19.6		
21.5	0.0547	1.1916
23.5	0.0796	1.1370
25.2	0.0917	1.0573
26.9	0.0949	0.9656
29.3	0.1518	0.8708
31.5	0.1444	0.7189
34.1	0.1447	0.5745
36	0.1135	0.4298
36.6	0.0163	0.3163
37.5	0.0626	0.3000
40	0.1294	0.2374
42	0.1080	0.1080

A linear curve fit between (1/T) in Kelvin and $\log_{10}(\alpha_t)$ yields q as the slope, as shown in Figure 20.

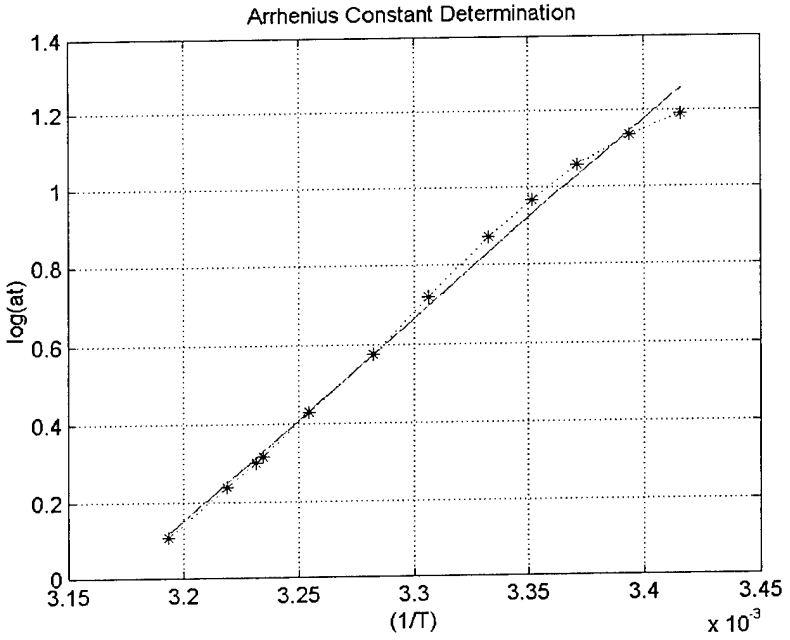

Figure 20: Linear fit used to determine arrhenius shift constants. (42.0° C ref. temp.)

Figure 20 shows the linear fit used to find the constant q. Note that the actual $\log(\alpha_t)$ deviates from the linear fit for low temperatures (i.e. in the right portion of the curve). This is primarily due to noise in the test data at low temperatures, as seen previously. At higher temperatures the test specimen effectively damps noise and resonances due to the test fixture,

resulting in cleaner data. It is also possible that the arrhenius temperature-frequency constants may change at very low temperatures. At lower temperatures the viscoelastic becomes very stiff, and the viscoelastic-composite combination begins to exhibit the less-frequency dependent properties of the composite more strongly.

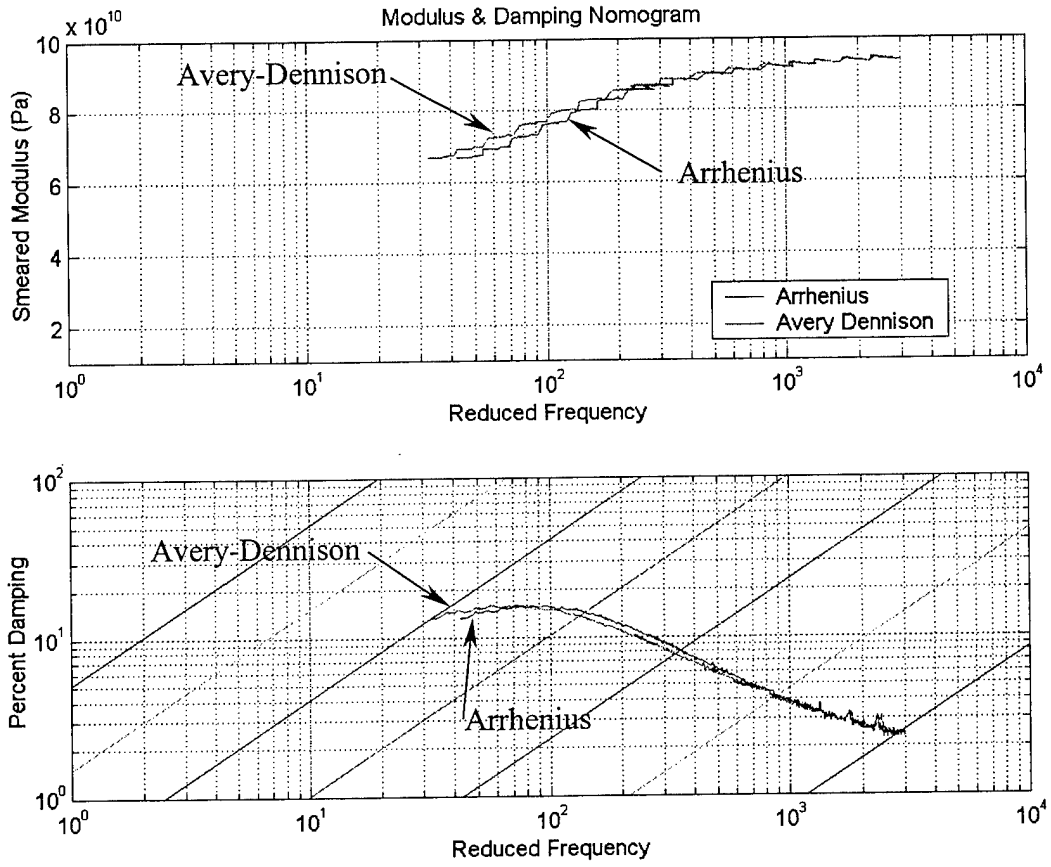

Figure 21: Shifted stiffness & damping curves

Figure 21 shows the data from Figure 18 shifted with the value for q determined previously (q = 5150). The same data is also shifted using shift constants determined by Avery Dennision for the viscoelastic alone (q = 5555.56, T_0=25°C). We can see that the curves agree very well. The composite takes on the frequency-temperature characteristics of the viscoelastic. If available, the manufacturer's shift constants can be used to give a good approximation. Test results suggest that the viscoelastic-composite combination may in fact produce a broader damping peak, though shift constant determination is very sensitive to error and more research is needed to understand this completely. This will be discussed in more detail in Section 4.3.4.

4.3.3. WLF Constant Determination

The method of determining the constants for the WLF equation is similar to the method used to determine the Arrhenius constants presented in Section 4.3.2 (Sperling 1989). The shift constants $\delta\alpha_t$ and $\log(\alpha_t)$ are found as described previously, though a different linear fit is used to find the shift constants c_1 and c_2, as shown in Figure 22.

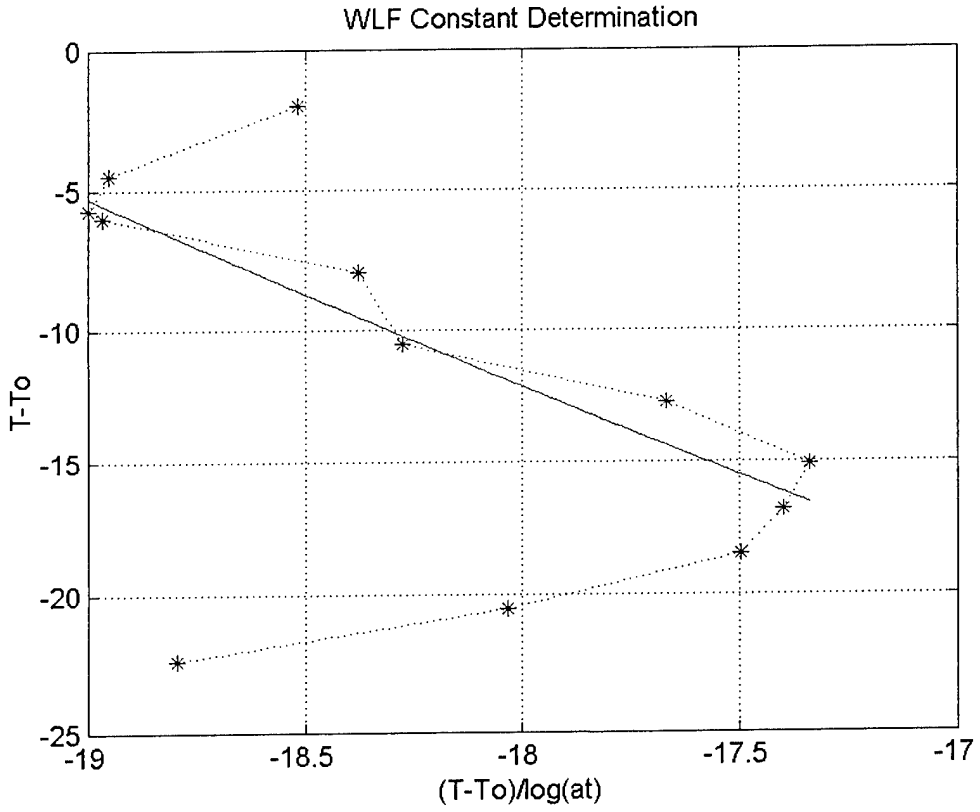

Figure 22: Linear curve fit used to determine WLF constants.

Equation 21 can be re-written as Equation 23.

$$T - T_0 = -c_1\left(\frac{(T - T_0)}{\log_{10}[\alpha(T)]}\right) - c_2 \qquad \text{Equation 23}$$

Thus a linear curve fit between $(T\text{-}T_0)/\log_{10}(\alpha t)$ and $(T\text{-}T_0)$, as shown in Figure 22, yields $-c_1$ as the slope and $-c_2$ as the intercept. Note that there was considerable scatter in data. There was typically a significant amount of scatter in the curve fit when finding the WLF shift

constants. Generally, the linear fit was only good for a narrow range of temperatures near the damping peak.

The constants can now be adjusted for any reference temperature using Equation 24 and Equation 25.

$$c_{1,new} = \frac{c_1 c_2}{c_2 + T_{0,new} - T_0} \qquad \text{Equation 24}$$

$$c_{2,new} = c_2 + T_{0,new} - T_0 \qquad \text{Equation 25}$$

Shifting the constants found in Figure 22 to 25° C yields $c_1 = 7.78$ and $c_2 = 117$.

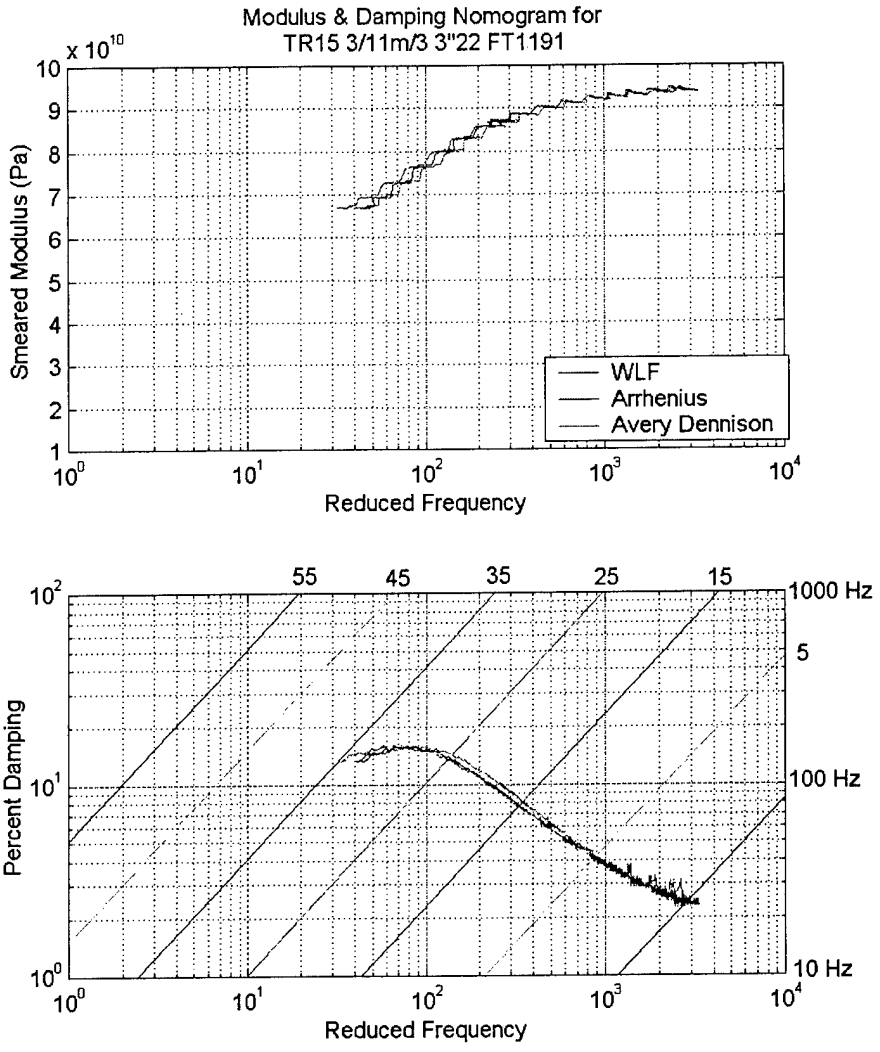

Figure 23: Data for 3"22° tube shifted by three methods.

Figure 23 shows the data from Figure 21 shifted using the WLF constants, Arrhenius constants and Avery-Dennison's viscoelastic constants. Note that the agreement is excellent for this tube. Other results will be examined in Section 4.3.4.

Nomogram lines and temperature labels have been included in Figure 23. As discussed earlier, since this nomogram is referenced to 25°C, the frequency in Hertz can be read directly on the reduced frequency scale. For other temperatures the stiffness and damping can be read by using the temperature lines. For example, if the stiffness and damping at 1000 Hz and 35° C is desired: First locate 1000 Hz on the far right axis. Follow this line to the left until reaching the diagonal temperature line labeled 35° C. (Note that the reduced freqency value at this point is approximately 230 Hz. Thus 1000 Hz at 35° C is equivalent to 230 Hz at 25° C). Now read up or down to the stiffness or damping master curves. From this point the stiffness or damping value can be read by traveling horizontally to the far left scale. The values are approximately 87 GPa for the axial stiffness and 10% damping.

4.3.4. Experimental Shift Constants vs. Viscoelastic Only Constants

As discussed previously, the wavy composite-viscoelastic combination tends to take on the time-temperature superposition characteristics of the viscoelastic alone, and when available the shift constants of the viscoelastic alone can be used to give a good approximation. This section will explore this in more detail. First, a tube made with 7.5 cm (3.0 in.) 30° wavy material using 0.28 mm (0.011 in.) thick Avery-Dennison FT1191 viscoelastic will be analyzed (named TR16).

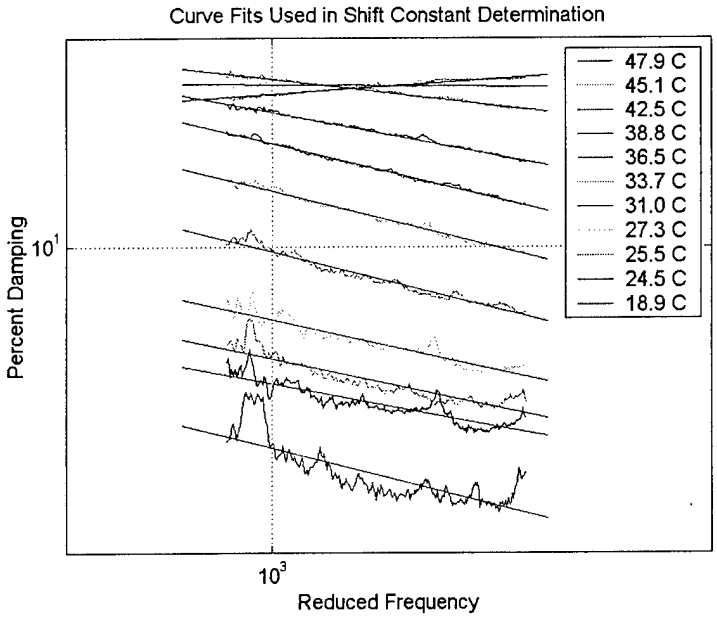

Figure 24: Curve fits used for damping data TR16

The linear fits are exceptional for this tube above 27°C, as seen in Figure 24. Below 27°C the data begins to appear noisy. The slope of the curve fit lines seems representative of the data at every temperature, though at 18.9°C the data is very noisy and it is difficult to say what the true slope should be.

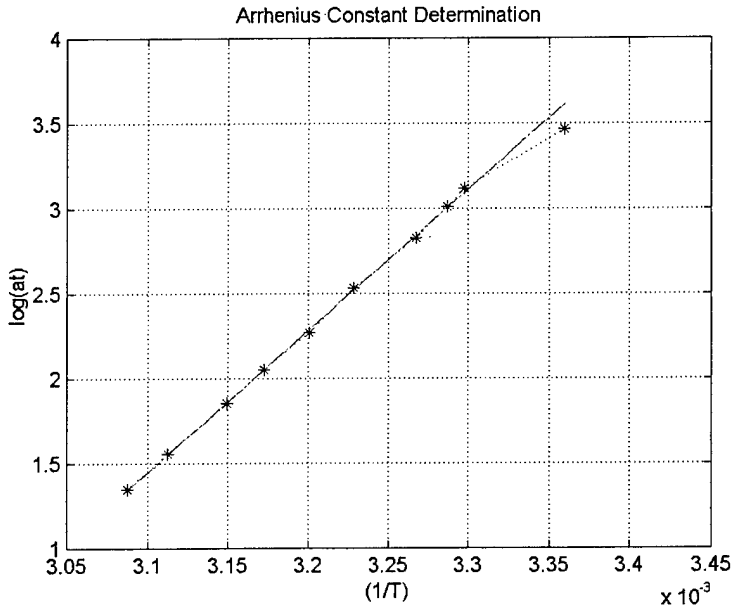

Figure 25: Linear fit used to find Arrhenius constants

Figure 25 shows the linear fit used to determine the Arrhenius shift constant, q. Once again, the data seems to diverge slightly at lower temperatures. In this case, the low temperature

divergence is probably due to noise in the data at low temperatures, as seen in Figure 24. The curve fit results in $q = 8357$.

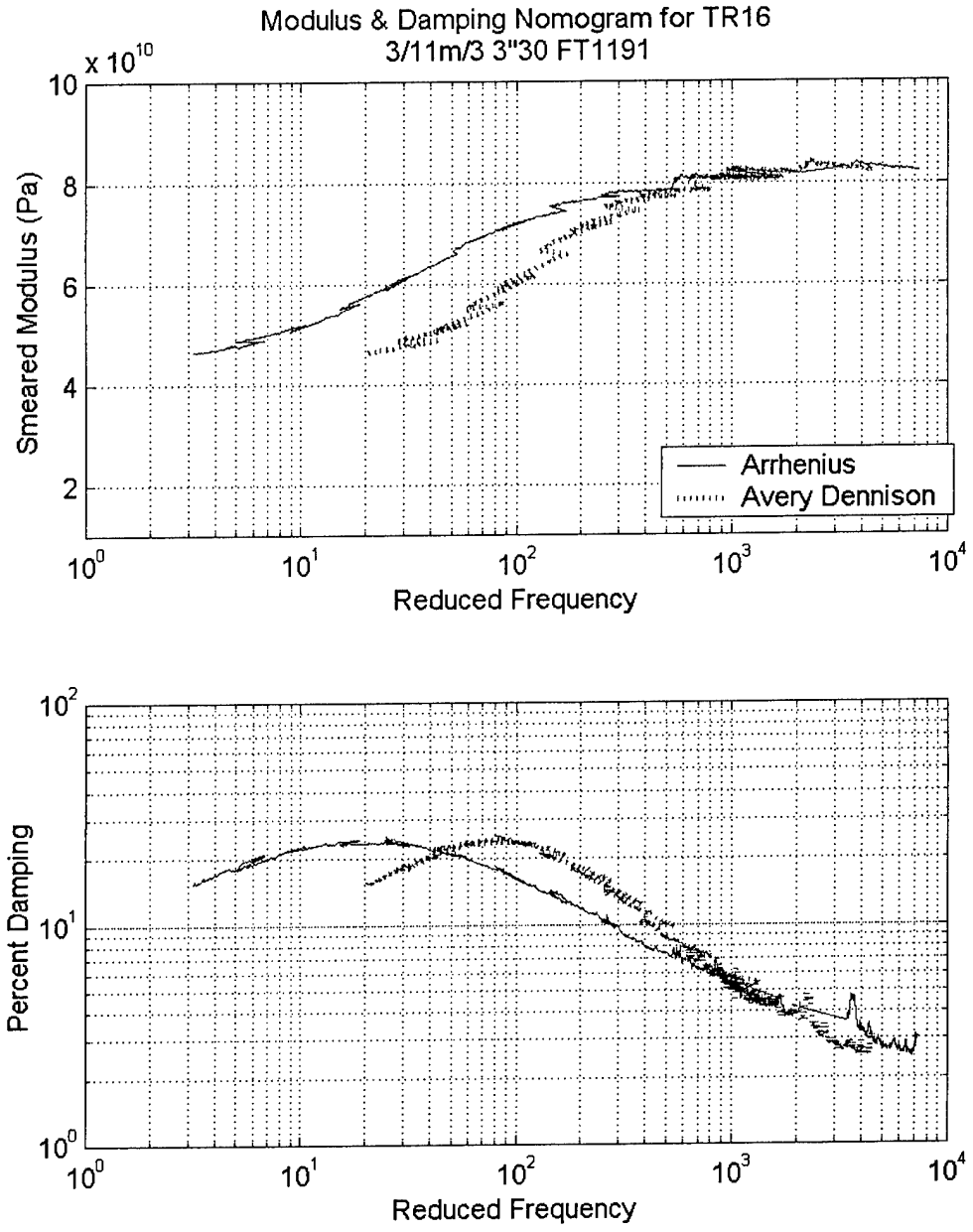

Figure 26: TR16 Data shifted according to Arrhenius and Avery-Dennison constants

Figure 26 shows the stiffness and damping data shifted using both Arrhenius and Avery-Dennison's constants. The Arrhenius constant places the damping peak at about 20 Hz. The Avery-Dennison shift constant placees the damping peak at about 85 Hz. The Arrhenius curve visually appears smoother than the Avery-Dennison curve. In terms of temperature, the spacing between these damping peaks is about 10°C. Much of the discrepancy seen above could be due

to inaccuracies in the temperature measurement, or variations in the temperature of the tube from top to bottom.

One more tube will now be examined. This is a 5.0 cm (2.0 in.) 30° tube made with 0.28 mm (0.011 in.) thick Avery-Dennison FT1191 viscoelastic (named TR17). First, the curve fits through each segment of damping data will be analyzed.

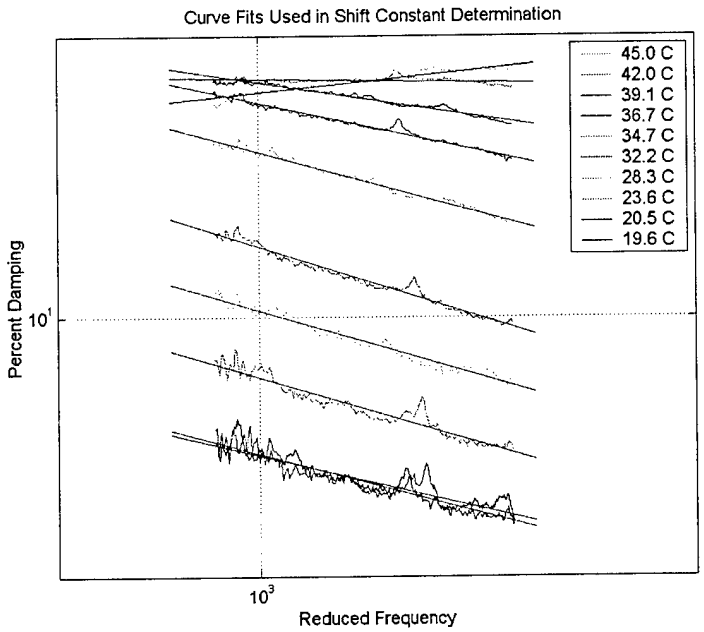

Figure 27: Curve fits through damping data at discrete temperatures—TR17

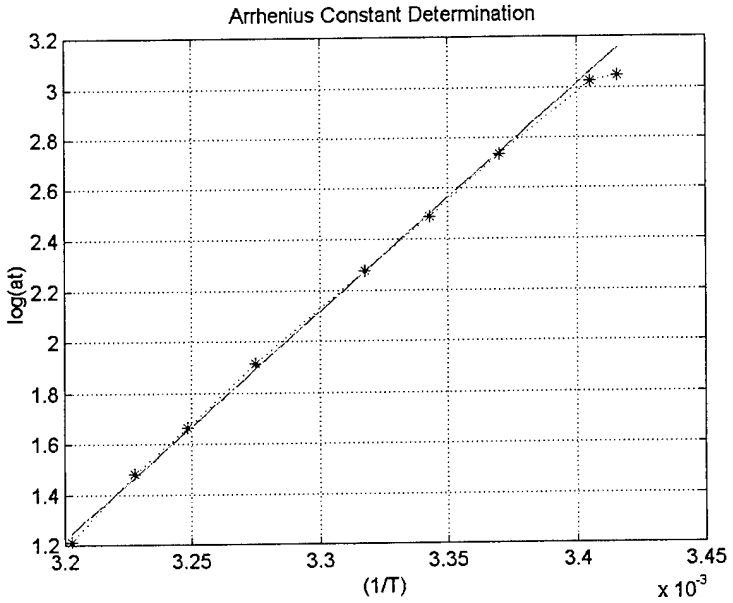

Figure 28: Linear fit used to find Arrhenius shift constants for TR17

As shown Figure 27, the curve fits through this data are all excellent, even for the data at low temperatures. Visual inspection of the data and linear fit gives no reason to suspect that these curve fits might give erroneous results. Figure 28 shows the linear fit which yielded $q = 8971$. The line fits the test data almost perfectly.

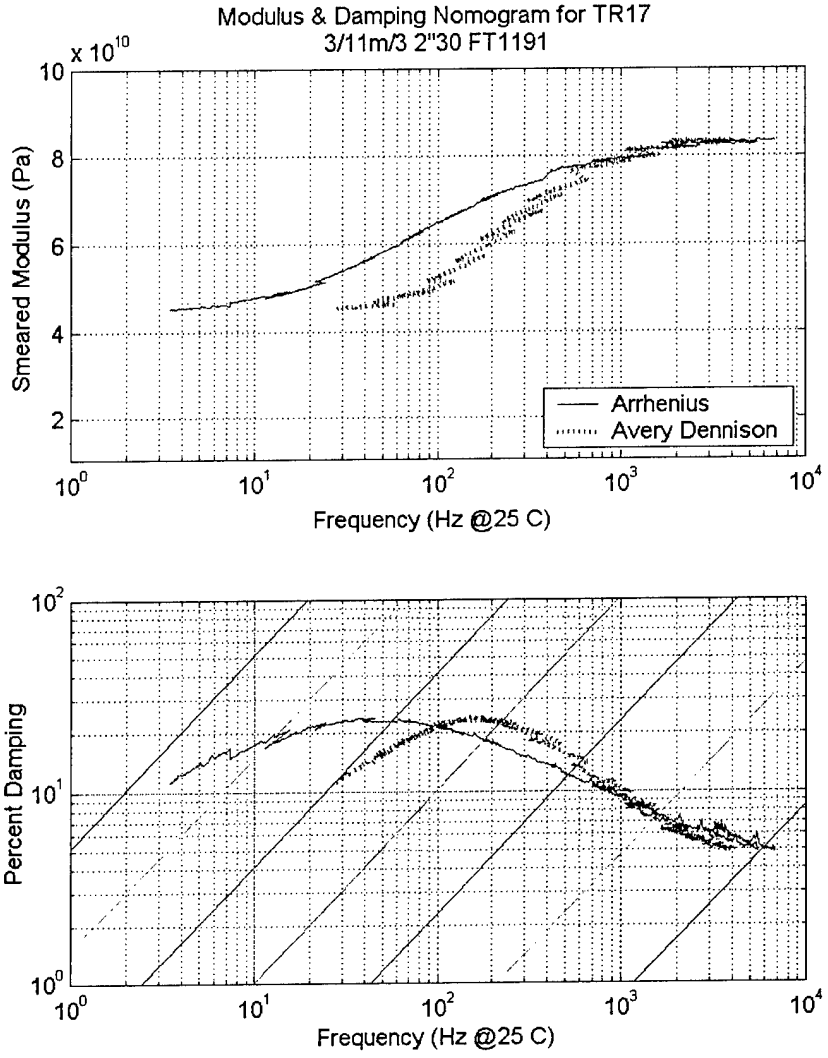

Figure 29: Data for TR17 shifted according to Arrhenius and Avery-Dennison

Figure 29 shows the data for TR17 shifted according to two methods. Once again, the Arrhenius constants place the damping peak at a significantly lower frequency than the Avery-Dennison constants. The resulting master curve looks significantly smoother when the Arrhenius constants are used. The horizontal spacing between the two damping peaks represents a temperature shift of 6-7°C.

In this section, the challenge involved in extrapolating to low frequencies using time temperature superposition has been demonstrated. When the Arrhenius shift constants are determined experimentally, the resultant master curve tends to be shifted to lower frequencies than expected.

The differences in the shift constants seen previously may be explained by a number of factors. First, the Avery-Dennison viscoelastic curve fits were quite noisy, and there may be error in the viscoelastic shift constant reported. Second, the wavy composite test stand allows for small temperature gradients between the top and the bottom of the tube as heat is conducted away through the piezoelectric actuator, into the steel base. The temperature measured at the center of the tube may not always be representative of the average temperature of the tube. Finally, error in the measured transfer function can affect the slope of the damping and stiffness curves, and thus affect the accuracy of the shift constants obtained from the data, especially if there is a bias in the test set-up as discussed in Section 4.3.5. The extension of the master curve to lower frequencies is subject to significant error because the shift required for high temperature, low frequency data is a cumulative of all previous shifts. If error is biased due to some anomaly in the test set-up, the result would have a tendency to cause large variations in the shift constants as will be seen in the next section.

The data presented in this section suggests that the actual Arrhenius shift constant for the composite-viscoelastic combinations examined here is 8000-9000. This large variation seems excessive at first, though differences of $\pm$ 500 in the shift constant produce a shift in the damping peak that is almost indiscernible. Further testing will be necessary to determine the actual shift constant for the composite-viscoelastic combination, and to verify that the constant for the viscoelastic alone is indeed correct. The effect of fiber angle, wave period, and thickness on the shift constant will also need to be examined. Since a more statistically significant dataset has not been examined, the manufacturer-supplied value will be used in the results presented here.

If it is assumed that wave angle, period, and thickness do not affect the shift constant, comparisons between the various test samples would be unaffected by the shift constant used. The agreement between the test data presented in Chapter 5 and the FEA analysis using the same shift constant suggests that this assumption is valid. The sensitivity analysis in section 4.3.5 will

illustrate the sensitivity of the shift constant to very small errors in the measured transfer function.

4.3.5. Time-Temperature Superposition Sensitivity Analysis

Simulated test data was generated using a curve fit of the results for a 7.5 cm (3.0 in.) 30° wavy composite tube. The simulated test data was generated by curve fitting the complex stiffness and damping as a function of frequency and temperature. This data was then used to construct a transfer function from 500 to 3200 Hz at discrete temperatures. 1% error was then added or subtracted from the magnitude and phase data to simulate noise in the data. This data was then analyzed using the same algorithms used in testing, resulting in stiffness and damping as a function of frequency at a number of temperatures. Time temperature superposition was then used to find the best-fit Arrhenius shift constants for this data.

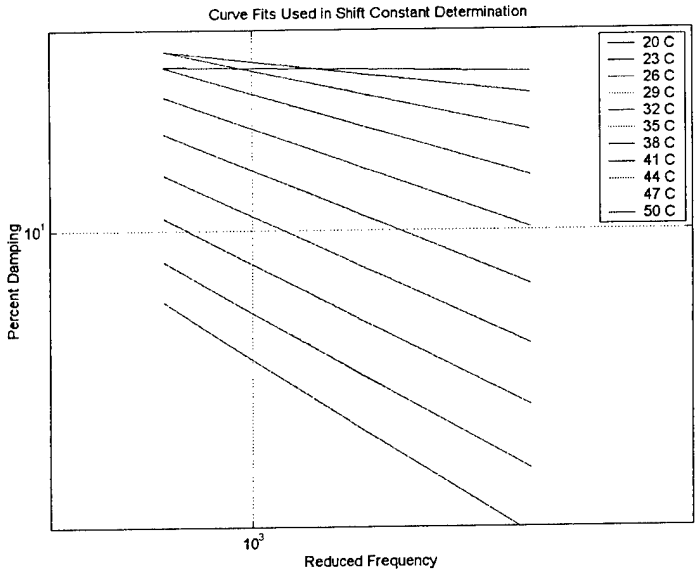

Figure 30: Curve fits on segments of simulated data with 1% error

Figure 30 shows the linear fits used on each segment of simulated damping data. Notice that there is no visible sign of error. A 1% error has been imposed on the transfer function over the entire test frequency range, so the error only appears in the slope of the damping curve.

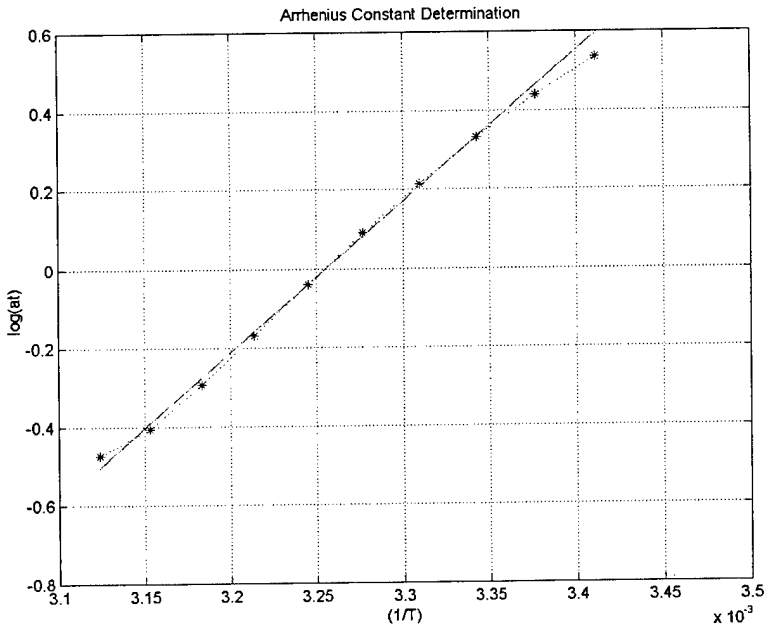

Figure 31: Arrhenius Fit on Simulated Data with 1% Error.

Figure 31 shows the linear fit used to determine the Arrhenius constant for the simulated data with +1% error imposed on the transfer function. Once again, there is nothing in the linear fit that would indicate that the error is there. With +1% error the fit yields q = 3816. With –1% error the fit yields q = 8352. The Arrhenius constant used to generate the data was q = 5555.56.

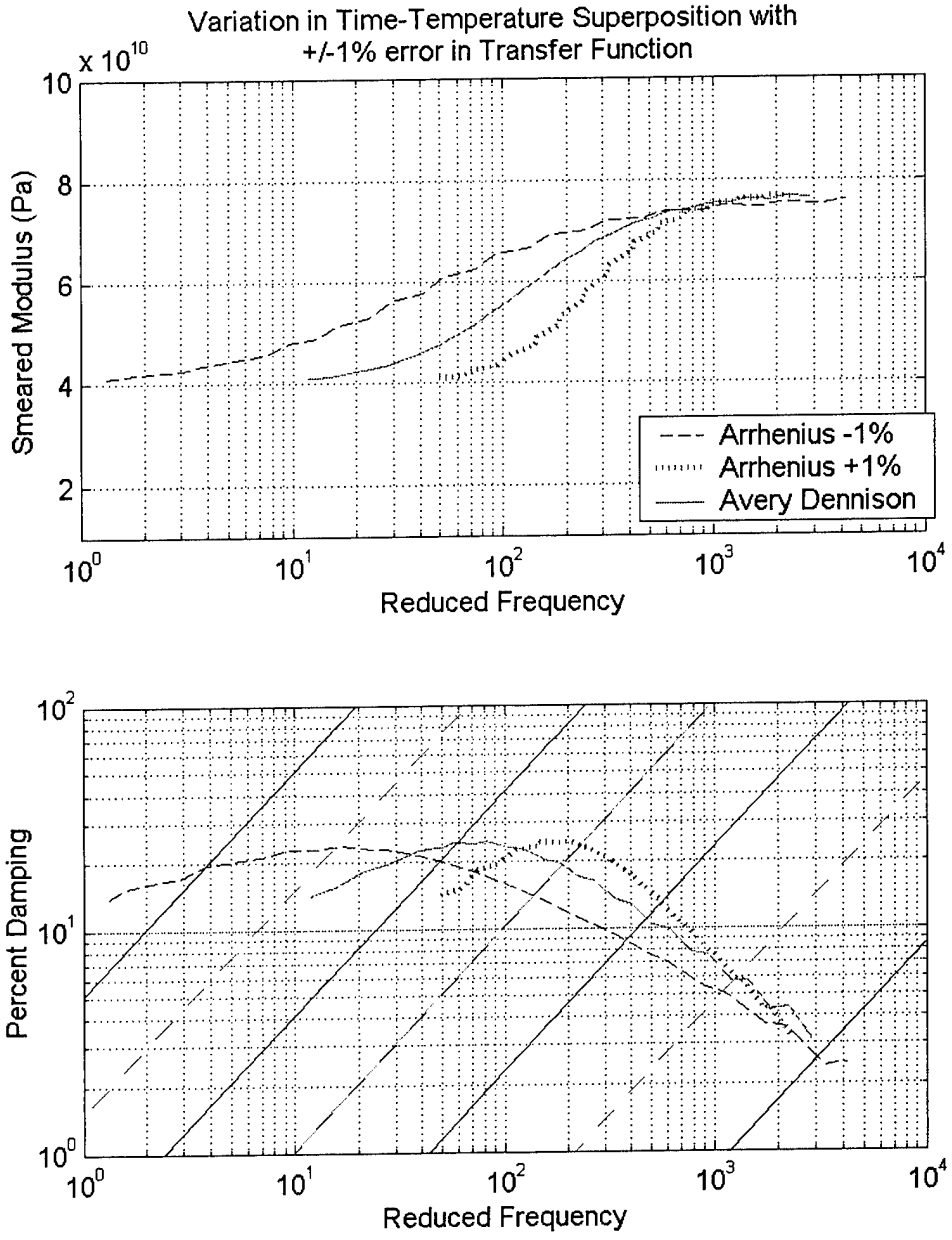

Figure 32: Resulting Shifted Curves with +/- 1% Error in Transfer Function

Figure 32 shows the shifted stiffness and damping curves obtained using the Arrhenius shift constants for the erroneous data. Imposing only 1% error on the transfer function has resulted in large shifts in the master curves. This suggests that small amounts of noise in the transfer function may be causing the discrepancies seen previously in Figure 19 through Figure 29.

Analysis has demonstrated that the time temperature superposition shift constants are susceptible to error. Nevertheless, it has been shown that the wavy composite certainly does take on the time-temperature properties of the viscoelastic. The shift constants determined experimentally for three different tubes ranged from 5000 to 9000. The sensitivity analysis in Figure 24 through Figure 32 indicates that variation much wider than this is observed if only 1% error is imposed on the transfer function. In the worst case, it appears that the error in determining the frequency of the damping peak is between 0.3 and 0.5 frequency decades. This corresponds to a temperature shift of 5-10°C. Over most of the curve, this results in only a few percent error in the stiffness and damping, though at the low frequency extreme the error becomes much larger. For this reason great care should be taken when extrapolating to very low frequencies. Since the shift constant is highly susceptible to error, a more detailed investigation must be performed in order to verify that the shift constants found are accurate for any viscoelastic-carbon fiber composite combination.

The data presented in this section reveals an interesting fact. The stiffness and damping *value* is unaffected by time-temperature superposition, and has been shown to be very accurate, especially at resonance. However, the *frequency* at which a particular value of stiffness and damping exists is in question because of errors in the slope of the data that determines the *frequency* shift constant. Mechanical tests accurately determine the stiffness and damping of the tube and can be performed between 1000 and 2000 Hz for any reasonable temperature.

Three points are required to define a second order curve exactly. Since the damping curve is parabolic in the useable range of interest, three points where the damping and frequency value are known would be necessary to complete an accurate nomograph. A room temperature test is unshifted by the Arrhenius equation, so the far right portion of the curve can be trusted. The peak value of damping can be accurately determined from the curve and represents a known second point. However it is the value of the damping at room temperature and at a very low frequency that is unknown because of the limitations in testing. Using the procedures outlined in this chapter, this low frequency point in the curve can be determined using shifted data but it has been shown that the shifted data at low frequencies is very susceptible to error. If a single low frequency test was available to "anchor" the lower end of the curve, the shift constant could be adjusted to agree so that every point in between would also be known with high accuracy.

Future testing is recommended at some very low frequency (ie 1 to 10 Hz). This may even be possible on existing tensile equipment. This could serve to anchor the damping master curve at low frequency. Another alternative involves determining time-temperature superposition constants experimentally on a large body of experimental data until the uncertainty in the shift constant is reduced to an acceptable level. Once again, it is important to remember that despite the difficulty in determining the time-temperature superposition shift constant, the *value* of the stiffness and damping at low frequency is not in question, only the exact *frequency* at which that stiffness and damping occurs.

4.4. TORSION & BENDING

A number of different samples were also tested in bending and in torsion, though testing in these areas was not as comprehensive. This section will outline some of the testing that was accomplished with foam core panels, tubes tested in bending, and tubes tested in torsion. The derivation of a test algorithm for broadband torsional testing will also be described.

4.4.1. Panel testing

A number of foam core composite panels were tested. A broadband testing algorithm was derived as for the axial and torsion testers. Unfortunately, it proved much less robust, and it was very difficult to obtain clean test results. Since broadband testing wasn't practical, another method had to be used. The panels were excited in bending by a stinger attached to one end of the panel. Two accelerometers were used, one directly above the stinger and one on the opposite edge of the panel. The transfer function between the accelerometers was recorded and the half power method was used to determine the damping at the first few bending modes. Figure 33 shows a schematic of the panel test setup.

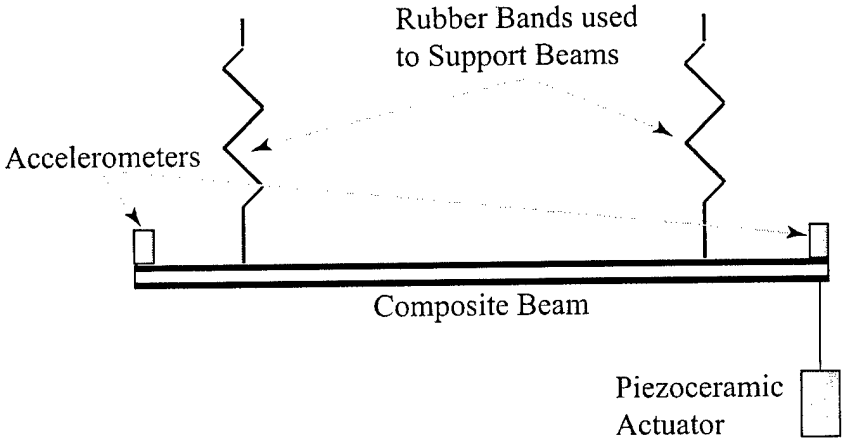

Figure 33: Beam Test Apparatus

Figure 34 shows a comparison between the transfer function measured from damped and undamped panels of similar stiffness and weight. Note that when testing the undamped panels the measurement may have suffered from slight inaccuracy because the point density used in the FFT may not have been sufficient to resolve the damping peak.

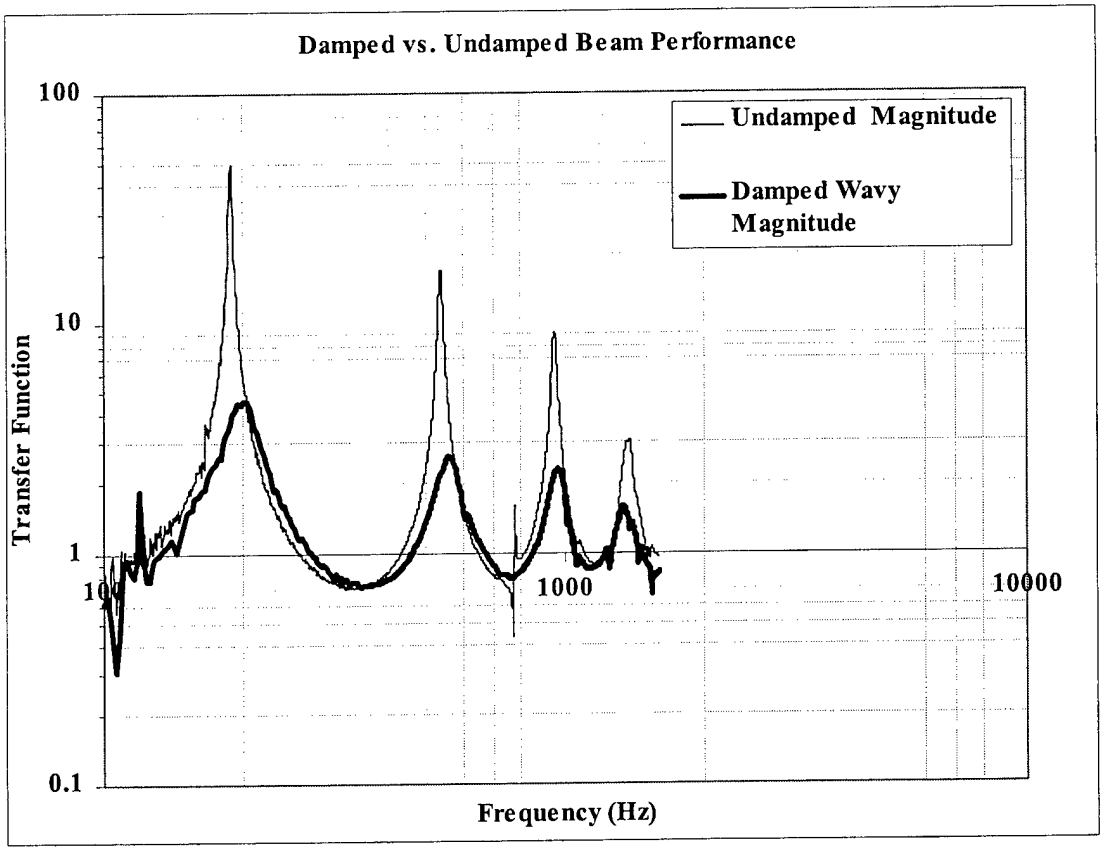

Figure 34: Magnitude response of Damped and Undamped Panels

Since the half power method was used at a number of frequencies at each test temperature, time-temperature superposition can be applied to create the master curve for the panel by shifting all of the tests at various temperatures to a reference temperature. Rather than try to find shift constants with such a small dataset, it was assumed that the viscoelastic shift constants would be sufficiently accurate. The smoothness of the shifted data will serve as an indication of the validity of this approximation.

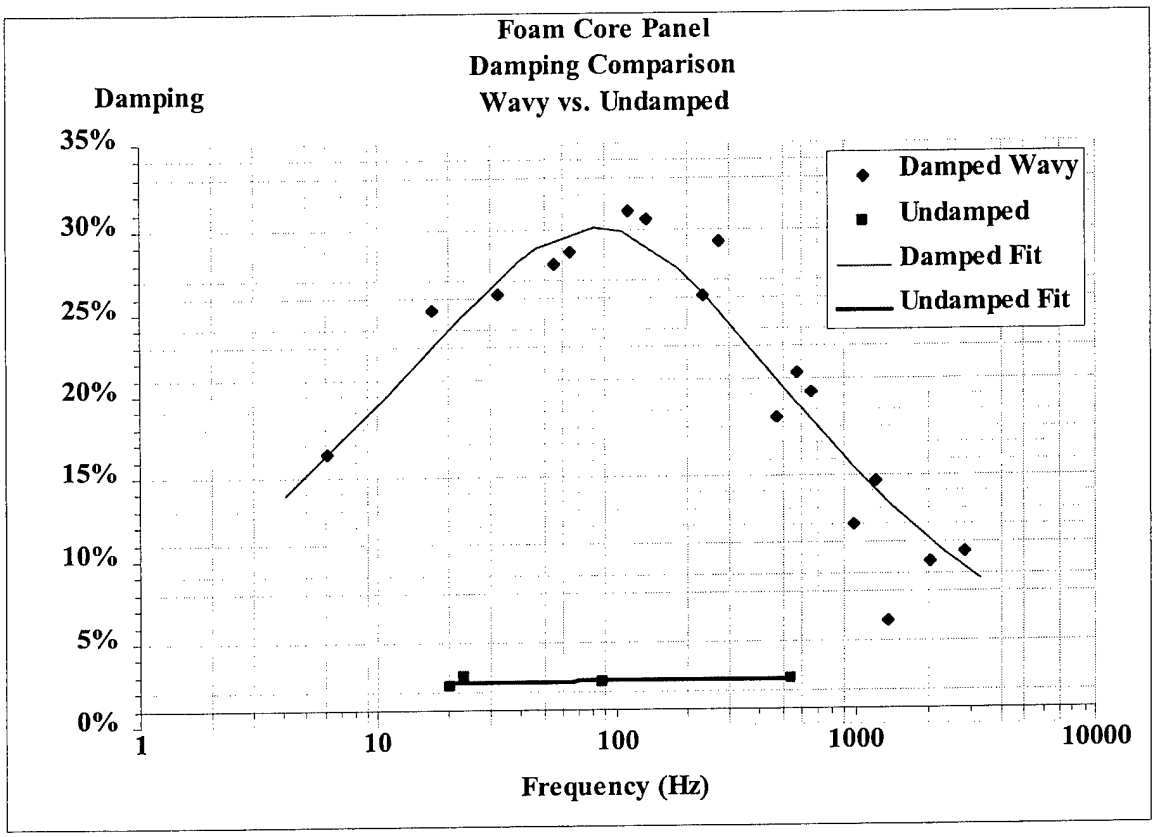

Figure 35: Panel master curves. Damped and Undamped

Figure 35 shows the damping master curve for a panel constructed with 3.75 cm (1.5 in.) 30° wavy face sheets on a 1.3 cm (0.5 in.) – thick Rohacell foam core. (The lay-up for the face sheets was the same as used for the tubes: 0.38 mm (0.015 in.) thick composite—0.28 mm (0.011 in.) thick viscoelastic—0.38 mm (0.015 in.) thick composite, opposing wave.) Also shown are the damping results for a panel constructed with conventional ± 30° unidirectional fiber facesheets on a 1.3 cm (0.5 in.) – thick Rohacell foam core. The damped panel has a damping peak of about 30% at 90 Hz. The damping of the undamped panel is essentially constant at about 2.7%. For comparison purposes, the data for the undamped panel has been shifted using the same

shift equation. Obviously, the frequency-temperature properties of the undamped panel are substantially different from those for the damped panel. The same shift equation has been used for both only to illustrate the fact that the properties of the undamped panel are not a strong function of frequency.

It is interesting to note that the tubes tested axially experienced a damping peak of significantly lower magnitude (23%), and at a different frequency (230 Hz), though the tube walls were identical to the foam core face sheets. When subjecting the panel to bending, slightly higher damping is expected since bending shears the viscoelastic layer, resulting in an additional damping component similar to that achieved in conventional constrained-layer damping. The damping peak also appears to be broader.

4.4.2. Tubes in Bending

The shifted damping peak and higher than expected damping observed in the panels raises questions. Does the material perform better in bending because of a component of conventional constrained-layer damping? Does the damping peak occur at a different frequency when the same structure is excited in bending as opposed to axially? A method is also sought that would allow testing the same sample at very low frequencies to confirm that the time-temperature superposition shift constants are indeed accurate. Though the data in this section is in nowise complete, it does provide an interesting preview to future testing.

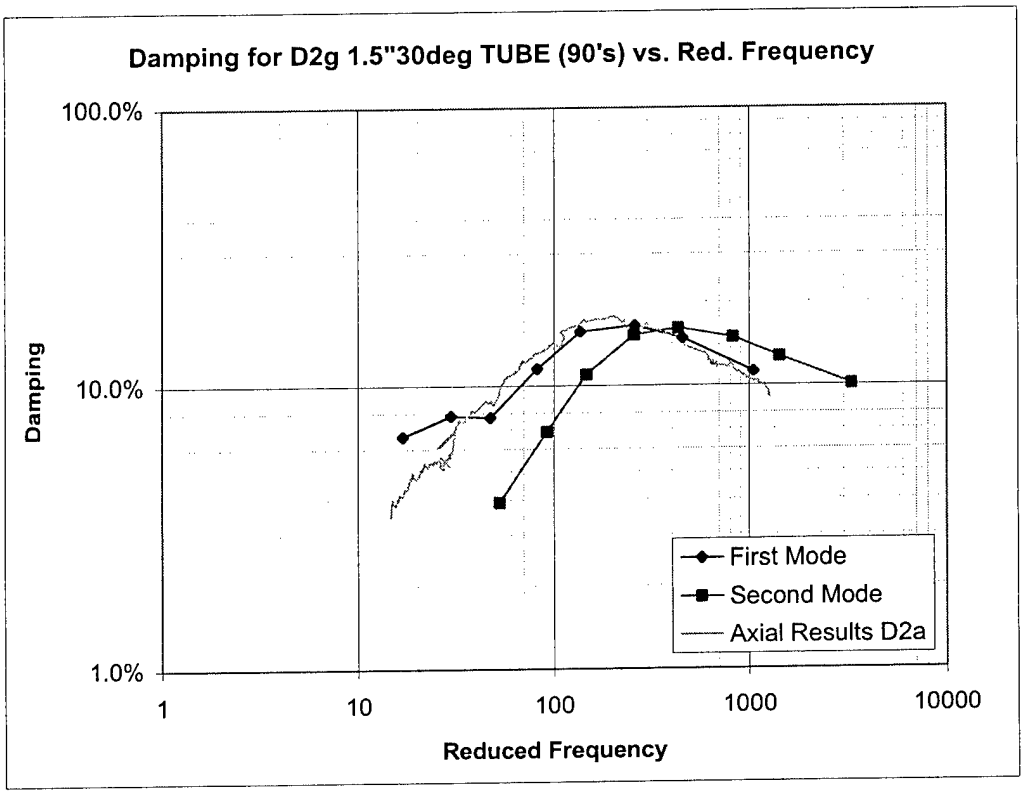

Figure 36: Bending results for Wavy Composite Tube

Figure 36 shows various results for a tube constructed with 3.75 cm (1.5 in.) 30° wavy composite material. The tube was constructed similarly to those tested axially, though a 0.13 mm (0.005 in.) thick layer of 80° unidirectional composite was added on either side of the viscoelastic for increased hoop strength. This tube was tested in bending using the same methods described previously for panels. The half power method was used to determine the bending at the first two resonances at a number of temperatures. All of the curves have been shifted using the Avery-Dennison shift constants (q=5555.56, Tref = 25°C.) The bending results using this method at the first and second modes are plotted as "First Mode" and "Second Mode." The axial test results have been overlaid on the same figure.

The axial test data in Figure 36 agrees fairly well with the bending data for the first bending mode. The data for the second mode seems to be shifted in frequency. The reasons for the phenomena seen in Figure 36 have not been determined.

These test methods were only used once with this tube, and it would not be wise to draw any major conclusions from such a small data set, though the combination of the methods described above in the future may provide a better understanding of the performance of wavy

composite structures under various loading conditions. One advantage to testing in bending is that cantilever-bending modes can be excited at very low frequencies. This provides an opportunity to obtain substantial evidence to support the time-temperature superposition constants, as it may be possible to anchor the low frequency end of the curve to some actual low frequency test points.

4.4.3. Derivation of Torsional Test Algorithm

A test setup was also constructed for testing tubes in torsion, similar to that used for testing the tubes axially. The test system can be approximated as a tube with inertial discs at either end. Accelerometers were attached to the inertial discs perpendicular to the tube and at a known radius. A thin wire stinger driven by a piezoceramic actuator was attached beneath the accelerometer on the base piece. The equation for the angular deflection of a tube in torsion according to Dimaroganos is: ((Dimarogonas 1995) p.423)

$$\theta(x,t) = \sum_{i=1,2,3\ldots}^{\infty} \left\{ \left(A_i \cos(w_i t)\right)\left(B_i \sin(w_i t)\right)\left[C_i \cos\left(\frac{w_i t}{c}\right)\right]\left[D_i \sin\left(\frac{w_i t}{c}\right)\right]\right\} \qquad \text{Equation 26}$$

Subject to:

$$J_1 \frac{\partial^2 \theta}{\partial t^2} = GI_p \frac{\partial \theta}{\partial x} \text{ At } x = 0 \qquad \text{Equation 27}$$

$$J_2 \frac{\partial^2 \theta}{\partial t^2} = -GI_p \frac{\partial \theta}{\partial x} \text{ At x = L} \qquad \text{Equation 28}$$

Where G is the shear modulus of the tube material, I_p is the polar area moment of the tube, and J_1 and J_2 are the inertia of the discs attached at x = 0 and x = L respectively. Using the initial conditions above the following is found for the first mode.

$$\beta = wL\sqrt{\frac{\rho}{G}} \qquad \text{Equation 29}$$

$$TF = \cos(\beta) - \beta \frac{J_1}{L\rho Ip} \sin(\beta) \qquad \text{Equation 30}$$

The form of the equations is similar to that used in the axial test algorithm. Thus by simply modifying the parameters in the solver, the axial test algorithm can be used for torsional testing.

4.4.4. Torsional Test Stand Performance

A major challenge when testing the composite tubes in torsion was that even with very small inertial discs on either end, the long, thin walled tubes tested axially resonated in torsion between 200-400 Hz. At these low frequencies noise in the accelerometers was troublesome. By reducing the inertial disc at x = L to the minimum that would hold the accelerometer, and by building thicker, shorter tubes it was possible to obtain fairly clean test data, as seen in Figure 37.

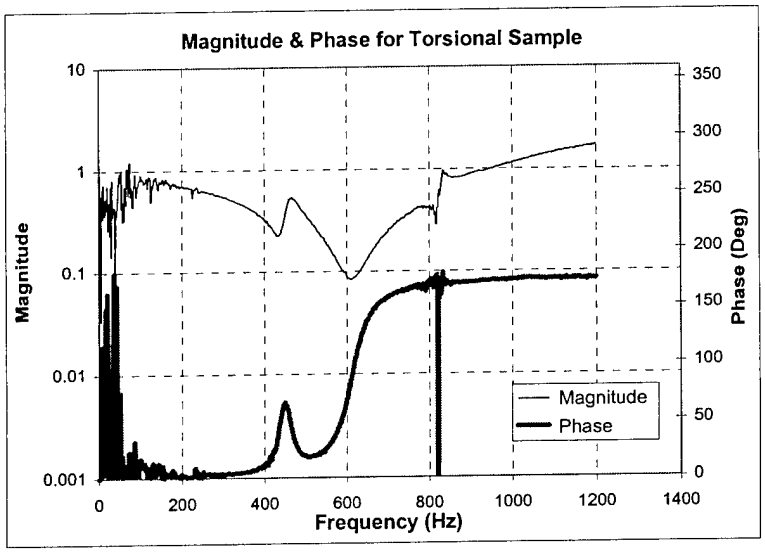

Figure 37: Magnitude and Phase results for torsion tester

Figure 37 shows the magnitude and phase results for the torsion tester. The sample tested was named T02. This tube construction, from the inside out was as follows: A four layer cross-ply (as discussed in chapter six), followed by a 0.28 mm (0.011 in.) thick viscoelastic layer, a 0.51 mm (0.020 in.) thick 3.75 cm (1.5 in.) 30° wavy composite layer. This was followed by another 0.28 mm (0.011 in.) thick viscoelastic layer and a 0.51 mm (0.020 in.) thick 3.75 cm (1.5 in.) 30° wavy composite layer with the waveform 180° out of phase with the previous layer. Note that a number of significant spurious resonances can be seen in the test data. When testing in torsion it was much more difficult to avoid exciting the natural modes of the test setup. A number of the bending modes may also be present. (The accelerometers were positioned

perpendicular to direction of the major bending plane to minimize this, though they are 5-10% sensitive to out of plane acceleration.)

The main challenge when testing in torsion was imparting enough torsional energy to the structure to obtain a strong signal. The accelerometer signals were much closer to their noise floors when testing in torsion than in bending or axial testing. Also, if a bearing was used to constrain the base piece unacceptable noise resulted. For this reason, the test system was suspended by rubber bands, connected to ground only through the stinger. With this setup, much of the energy imparted to the structure went into translating the base and only a fraction went into torsion. A better actuation method will have to be derived before higher accuracy can be obtained.

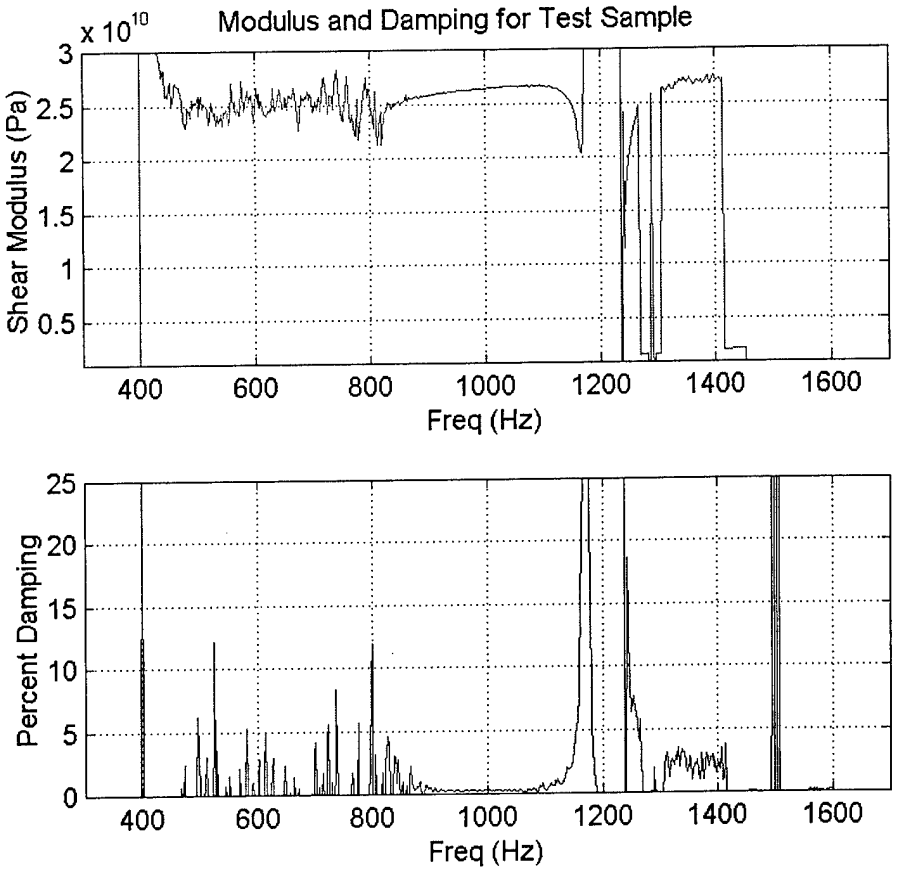

Figure 38: Shear Stiffness and Damping for Aluminum Test Specimen.

The torsional test stand was validated by testing a short aluminum tube of known properties. This was used to calibrate the test setup, since the inertia of the end pieces is difficult

to determine precisely. Further testing and evaluation will be necessary before reliable data can be obtained with the torsion tester, though it appears that the results to date are reasonable.

Figure 38 shows the shear stiffness and damping results for aluminum. The data is only reliable between about 800 and 1150 Hz. Note that there is still some erroneous curvature in this section, which may be due to spurious resonances just outside of this range altering the magnitude and phase results. As seen in Figure 37 there are large spurious resonances on either side of the resonance in test data for the composite tube. Similar noise patterns were seen in the test data for the aluminum sample. These large spurious resonances can change the slope of the stiffness and damping curves.

Time-temperature superposition was applied to the wavy composite, torsional test data. The resultant nomogram showed the typical damping peak and increasing stiffness with frequency.

4.5. CONCLUSIONS

The axial test stand is an effective tool in characterizing the performance of stiff, highly damped composites. Investigations into all of the possible sources of error have shown that the test stand is accurate and robust. Sensitivity analyses have shown that the data at resonance is highly reliable, though the data is somewhat sensitive to error away from resonance. The magnitude of this error away from resonance is normally very small.

Time-temperature superposition has been applied to create master stiffness and damping curves over a very broad frequency range. The Arrhenius time-temperature superposition constant has been shown to be highly sensitive to error in the slope of the stiffness and damping data. Experimentally determined shift constants vary between 5000 and 9000, while the value for the viscoelastic alone is reported as 5555.56. The scatter seen in testing has been shown to be significantly less than occurs when a 1% error is imposed on the magnitude and phase curves. Because of this high sensitivity to error, the low frequency properties determined through time-temperature superposition are susceptible to error. It is important to remember that despite the difficulty in determining the time-temperature superposition shift constant, the *value* of the stiffness and damping at low frequency is not in question, only the exact *frequency* at which that stiffness and damping occurs.

Wavy composite takes on the properties of the viscoelastic, and the viscoelastic curve fit constants appear to be a reliable approximation that can be used to shift test data and form master nomograms. Further testing at very low frequencies or on a larger body of data will determine the time-temperature superposition shift constant more accurately.

Methods for testing in bending and in torsion have revealed that the material behaves similarly in bending and torsion, though further research will be necessary to make these methods as robust and reliable as the axial test.

CHAPTER 5: DOE AND MODEL CORRELATION

5.1. GENERAL

The purpose of this chapter is to evaluate the accuracy of the finite element code discussed in Section 3. To do this, the stiffness and damping master curves for various tubes will be compared to the FEA predicted master curves. Some of the material constants for the composite were obtained by testing a number of unidirectional tubes and others through a rule of mixtures analysis. The viscoelastic properties were determined from data sent by the viscoelastic manufacturer (Avery-Dennison) and through independent in-house testing. A number of tubes were built and tested using the methods described in chapter four. This evaluation focuses on testing the performance of the FEA code for predicting axial material properties of simple wavy composite—viscoelastic—wavy composite lay-ups. The wavy composite wavelength and maximum angle are varied, as well as the composite and the viscoelastic thickness.

Since the viscoelastic properties, and hence the composite properties, are frequency dependent, to adequately test the FEA code it was necessary to compare test data to FEA predictions at a number of frequencies. Typically, thirteen predictions were performed at uniformly logarithmically spaced frequencies between 1 Hz and 10,000 Hz.

The analysis shows that the FEA model is typically accurate to within 5% when predicting stiffness and within 2% or better when predicting damping. The FEA model retained high correlation even when wavelength, max angle, and layer thickness were varied.

5.2. MATERIAL PROPERTIES

In order to obtain accurate correlations, the properties of the composite and the viscoelastic had to be determined. The FEA code requires the following properties for the composite: E_{11}, E_{22}, G_{12}, G_{23}, ν_{12} ,ν_{23} ,D_{11} ,D_{22} ,D_{12} , and D_{23}. Where E, G, ν, and D represent the Young's modulus, shear modulus, Poisson's ratio, and loss factor respectively. The subscripts indicate the directions. Many of these properties could be determined by testing sample tubes on the axial test stand. A number of unidirectional tubes were made with the fibers laid in the 0° direction (along the length of the tube) and others with fibers laid in the 90° direction (around the tube) to determine E_{11}, E_{22}, D_{11} and D_{22}. Table 3 shows that there was little variation in the measured properties.

Table 3: Test Results for Unidirectional Tubes

Layup	Tested for:	Modulus (Gpa)	Modulus (Msi)	Damping
8 layers 0°	E_{11}, D_{11}	132	19.14	0.25%
15 layers 0°	E_{11}, D_{11}	135	19.58	0.25%
9 layers 90°	E_{22}, D_{22}	10.4	1.51	1.00%
14 layers 90°	E_{22}, D_{22}	9.8	1.42	0.80%

Values for the other constants were chosen by experience using a rule of mixtures analysis. The properties of the carbon fibers and viscoelastic were known, so the rule of mixture analysis was modified until it resulted in the measured values for E_{11} and E_{22}. The resulting rule of mixtures solution for G_{12}, G_{23}, ν_{12}, ν_{23} was then assumed to be correct. Experience dictates that a typical ±45° tube has between 1-2% damping, so an average value was taken as the D_{12} and D_{23} damping.

Table 4: Values used in analysis and correlation

Property	Value
G_{12}	5.2 GPa (0.75 Msi)
G_{23}	5.0 GPa (0.72 Msi)
ν_{12}	0.312
ν_{23}	0.463
D_{12}	1.5%
D_{23}	1.5%

The FEA code is highly sensitive to the properties of the viscoelastic. The manufacturer of the viscoelastic supplied curve fit equations for the stiffness and loss factor of the viscoelastic. Before this data was available, in house testing was performed on samples of viscoelastic to determine it's damping and shear modulus.

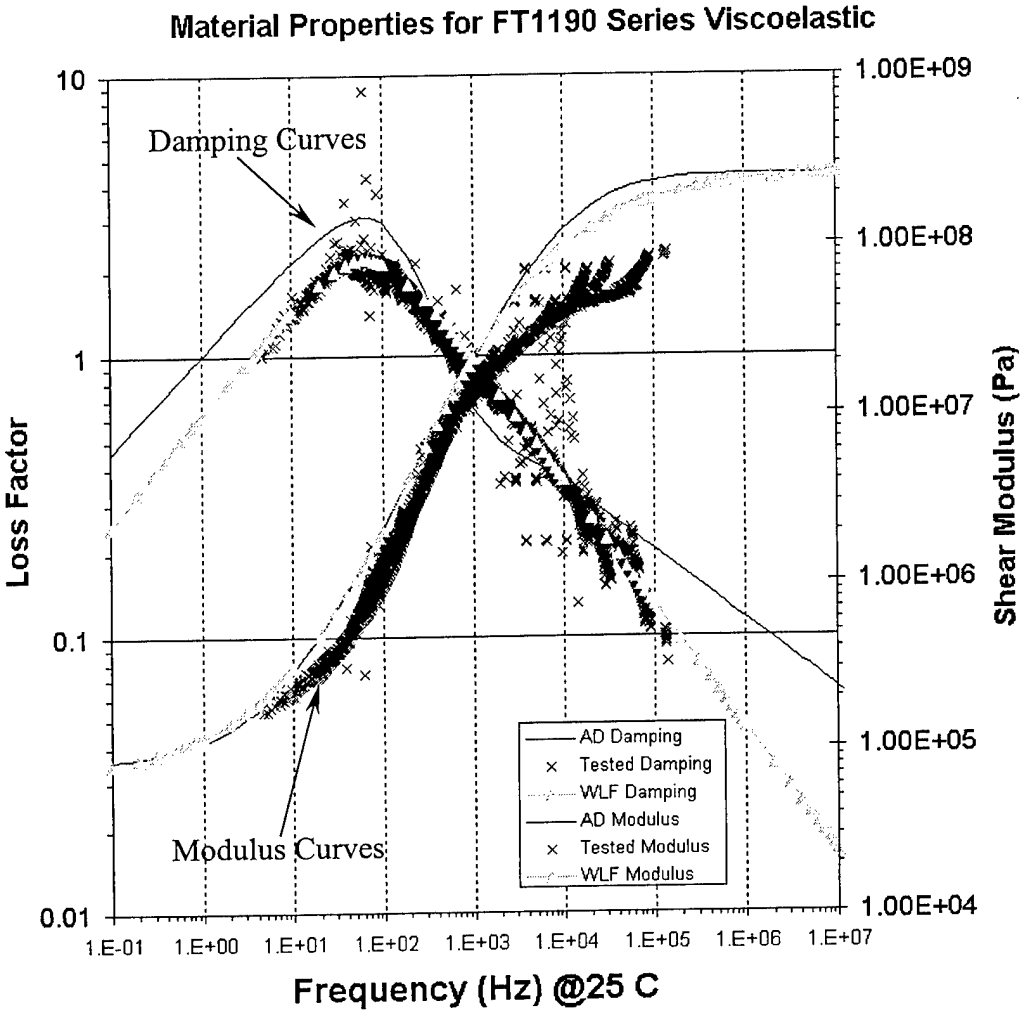

Figure 39: VEM Test Data vs. Avery-Dennison and WLF Curve Fits

Figure 39 shows the results of the in-house testing of the viscoelastic properties and the curve fits supplied by Avery-Dennison. Also shown are curve fits for another set of curve fit equations. (We have chosen to call them WLF curve fits since their original users used the WLF equation extensively.) It is readily apparent that the damping test data doesn't agree strongly with Avery-Dennison's curve fit. Also, our damping test data does not show an elbow in the damping curve as seen in the Avery-Dennison curve fit equation.

When used in the FEA program, the Avery Dennision curve fit equation gave good overall quantitative correlation with the test data, though the FEA code would predict a damping peak that was too high. Furthermore, when the Avery-Dennison curve fit was used, FEA code

predicted an elbow in the damping curve which was never observed in the test data. Avery-Dennison's equations were fit to very nosy damping data. If the high peak and elbow are taken to be anomalies of their testing, then it seems reasonable that the actual damping performance is much closer to our test data shown above. Unfortunately, we are less confident in our ablilty to determine the modulus of the viscoelastic, because it depends on the thickness of the viscoelastic sample, which is hard to measure accurately using our test setup. Thus a compromise was struck between the two. The WLF viscoelastic curve fit equation for the modulus was fit to Avery-Dennison's modulus data, though the damping curve fit equation was modified to reflect in-house test results. With these modified WLF curve fit equations used to model the viscoelastic, the FEA code predicted the actual performance of the tubes very precisely. The WLF and Avery-Dennison curve fit equations are shown below. Table 5 shows the constants used in these curve fit equations.

WLF curve fit equation for shear modulus:

$$\log_{10}(G) = \log_{10}(ml) + \frac{2 * \log\left(\frac{mrom}{ml}\right)}{1 + \left(\frac{fqrom}{f}\right)^{slope}} \qquad \text{Equation 31}$$

WLF curve fit equation for damping:

$$\log_{10}(\eta) = \log_{10}(etafrol) + \left(\frac{c}{2}\right)\left\{(sl + sh)\left(\frac{\log_{10}(f) - \log_{10}(frol)}{c}\right) + (sl - sh)\left(1 - \sqrt{1 + \left(\frac{\log_{10}(f) - \log_{10}(frol)}{c}\right)^2}\right)\right\}$$

Equation 32

Avery Dennision curve fit equation for shear modulus:

$$G = Gmid - \frac{(Gmid - Gmin)}{(1 + K1a * (f)^{na})} + Gmax - \frac{(Gmax - Gmin)}{(1 + K1b * (f)^{nb})} \qquad \text{Equation 33}$$

Avery Dennision curve fit equation for damping:

$$\eta = K2a * \frac{(f)^{(Pa-1)}}{(1 + K3a * (f)^{Pa})^{ma}} + K2b * \frac{(f)^{(Pb-1)}}{(1 + K3b * (f)^{Pb})^{mb}} \qquad \text{Equation 34}$$

Table 5: Avery-Dennison and WLF curve fit equation constants

AVERY-DENNISON CURVE FIT CONSTANTS:			
Gmid	3.44E+09 Pa	K2a	0.0371
Gmin	1.08E+04 Pa	K2b	0.965
Gmax	2.57E+08 Pa	K3a	0.000038
K1a	0.00002	K3b	0.00072
K1b	0.00007	Pa	1.369
na	0.053	Pb	1.34
nb	1.026	ma	0.453
		mb	1.72

WLF CURVE FIT CONSTANTS			
WLF Model		Damping Constants	
ML	6.00E+04 Pa	ETFROL	2.2
MROM	4.00E+06 Pa	C	0.5
FQROM	200	SL	0.4
SLOPE	0.5	SH	-0.45
		FROL	70

5.3. TEST AND EVALUATION OF WAVY COMPOSITE TUBES

Once an accurate model for the viscoelastic properties had been obtained, the FEA code was tested by comparing master curves created from test data to master curves produced by the FEA code. The FEA predictons were performed using a shell model of a 0.875-in diameter tube with twenty-four elements. (Six elements around the circumference and four elements along the length.) The model was scaled in the lengthwise direction to include one full wavelength for each material analyzed. Tubes were used because the analysis determines material properties directly, as described in chapter four. Each analysis took between 45-90 seconds on a Pentium 450 MHz machine, for a total of about 15 minutes to create the entire master curve (ie. analysis at 13 frequencies.) The finite element code outputs complex displacements, from which the damping was calculated from the ratio of the imaginary part of the displacement over the real part of the displacement. The smeared axial modulus was found by dividing the stress (1000 psi) by the strain. Thus the smeared stiffness is the stiffness of an equivalent homogeneous material.

The test data was taken to reflect the smeared stiffness of carbon fiber layers only. This was convenient because, as described in chapter two of the software operating instructions, the FEA code welds the viscoelastic layers together at the end, effectively applying pressure only on the carbon fiber layers. Because the viscoelastic is a few orders of magnitude less stiff, if pressure were applied directly to these layers they would essentially pull out from between the

carbon fiber layers. Also, in practice tubes are always made with welds on the ends to encapsulate the viscoelastic.

Stiffness that reflects the smeared stiffness of the carbon fiber layers only will be called "Carbon Only" stiffness. To convert from carbon only stiffness to a stiffness that accounts for the entire tube cross section including viscoelastic layers, simply multiply the carbon only stiffness by the ratio of the area of the carbon fiber layers over the entire area of the tube, (including viscoelastic layers).

A wave with a 7.5 cm (3.0 in.) wavelength, 0.38 mm (0.015 in.) thick composite layers and 0.28 mm (0.011 in.) thick viscoelastic was taken as a baseline. This layup is called a +3/11m/-3 for brevity where "+3" represents three plies (0.127 mm (0.005 in.) each) of wavy composite with the wave starting in the positive direction and "-3" represents three plies of wavy composite with the wave starting in the negative direction, or 180° out of phase with the positive layers. "11m" represents the thickness of the viscoelastic layer in thousandths of an inch.

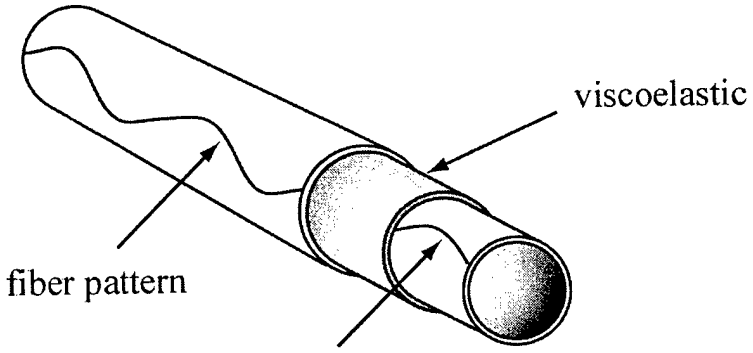

Figure 40: Basic Tube Design

A fairly simple experiment was designed to test the effect of varying the wavelength, max angle, composite thickness, and VEM thickness in a minimum number of tubes. This allowed evaluation of the performance of the FEA code for all of the basic design parameters. All of the tubes consisted of a viscoelastic layer sandwiched between two composite layers with opposing wave patterns, as seen in Figure 40. All of these tubes were constructed using Avery-Dennison FT1190 series viscoelastics. A number of 5.0 cm (2.0 in.), 10 cm (4.0 in.) and 12.5 cm (5.0 in.) (wavelength) tubes were also constructed. The results for these tubes will not be discussed here, but can be found in the Appendix.

Table 6: Properties Varied and Levels

Property	Levels Tested
Wavelength	3.8 cm, 7.5 cm, 15 cm. (1.5, 3.0, 6.0 in.)
Max Angle	22°, 30°
Composite Thickness	0.38 mm, 0.76 mm (0.015, 0.030 in.)
VEM Thickness	0.15 mm, 0.28 mm, 0.56 mm (0.006, 0.011, 0.022 in.)

Table 6 shows the properties and values used to build test tubes in a design of experiments conducted to evaluate and correlate test results to the FEA program. Table 7 shows the properties of the various tubes and the specific factors used in each tube. Thickness in either table refers to the individual layer thickness and not to the overall thickness of total composite used in the construction of the tube. The thickness of the pre-preg used in their construction was approximately .12 mm (.005 inches), thus a .38 mm thick layer of composite was fabricated by stacking three plies of pre-preg. The construction of the tube consisted of two constraining layers of wavy composite of the thickness shown, sandwiching a single viscoelastic damping layer as shown in Figure 40.

Table 7: Tubes Properties and Names

Max Angle	Wavelength	VEM Thickness	Composite Thickness	Tube Names
30°	3.8 cm (1.5 in.)	0.28 mm (0.011 in.)	0.38 mm (0.015 in.)	TR6, TR8
30°	7.5 cm (3.0 in.)	0.28 mm (0.011 in.)	0.38 mm (0.015 in.)	TR1, TR16
30°	15 cm (6.0 in.)	0.28 mm (0.011 in.)	0.38 mm (0.015 in.)	TR2,TR3
30°	3.8 cm (1.5 in.)	0.15 mm (0.006 in.)	0.38 mm (0.015 in.)	TR28, TR29
30°	3.8 cm (1.5 in.)	0.56 mm (0.022 in.)	0.38 mm (0.015 in.)	TR13, TR27
30°	3.8 cm (1.5 in.)	0.28 mm (0.011 in.)	0.76 mm (0.030 in.)	TR14, TR30
22°	3.8 cm (1.5 in.)	0.28 mm (0.011 in.)	0.38 mm (0.015 in.)	TR10, TR19
22°	7.5 cm (3.0 in.)	0.28 mm (0.011 in.)	0.38 mm (0.015 in.)	TR12, TR15

The FEA code predicted the damping performance of the tubes very accurately. The model predictions for the 3.8, 7.6 and 15.2 cm 30° tubes with 0.38 mm (0.015 in.) and 0.28 mm (0.011 in.) composite and VEM layers follow. In the figures which follow the FEA predictions are shown by astrices connected by a dotted line. The actual test data appears as a solid thin line. Note that in all of these figures, Avery-Dennison's shift constant (q = 5555.56) was used for the viscoelastic. The FEA can also perform tests at a single frequency, at a number of temperatures, thus replicating testing. Thus test data and FEA data will always agree no matter what shift constant is used, so long as the same shift constant is used for the test data and the viscoelastic.

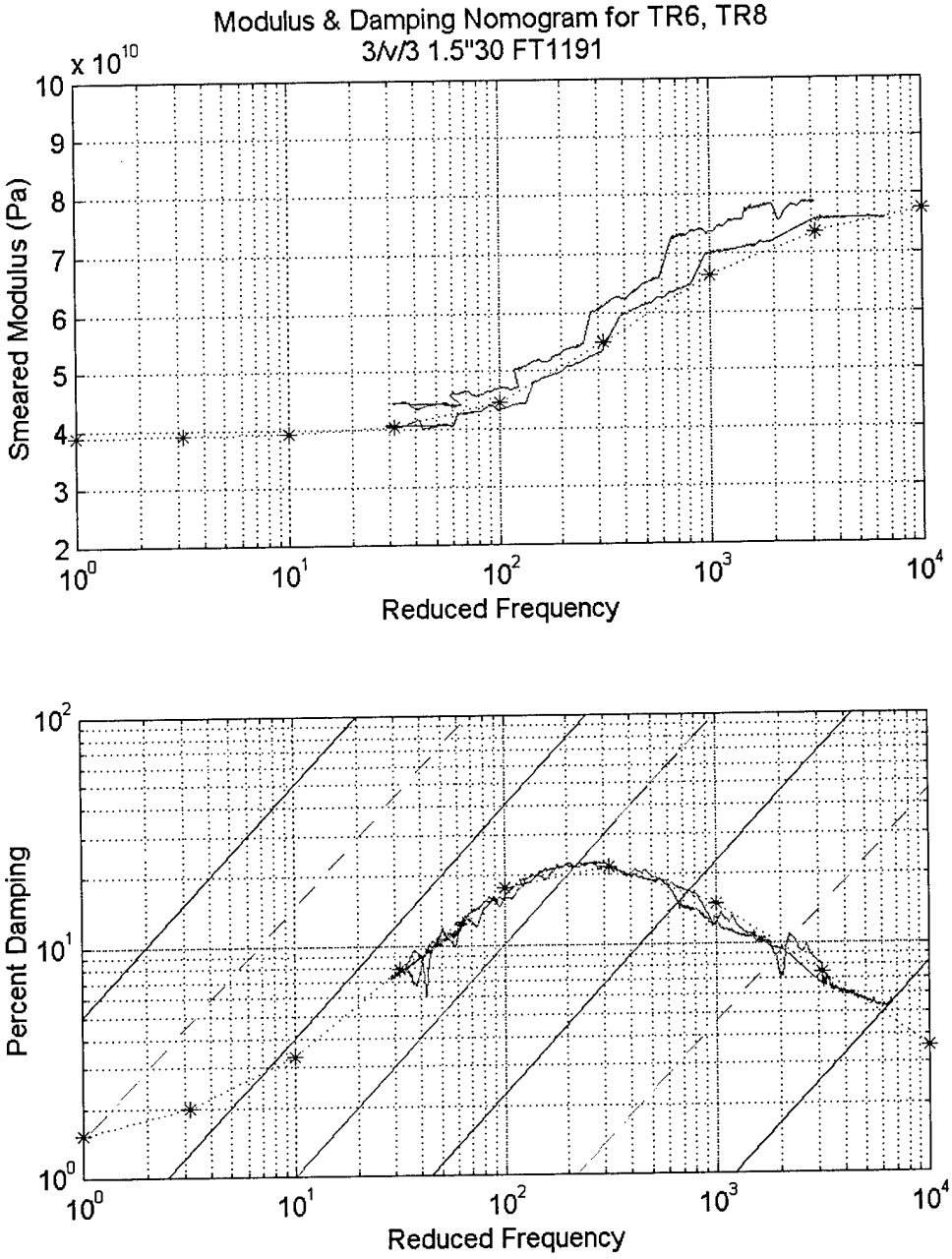

Figure 41: FEA prediction vs. test results for 3.75 cm (1.5 in.) 30° tubes

Figure 41 shows the stiffness and damping master curve for two +3/11m/-3 tubes with 3.8 cm (1.5 in.) 30° wavy layers, overlaid on the FEA prediction. The stiffness asymptotes are 40 and 80 GPa. The damping prediction shows no noticeable error, though there is 5-10% scatter in the stiffness data. Peak damping is 23% at about 230 Hz and 25 °C.

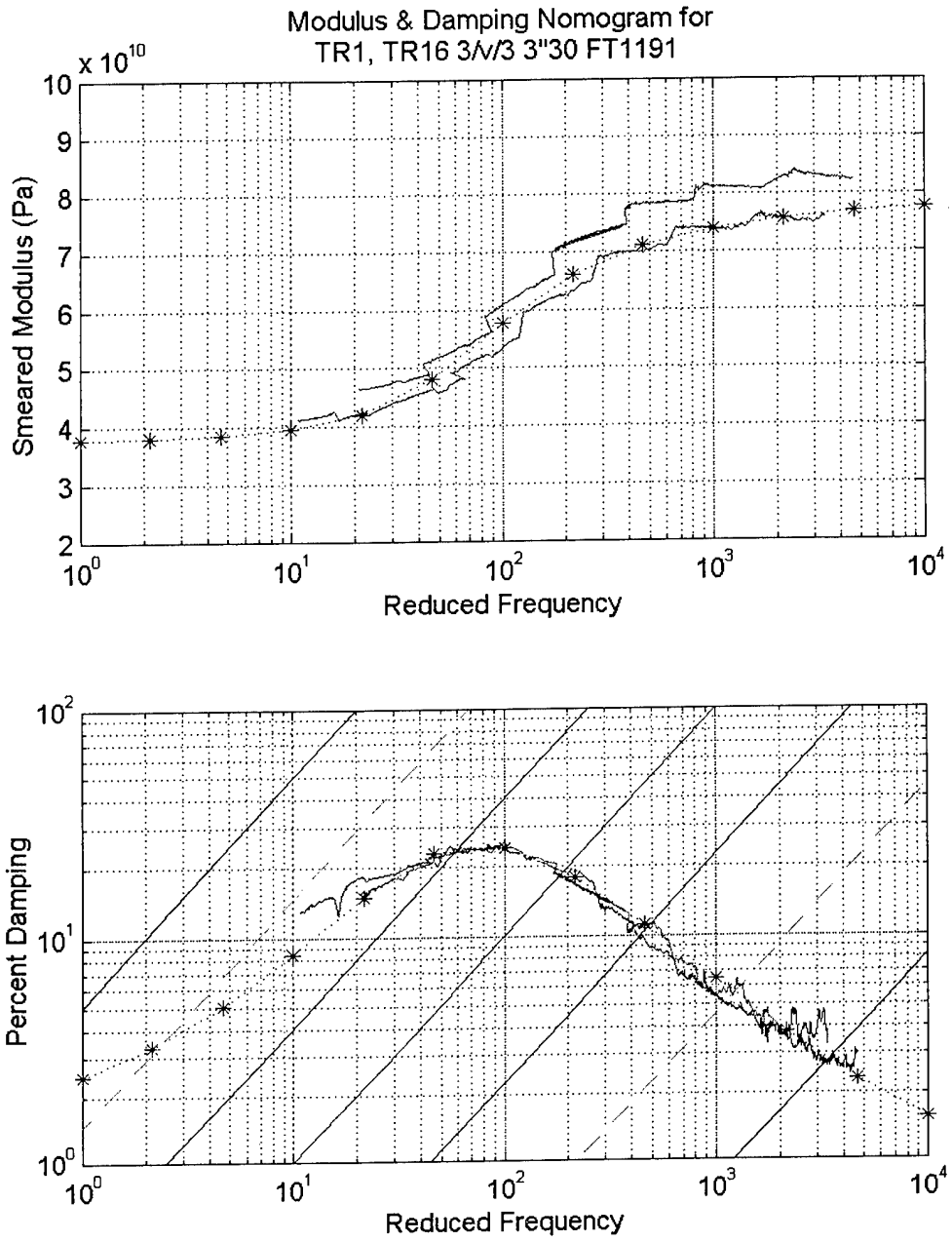

Figure 42: FEA prediction vs. test data for 7.5 cm (3.0 in.) 30° tubes.

Figure 42 shows the test data vs. the FEA prediction for two +3/11m/-3 tubes with 7.6 cm (3.0 in.) 30° wavy layers. The stiffness asymptotes are about 38 and 78GPa. The damping prediction shows no noticeable error, though the test data may diverge at very low frequencies. There is about 10% scatter in the stiffness test data. The peak damping for this 7.6 cm (3.0 in.) 30° tube was 24% at 75 Hz.

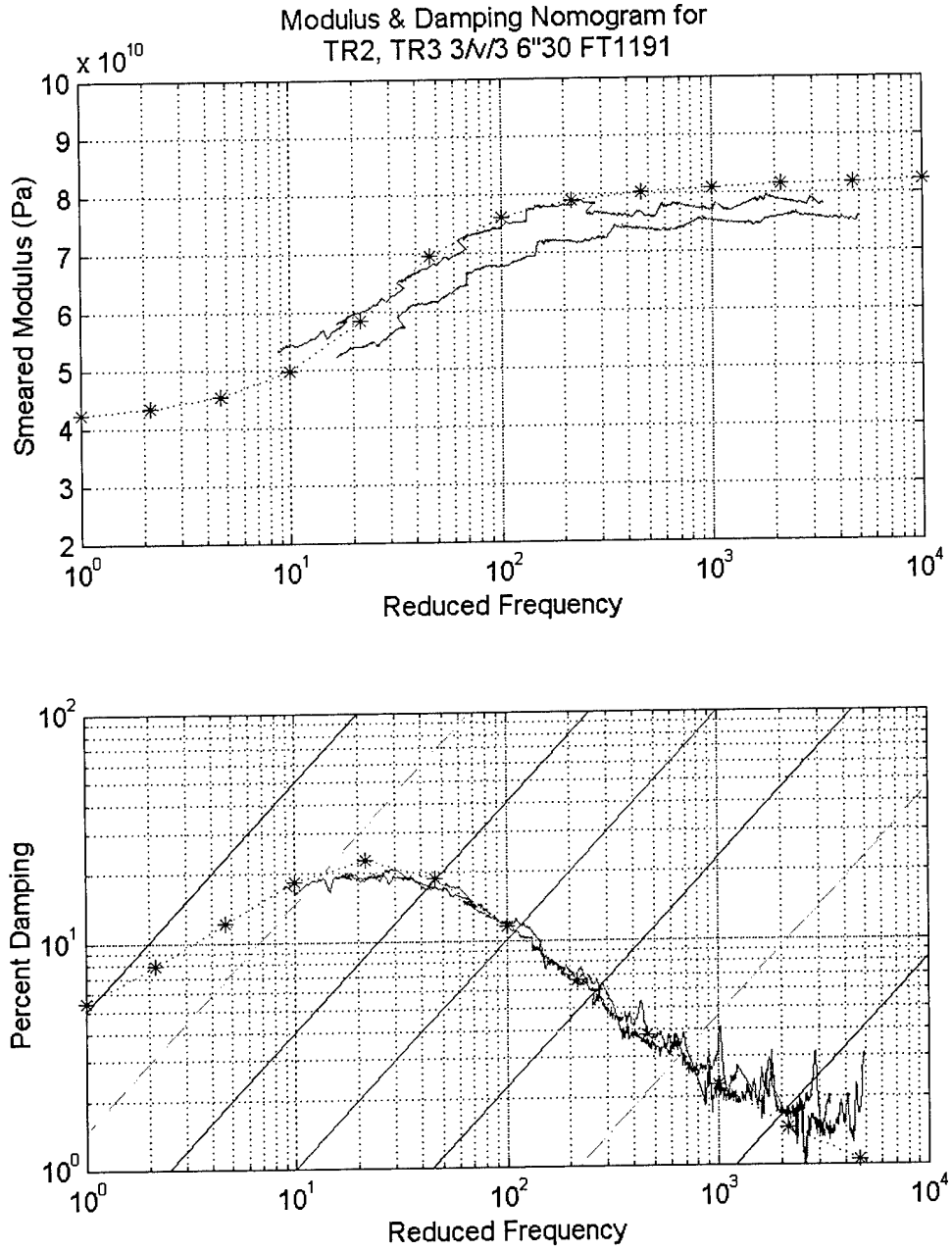

Figure 43: FEA prediction vs. test data for 15 cm (6.0 in.) 30° tubes.

Figure 43 shows the results for two +3/11m/-3 tubes with 15.2 cm (6.0 in.) 30° wavy layers. The stiffness asymptotes are 42 and 82 GPa. The FEA code has over predicted the peak damping slightly, though the error is less than 10%. This 15.2 cm (6.0 in.) 30° tube shows peak damping of 20% at about 21 Hz at 25°C. (This material would be well suited to high temperature or low frequency applications.)

In Figure 43 the actual performance deviates from the model prediction at very high frequencies (low temperatures). In the viscoelastic model the damping is approximated as a simple hump where the damping drops off logarithmically as the frequency increases or decreases from the peak damping frequency. The test performance shows that at very low temperatures the damping begins to fall off more slowly, asymptotically approaching some minimum value.

Note that for all of the 30° waveforms the lower and upper assymptotes on stiffness are approximately 40 and 80 GPa respectively. Thus the wavelength has no significant effect on the stiffness assymptotes. It is interesting that these 30° tubes are significantly stiffer than conventional ±30° unidirectional composite. ±30° tubes tested had stiffness ranging between 35-45 GPa. At very low frequency the wavy composite tubes will have about this stiffness, but at higher frequencies they are twice as stiff.

It is interesting to note that changing the wavelength had little effect on the stiffness asymptotes, though it did affect the frequency at which the stiffness of the composite began to increase. The magnitude of the damping peak didn't change significantly either, though increasing the wavelength did decrease the frequency at which the damping peak occurred. This is the first principle of design with wavy composites: Increasing the wavelength has little effect on stiffness, though it does decrease the frequency at which the damping peak occurs. (This is discussed in more detail in Chapter 6.) Finally, notice that the 7.6 cm (3.0 in.) tube had the highest damping peak (24% at 70-80Hz). The peak damping for the viscoelastic alone occurs at 70 Hz. The peak damping performance for any viscoelastic will be realized when a waveform is used that places the damping peak of the composite-viscoelastic combination on the frequency of the damping peak of the viscoelastic alone.

There was considerable scatter in the stiffness measurements. The average wall thickness of these tubes was about 1.0 mm (0.040 in.) The tube diameter was measured using digital calipers at eight different places along the length of the tube. They were measured while still on the mandrels so that the nominal inside diameter was 22.225 mm (0.8750 in.) The eight measurements were averaged to find the wall thickness. The calipers read to a precision of ± 0.01 mm (0.0005 in.), though in practice they are only accurate to about ± 0.025 mm (0.001 in.) because of differences in pressure from one measurement to the next. Even though all the tubes

were made with the same thickness and width of material, the standard deviation of the wall thickness was 0.036 mm (0.0014 in.), thus statistical analysis tells us that at 95% confidence we expect 5-10% error. For present purposes, the stiffness predictions are adequate. Further experimentation with more accurate measuring devices or thicker walled tubes will confirm that the FEA code has better accuracy than suggested in the previous figures. The results for the thicker walled tubes with less scatter in the test data showed that the FEA code was accurate to 2-5% in the stiffness prediction.

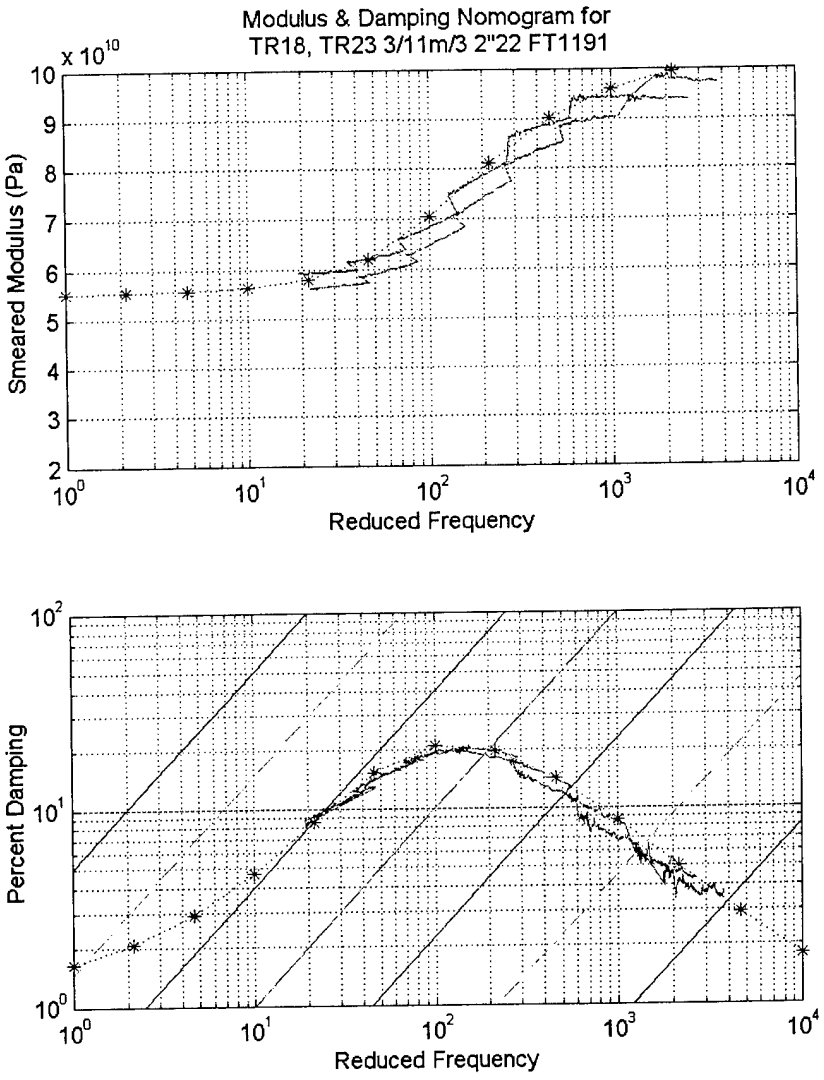

Figure 44: FEA prediction vs. test data for 5.0 cm (2.0 in.) 22° tubes.

The comparisons for the three tubes shown above validate that the code adequately models changes in wavelength with constant layer thickness. Agreement was also excellent for

the 5.0 cm (2.0 in.), 10.0 cm (4.0 in.) and (12.5 cm (5.0 in.) tubes (See the Appendix for figures.) Figure 40 through Figure 43 have shown that the FEA code accurately models changes in wavelength. Tests were also performed varying the max angle of the wavy composite from the 30° baseline.

Figure 44 shows the stiffness and damping results for two +3/11m/-3 tubes made with 5.0 cm (2.0 in.) 22° wavy material. The damping prediction is highly accurate, while once again there is considerable scatter in the stiffness data. This material has a damping peak of 20% at about 130 Hz. Note that by decreasing the max angle from 30° to 22° the stiffness asymptotes increase from 40 and 80 GPa to 55 and 100 GPa. The stiffness has increased by 25-40%, though the damping is still exceptional. (The 5.0 cm (2.0 in.) 30° tubes tested had 24% peak damping, thus the damping has decreased by 20%, though it is still exceptional.) The test results for other 22° tubes are found in the Appendix. These results conclude that the FEA code accurately models changes in max angle.

Another important design parameter is the layer thickness. A number of 3.75 cm (1.5 in.) 30° tubes were constructed using a number of layer thickness combinations. The following figures show the result when the layer thickness is varied.

Figure 45 shows the results when the thickness of the composite layers is increased. Two 3.75 cm (1.5 in.) 30° tubes were tested with 0.76 mm (0.030 in.) thick face sheets and the same 0.28 mm (0.011 in.) viscoelastic thickness used in the tubes seen previously. The damping peak is about 17% at 450 Hz. The lower stiffness asymptote is unchanged. The test data does not show the upper asymptote, though it appears that it will be 70-80 GPa. There is no noticeable error in the stiffness prediction, though the damping prediction is off by a few percent at low frequencies. Doubling the composite layer thickness has almost doubled the frequency at which the damping peak occurs (This will also be discussed in more detail in Chapter 6). The magnitude of the damping peak has decreased from 23 % to 17%.

Note that for this double thick tube there was very little scatter in the stiffness results. The FEA code predicts the stiffness very accurately. For this tube the error in measurement only represents 2-5% of the wall thickness. This suggests that the FEA code is actually accurate to 2-5% when predicting stiffness. Further testing with thick-walled tubes will continue to confirm the accuracy of the FEA code in predicting the material stiffness.

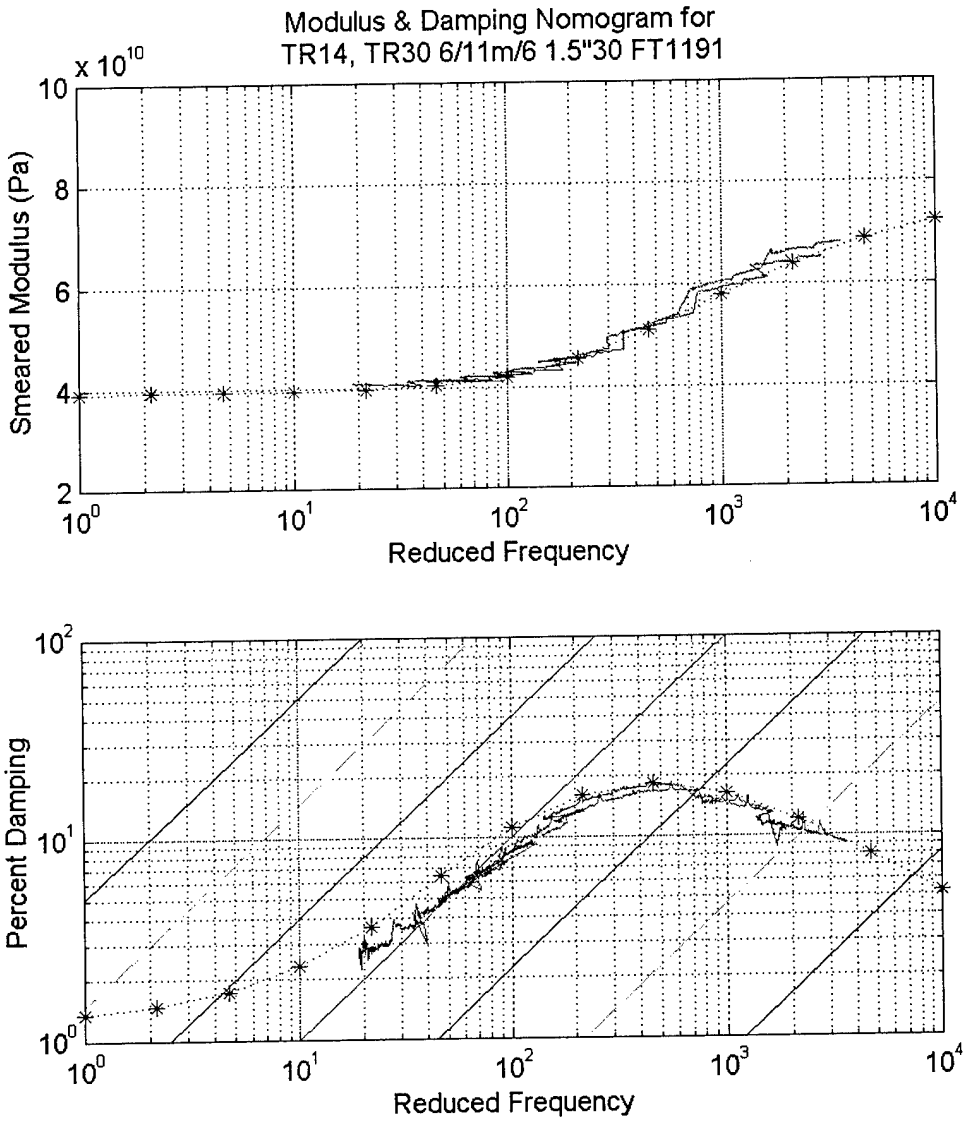

Figure 45: FEA prediction vs. test data for double-thick composite tubes.

Figure 46 and Figure 47 show the performance of the FEA code when the viscoelastic layer thickness is varied, while the composite layer thickness is constant at 0.38 mm (0.015 inches.)

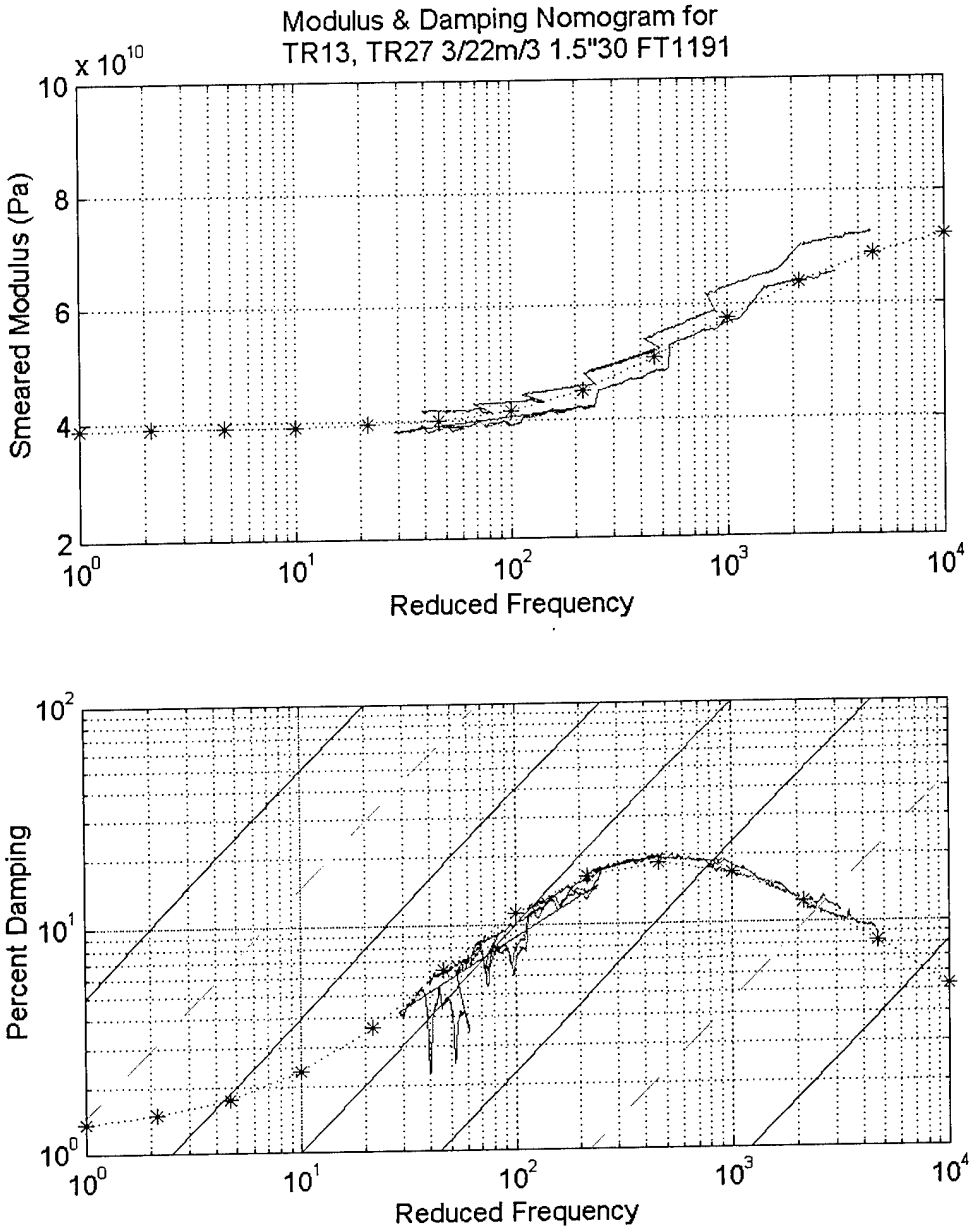

Figure 46: FEA prediction vs. test data with 0.56 mm (0.022 in.) thick viscoelastic layer.

Figure 46 shows the results for two +3/22m/-3 tubes constructed with 3.8 cm (1.5 in.) 30° wavy composite. Once again the stiffness asymptotes are 40 and 80 GPa. The magnitude of the damping peak has decrease slightly from 24% to 20%. The frequency of the damping peak has increased from 230 Hz to 450 Hz. It is interesting to note that increasing the thickness of the viscoelastic layer has the same effect as increasing the thickness of the composite layer. If high

frequency performance is desired, it is more efficient to increase the thickness of the viscoelastic layer rather than increasing the thickness of the composite layer since less weight is added when the viscoelastic layer thickness is increased. (The baseline +3/11m/-3 tubes averaged 106 g/m. The +6/11m/-6 weighed 196 g/m, an increase of 85%, while the +3/22m/-3 tubes weighed only 127 g/m increasing the weight by 20%.) The +3/22m/-3 tubes also had higher damping than the +6/11m/-6 tubes (20% vs. 17%). Figure 45 and Figure 46 show that the model performs very well when the thickness of the composite or the viscoelastic is doubled.

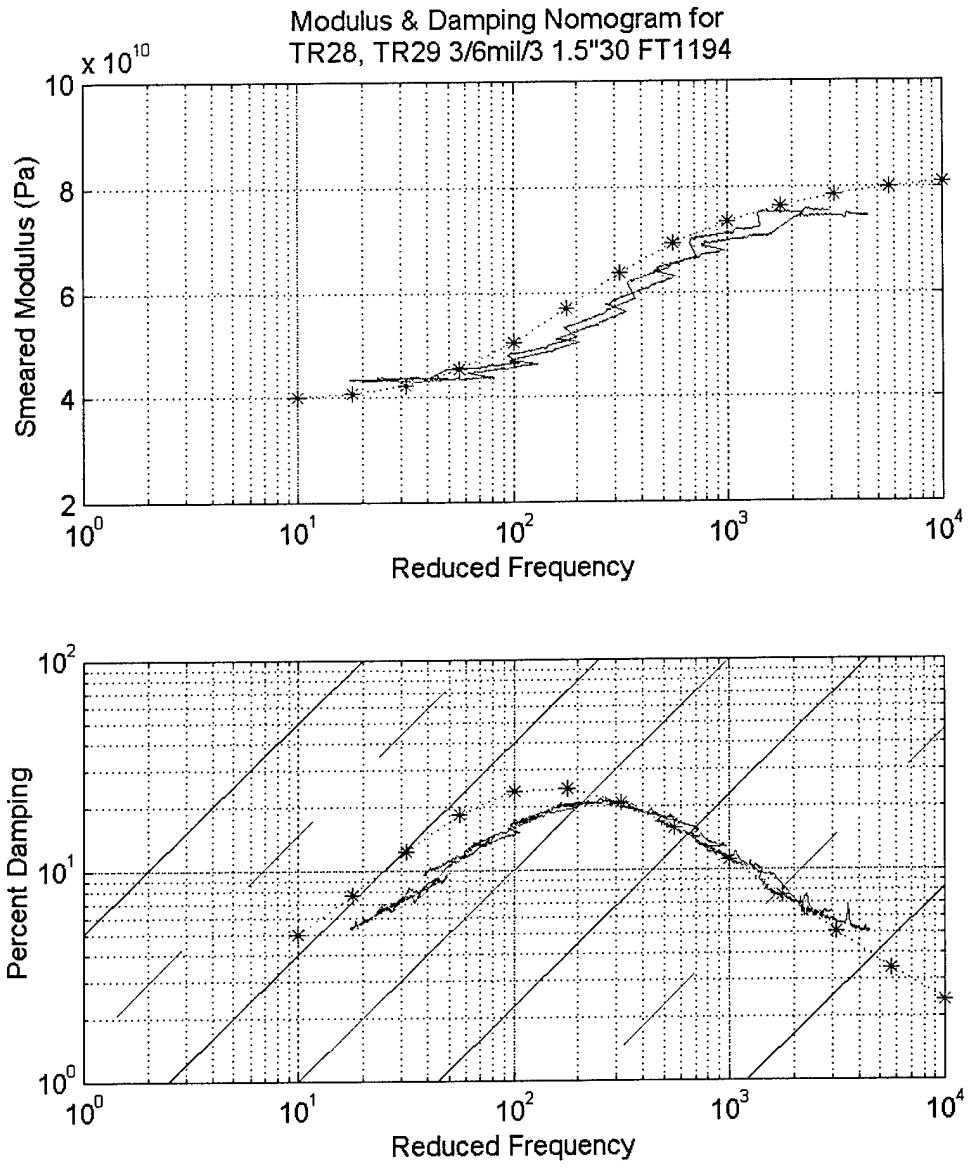

Figure 47: FEA prediction vs. test data for 0.15 mm (0.006 in.) thick viscoelastic layer.

Tubes were also constructed with a viscoelastic layer that was approximately half as thick (0.15 mm, 0.006 in.). Figure 47 shows the FEA prediction overlaid on the test data for these tubes. Figure 47 shows the result when the viscoelastic thickness if halved (0.15 mm, 0.006 in. thick). The FEA code predicts higher than observed damping for the +3/6m/-3, 3.75 cm (1.5 in.) 30° tube. Once again the stiffness asymptotes are 40 and 80 GPa. The test data shows a damping peak of 21% at 230 Hz, while the FEA model predicts 23% damping at 130 Hz. The stiffness prediction is still accurate to within 10%, though the FEA model predicts the transition at a lower frequency. There are a number of possible explanations for the phenomena observed above.

First, the interface between the viscoelastic and the composite is very rough, with the composite mixing with the viscoelastic as much as 0.05 mm (0.002 in.) on each side.

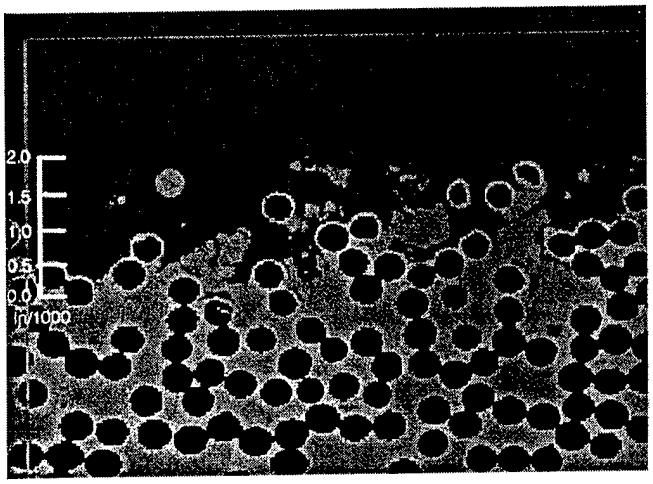

Figure 48: Optical microscope image of viscoelastic-composite interface.

The diameter of the individual carbon-fiber strands is about 7 micron (0.0003 in.) In Figure 48 we see that the ragged interface between the composite and the viscoelastic occupies about 4-5 diameters, 28-35 micron (0.0011 in. - 0.0014 in.) The discrepancies seen in Figure 47 are probably due in part to increased stiffness in the viscoelastic layer due to this ragged interface. In the other tubes, the interface thickness represents a smaller percentage of the total viscoelastic thickness, and the affect of the interface is diminished.

Also, a 0.15 mm (0.006 in.) viscoelastic was not available when these tubes were built, so they were constructed with three layers of 0.05 mm (0.002 in.) material. The 0.05 mm thick material was very difficult to work with, resulting in wrinkling and bubbling of the viscoelastic. This may also contribute to the deviation from ideal performance. The FEA code has predicted

the performance of tubes with 0.20 mm (0.008 in.) viscoelastic very accurately, though experience has shown that we must then be cautious when analyzing laminates where the viscoelastic is thinner than 0.20 mm (0.008 in.)

Figure 44 through Figure 46 show that the FEA model accurately predicts changes in the thickness of the composite or viscoelastic layers, as long as the viscoelastic is sufficiently thick.

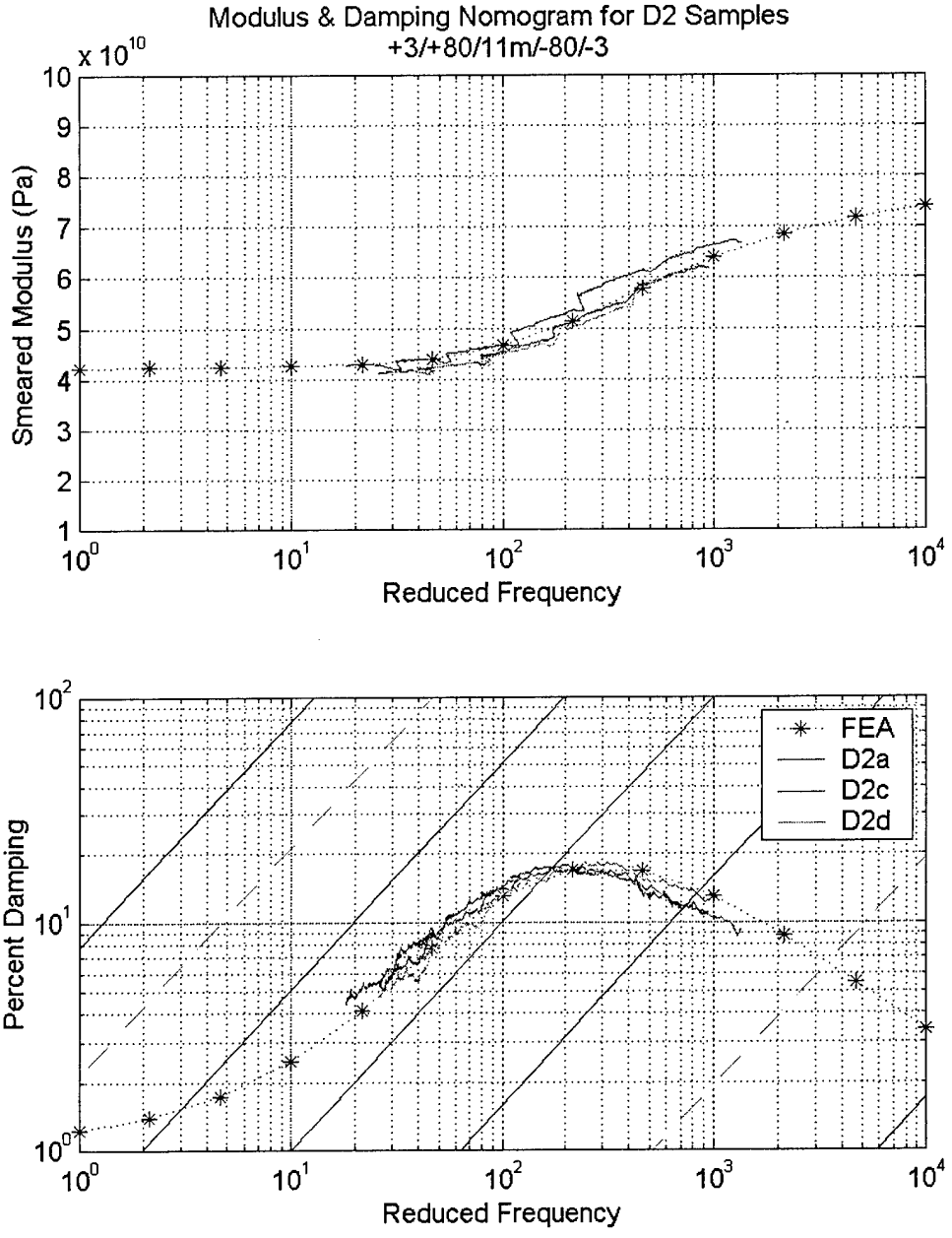

Figure 49: Stiffness and Damping results for +3/+80/11m/-80/-3 tubes.

A few tubes have been built and tested using more complicated lay-ups. As an example, a tube similar to those described previously was constructed where an extra layer of unidirectional material was wrapped on either side of the viscoelastic at about 80°. We will call this a +3/+80/11m/-80/-3 where the "+80" and "-80" represent a single extra layer at ±80°.

Figure 49 shows the results for three +3/+80/11m/-80/-3 tubes (D2a, D2c, D2d) made with 3.75 cm (1.5 in.) 26° composite. The addition of two 80° unidirectional layers has decreased the damping by a few percent. The FEA model prediction is within about 5% on both stiffness and damping. Future tests will further confirm the accuracy of the code with more complex lay-ups.

5.4. SUMMARY

This chapter has shown that the finite element code accurately models changes in waveform, max angle, and layer thickness. Though the test data shows some scatter, the FEA code has been shown to be accurate to 5% for predicting stiffness in tubes tested in the axial mode. The damping results are even more reliable, typically accurate within 2%, except when the viscoelastic thickness falls below 0.20 mm (0.008 in.)

CHAPTER 6: DESIGNING PRACTICAL STRUCTURES

6.1. THE VALUE OF MATERIAL DAMPING

Often we are asked, "what does damping do, how does it benefit aerospace applications?" While most engineers can tell you in general terms what damping does, few have experience either in designing with damped materials or assessing the impact of damping on "system performance". Probably the biggest reason for this lack of understanding is that practical material based damping has been unavailable. Most FEA codes do a very good job at estimating stiffness of a structure and mass-stiffness dynamics. Few FEA codes address damping adequately, and none can model the magnitude and characteristic damping offered by this new material (Pratt 1999).

When faced with an undamped resonant problem, the typical structural engineer will "make it stiffer". If this solution is possible and there is design latitude, it may in fact solve the immediate single frequency problem. Suppose the problem is more complex, i.e. the offending frequencies are broadband, or the dynamics of the structure change over time? In this case, simply modifying the stiffness (or mass) of the structure may not provide either a practical or a robust solution to the problem.

As will be seen in this chapter, the most efficient solution to a dynamic structural problem is to use a material that provides tailorable damping.

Aerospace vehicles can benefit from high damping in five major ways.

- Reduced settling times of vehicle vibrations, cantilevered antennas, mirrors, etc.,
- Control of vehicle resonance modes, "pogo effect",
- Reduced stress and strain amplitudes,
- Increased service life for airframes, avionics, and other sensitive equipment,
- And improved acoustic protection through the use of damped panels.

6.1.1. A new material paradigm

Wavy composite is unique and unparalleled in performance in that it exhibits both high damping and stiffness; no other material can do what this material can do. Standard graphite pre-preg (unidirectional) has a strong direction stiffness of about 137 GPa and damping of only 1 or 2 tenths of a percent. If a sample is made with fibers in two or more directions, the equivalent stiffness in any one direction will be considerably less than the strong direction value. Thus in

most cases the stiffness of a practical structure made from these materials will only rival that of aluminum, but the advantage of composite is that it has less than half the weight of aluminum. Hence its popularity. Wavy composite has comparable stiffness but considerably greater damping than either aluminum or conventional composite. Performance of wavy composite made with standard modulus fibers is comparable in stiffness to aluminum or conventional composite structures but damping can be as high as 30%. Using a stiffer fiber increases both stiffness and damping.

Table 8: Performance comparisons

Material (waveform)	Stiffness (GPa)	Damping (%)	Density (g/cc)
Std Graphite (3" 15°)	108*	15*	1.1
Std Graphite (3" 20°)	92*	21*	1.1
Std Graphite (3" 25°)	72*	25*	1.1
HiMod Graphite (3" 14°)	229*	32*	1.1
HiMod Graphite (3" 18°)	175*	38*	1.1
HiMod Graphite (3" 22°)	133*	42*	1.1
Aluminum	68	.1-.2	2.7
Titanium	110	.1-.2	4.5
Steel	203	.001-.01	7.4

* Stiffness at peak damping shown

Table 1 summarizes actual performance of wavy composite made from standard modulus Grafil 34-700 fiber and FEA projections for a high modulus wavy laminate made from a Mitsubishi Chemical fiber (K13710) that has been successfully used in the recent past, compared to aluminum, titanium, and steel. Note that it is now possible to have a standard graphite structure that rivals aluminum and titanium for stiffness but far exceeds both in damping performance with less than half the weight of aluminum and one-fourth the weight of titanium. With the use of stiffer fibers it is possible to create a laminate that exceeds the stiffness of steel, with thousands of times the damping and a fraction of the weight.

6.1.2. Settling times and space structures

Most structural materials have no or very low damping. When a space vehicle is perturbed by a course change, the structure will have a tendency to vibrate at its natural vibration modes for a considerable time especially in the vacuum of space where air damping is no longer a factor. **Figure 3** shows the effect of damping on settling time for two cantilevered tubular composite beams, one made from wavy composite with approximately 12% damping, and an

undamped tube of equivalent mass and stiffness with less than 1% damping. It should be noted that the settling time of the undamped tube is approximately 16 seconds in the lab, where air damping also effects the results. In space, the same tube would likely ring much longer. However, damping in the wavy tubular beam is unaffected by a change in environment since its damping properties are a characteristic of the material and air damping is only a very small fraction of the system damping.

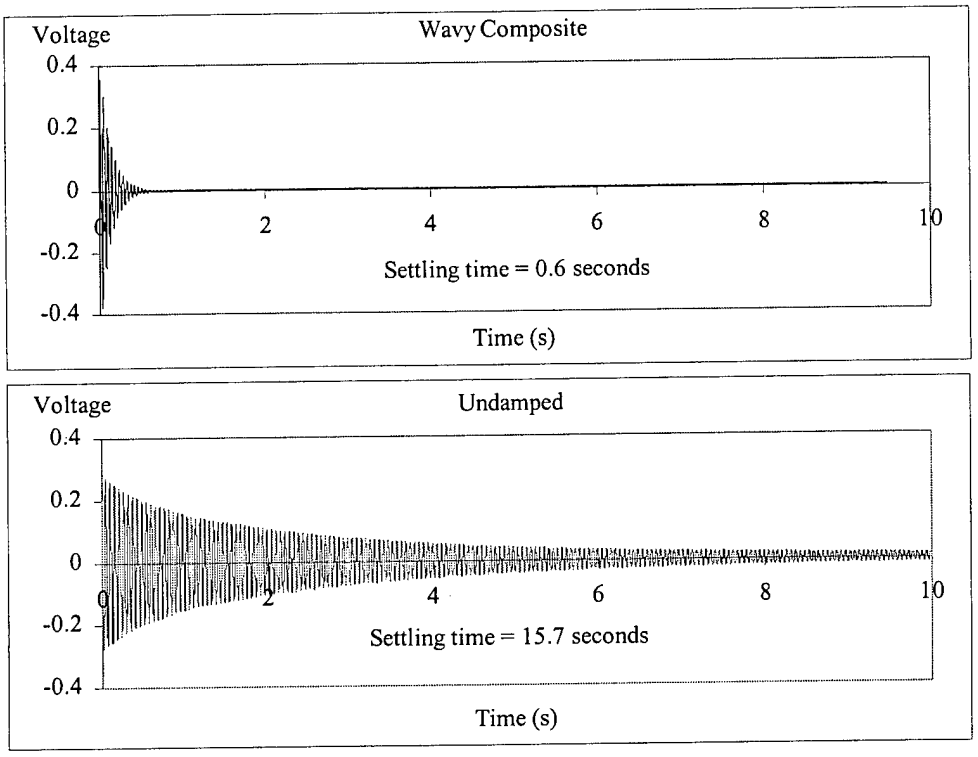

Figure 50: Actual settling time of two tubular beams, damped wavy vs. undamped

Settling time can be defined as the amount of time it takes for a structure's vibration amplitudes to be reduced to 1% of its initial value after being perturbed. As can be seen in Equation 1, settling time is inversely proportional to the product of damping (η) and natural resonant frequency (f_n). Since resonant frequency is proportional to the square root of stiffness (K) divided by mass (M) as shown, there are at least three ways an engineer can reduce settling time: increasing damping, increasing stiffness or reducing mass.

$$t_s = \frac{4.6}{\eta \pi f_n} \approx \frac{9.2}{\eta}\sqrt{\frac{M}{K}} \qquad \text{Eqn. 35}$$

Decreasing mass or increasing stiffness to raise the resonant frequency is simple in concept but often difficult to achieve, especially when design requirements dictate size

constraints, interface requirements, and structural properties. In short, there may be little design latitude to change the design. For every doubling of stiffness or halving of mass, there is only a 30% reduction in settling time. However, for every doubling of damping there is a 50% reduction in settling time. Thus it is more efficient to reduce settling time by the addition of damping.

The damped wavy composite tube shows a 96% reduction in settling time over the undamped tube. To get the same performance out of undamped composite, the designer would have to increase stiffness by a factor of 684 times, *if* there was no increase in mass. For example, if a baseline damped structure was 2.5 cm in diameter, the undamped version would have to be 20.3 cm inches in diameter to have the same settling time, with no additional material. While it is true that a structure that is 684 times more stiff will not deflect the same amount for a given load, the settling time for an initial deflection will remain unchanged. Only the magnitude of the deflection will be different. Suppose we approach the problem from a equivalent deflection point of view. If we make the deflection of both the damped 2.5 cm diameter tube and the stiffer undamped tube the same value at the same point in time (the settling time for the damped tube for example), the stiffness of the undamped tube need not be 684 times greater. In this case the structure only has to be 84 times stiffer or using our example the undamped tube diameter would have to be increased from 2.5 cm to 11 cm, again with no additional material.

The bottom line: Obviously, damping is a much more efficient way of getting a stable structure.

6.1.3. Vibration control and the pogo effect

Figure 51 illustrates what happens when the frequency of the driving force is close to the natural resonance of a structure. At very low frequencies (in this example 100-300 Hz) there is a one-for-one relationship between the driving amplitude (input side) and the free response of the output. As the driving frequency of the input approaches the natural resonance of the structure, the ratio of output to input is amplified until at resonance the output of the free end reaches its maximum. In the case of an undamped structure shown in Figure 51, the resonance magnitude can reach extremely high levels where an input of ± 1 is amplified 144 times. The damped wavy structure will limit amplification to 6 times the input.

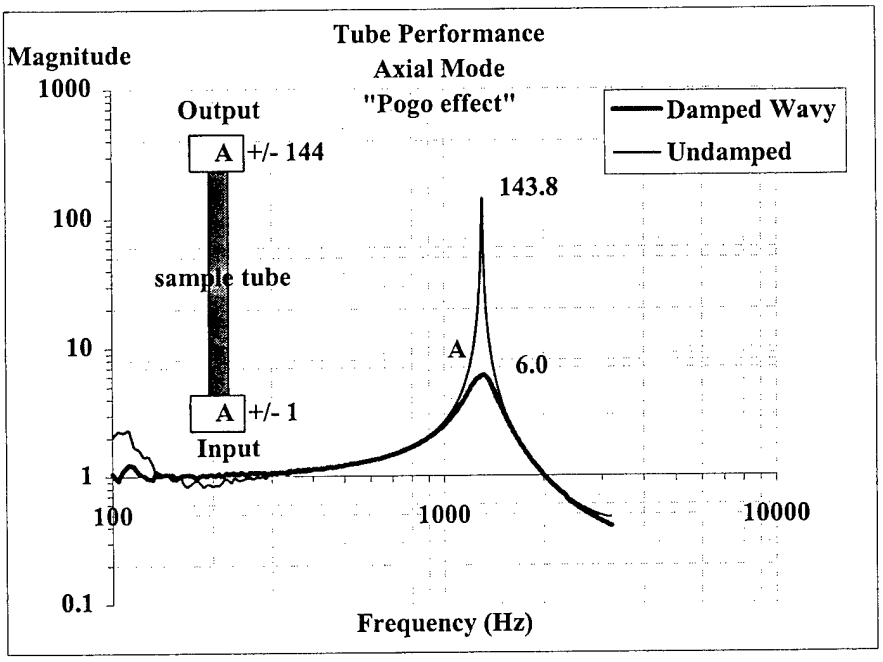

Figure 51: Actual vibration magnification or "Pogo effect" in wavy damped vs. undamped tubes excited in the axial mode.

This is known as the "pogo effect", an expression that was coined by the aerospace community to describe how unacceptable g-forces were showing up in the payload of rockets during launch. It happened on the Apollo 6 mission, and was a constant problem with the Titan rocket. Using the example in Figure 51, if fluctuation in the rocket motor caused just a $1/10^{th}$ "g" force at the resonant frequency, the payload would experience a 14^{+} "g" fluctuating force during the launch. If, however, the rocket had been made from wavy composites, the fluctuating g-forces on the payload would be limited to a maximum of 0.6 g's. Use of damped wavy composites would prevent catastrophic failure.

6.1.4. Sound attenuation

Test panels were made to optimize damping at the first bending mode of the panel (180 Hz). An undamped panel was made with equivalent stiffness and weight to provide an accurate comparison of performance. The results are shown below.

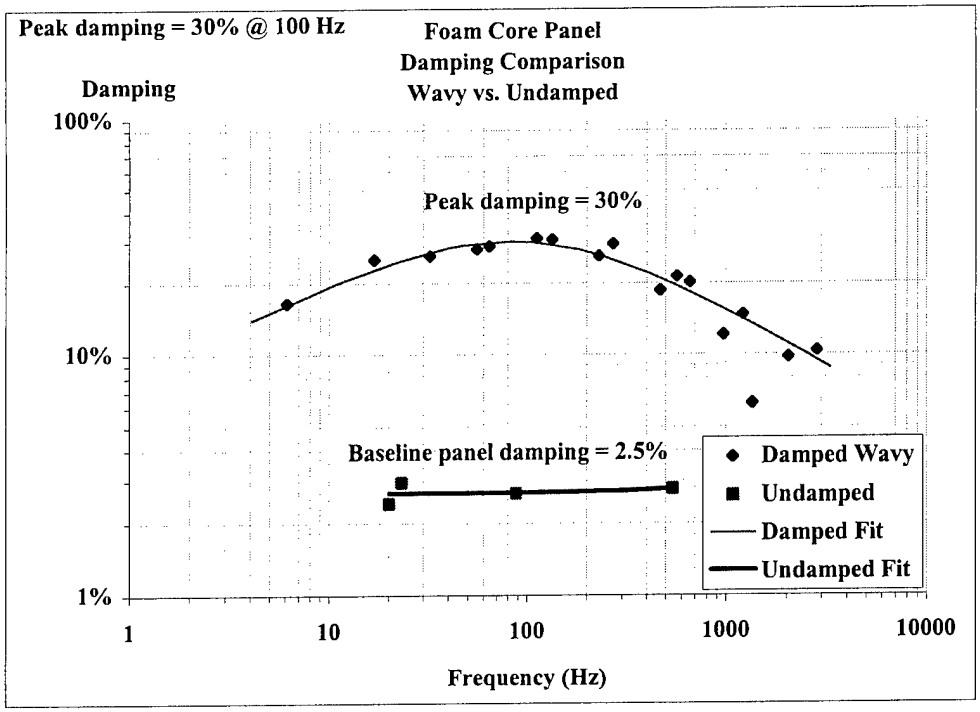

Figure 52: Test data showing damping measurements of wavy damped panel vs. equivalent undamped panel.

The damping of the wavy composite panel peaks at 30% (for reference critical damping is 100%) at about 100 Hz. In contrast, the undamped baseline panel averaged only 2.5% damping. It should be noted that this performance was accomplished with standard modulus pre-preg materials. Both higher damping *and* stiffness can be expected if high modulus fibers are used in the wavy pre-preg skins. Additionally, these results were obtained with a relatively weak foam core structure. Increasing the section modulus and using AFRL's grid stiffened concept is likely to further improve both stiffness and damping.

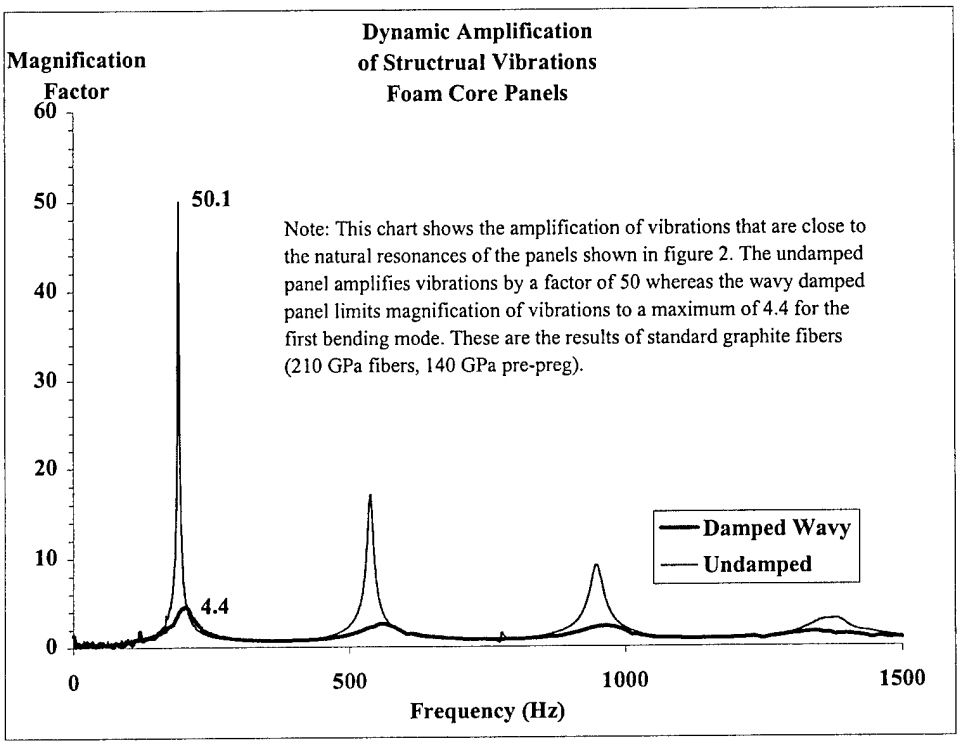

Figure 53: Amplification of vibrations, wavy damped vs. undamped foam core panels.

This level of damping translates into a much more dynamically stiff structure (from the effects of high damping) as shown in Figure 53 where the transfer function between the driving force and the free vibrations of the structure are amplified at or near resonance. The undamped panel amplifies the driving force by a factor of 50 whereas the wavy damped panel limits amplification to 5 or less for the first bending mode. Frequencies close to a natural resonance should be avoided whenever possible but more often than not, driving frequencies are not easily controlled. For example, the driving frequencies on a launch vehicle are caused by fluctuations of the rocket or exhaust rumble and can be classified as low frequency and broadband in nature. Avoidance of an overlay between the first bending modes of the structure and the frequency rich nature of the launch may be impossible. This means that amplified vibrations and acoustic energy will reach the payload and/or guidance system. Without damping, the results could be catastrophic.

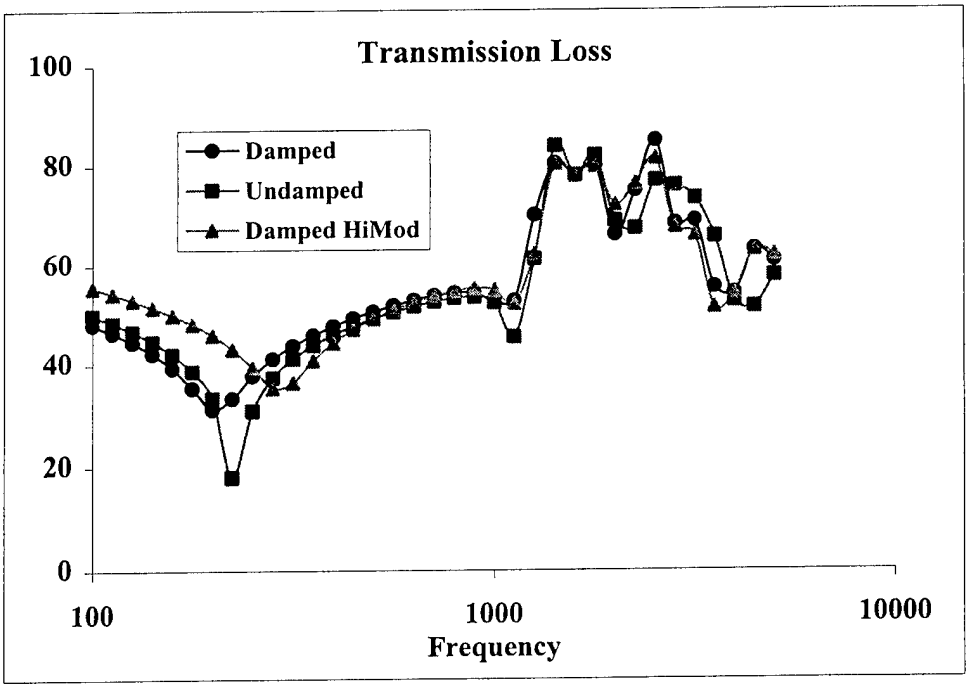

Figure 54: Projected transmission loss comparison, undamped vs. damped foam core panels made with standard graphite pre-preg and projections for high modulus wavy composite.

Figure 54 shows the effects of inherent damping on the transmission loss in three example panels. This information was derived from finite element analysis accomplished with Patterned Fiber Composites, Inc.'s FEA program. This analysis assumed only 20% peak damping instead of the measured 30% shown in Figure 52. Even so, the result is a predicted 20 dB greater transmission loss near the resonant frequency than available from an equivalent undamped panel.

6.2. DESIGNING WITH WAVY COMPOSITES, BASIC CONCEPTS

The figures shown in this section are model predictions generated by software developed by Patterned Fiber Composites, Inc. and verified experimentally by testing. Except where noted, all model results represent the axial stiffness and damping performance of damped wavy composite tubes fabricated from pre-preg made from Grafil 34-700 carbon fiber and a sports resin system, with a 60% ±1% fiber volume fraction. All waveforms used in this analysis were simple sinusoids defined by wavelength and maximum angle.

6.2.1. Assumptions

The FEA model has been shown to give very good experimental correlation (less than 5% error as discussed in Chapters 4 and 5) and is based on the following assumptions.

- Inherent damping and stiffness in the composite facesheet are independent of temperature and frequency over the useable range of the viscoelastic material (Adams et al. 1969). This was experimentally verified using unidirectional pre-preg made at the same time as the wavy composite material used in the fabrication of all samples. Typical values for damping in the fiber direction were 0.1 to 0.2 percent.
- Linearly elastic modeling of stiffness and damping; small strain assumption. The assumption of small strains is used i.e. strain will be less than 1-2%. Strain greater than this usually involves failure in composites. This has shown to give very good agreement between model and actual test results (Pratt et al. 2001).

6.2.2. Basic Concepts

The following paragraphs detail the most important concepts that must be understood to execute good designs with wavy composites. They are:

- The viscoelastic layer dominates the damping and stiffness performance of a wavy composite combination. As a result, all the concepts that apply for a linear viscoelastic material apply to the combination of wavy composite and viscoelastic material, namely:

1. Wavy composites exhibit glass transitional properties, i.e. there are defined asymptotic values for stiffness, and a defined damping peak as a function of temperature and frequency.
2. Frequency-temperature superposition, i.e. a change in temperature is equivalent to a change in frequency (Ferry 1980).
3. Viscoelasticity, i.e. damping can be approximated by factoring the modulus or stiffness of a material.

- Damping and stiffness in wavy composites can be tailored to the dynamics of the structure. Although the wavelength, maximum angle, thickness ratios of constraining to constrained layer, fiber type, and temperature, all combine to effect the location

and magnitude of the damping peak (and the stiffness). In general, the following is true for a given wavy composite-viscoelastic combination at a constant temperature:

1. The frequency of peak damping in a wavy composite structure is primarily driven by the wavelength.
2. The magnitude of the damping peak and the stiffness are driven by the maximum angle of the waveform.

It should be noted that the stiffness reported is based on the equivalent axial stiffness (stiffness in the strong direction) of load bearing material without the viscoelastic, i.e. stiffness does not include the volume of the viscoelastic material. This is normal for conventional constrained layer damping where the constraining layers of dead soft aluminum and viscoelastic adhesive are not considered in the determination of stiffness of the structure. This is done to provide a basis for comparison of the material characteristics of the composite.

6.2.2.1. Characteristics of wavy composites

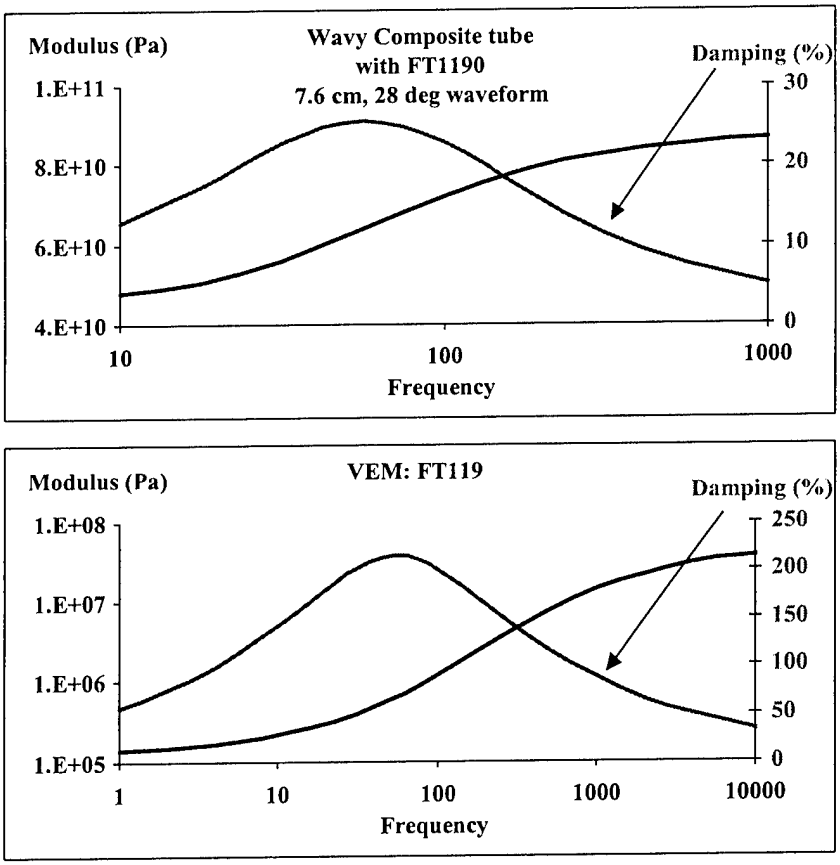

Figure 55: Modulus and damping of wavy composite tube made with FT1190 VEM (upper chart) compared with FT1190 series viscoelastic properties at 25° C (lower chart).

The viscoelastic layer dominates the damping and stiffness performance of a wavy composite combination. Comparison of the modulus and damping of the wavy composite – viscoelastic combination in Figure 55 (upper chart) and the viscoelastic (only) in Figure 55 (lower chart) shows the shape of the curves to be similar in every respect.

As is typical for a viscoelastic material, for wavy composite combinations there is a defined damping peak that coincides with the glass transition temperature of the material, and a shear modulus that has a lower and upper asymptote.

6.2.2.2. The effect of wavelength

While the performance of wavy composite is dependent on the properties of the viscoelastic used, the ability to change the stiffness and damping response of the structure by varying the waveform gives the designer significant latitude to pursue optimal designs. For example, the charts in Figure 56 and Figure 57 (room temperature response), show the damping and modulus for five different wavelengths where thickness, and maximum angle (of the sinusoidal waveform) are held constant.

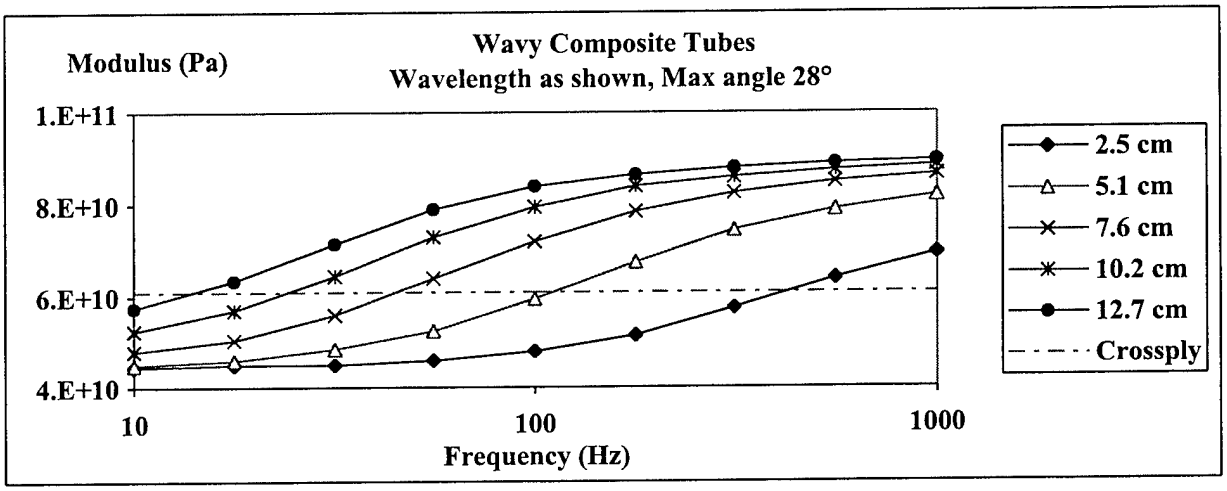

Figure 56: Equivalent axial modulus for carbon fiber wavy composite – viscoelastic tube.

The curves shown in Figure 56 represent the equivalent axial modulus as a function of frequency at room temperature. As can be seen, there are asymptotic values for the modulus of the wavy composite–viscoelastic structure that are attributable to the stiffness characteristics of the viscoelastic material. For reference, the stiffness of aluminum is approximately 68 GPa; the 0 degree properties for carbon composite material is 180 GPa; and a unidirectional crossply lay-up

(shown as "Crossply" on both figures) of the same maximum angle would have a stiffness of 61 GPa but damping of only 1.5%.

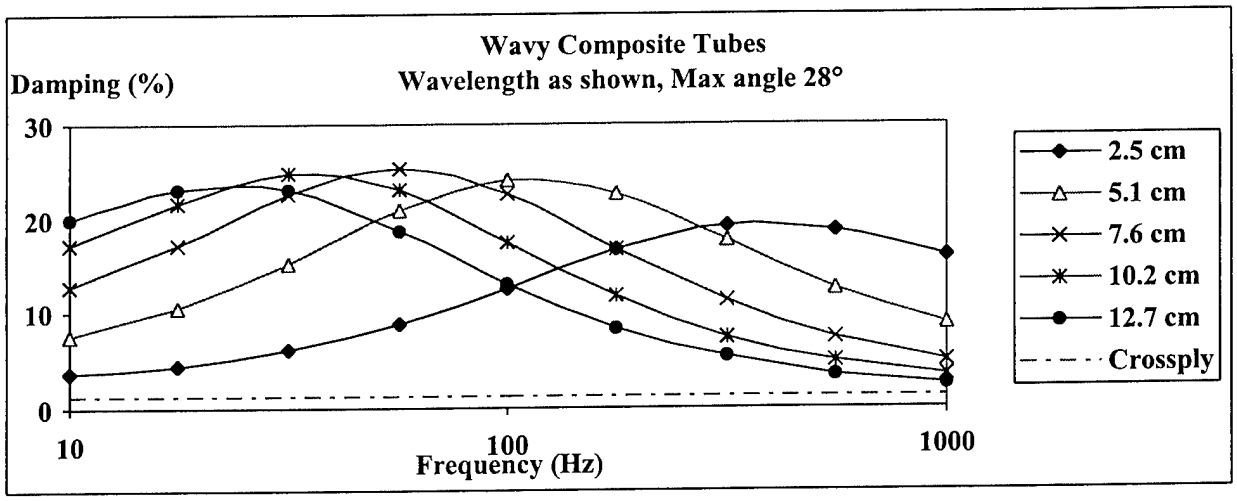

Figure 57: Damping (%) performance for carbon fiber wavy composite – viscoelastic tube.

Note in Figure 57 that the damping peak varies for the different waveforms and like the modulus, mirrors the shape of the viscoelastic material in every case. In Figure 57, the 7.6 cm period waveform produces the highest damping at the frequency (60 hertz) that coincides with the peak damping frequency of the viscoelastic. The fact that damping peaks for the 2.5, 5.1, 10.2, and 12.7 cm waveforms are lower than the 7.6 cm waveform is probably due to a less than optimal combination of viscoelastic modulus and loss factor. Despite this, appropriate selection of wave period can still provide high damping and provides greater design flexibility.

Using both figures, the designer has the option to maximize damping, or optimize the stiffness of the structure for a certain frequency band of interest by changing the wavelength of the sinusoidal wave. For example, if the frequency band of interest lies between 100 and 1000 hertz, the designer could select a waveform with a period of from 2.5 to 5.1 cm depending on the stiffness and damping desired. A 5.1 cm waveform would give a stiffer response and provide greater damping at lower frequencies. Thus the following is true:

Design principle 1: For a given temperature, the wavelength of a wavy composite structure determines the frequency of the damping peak.

6.2.2.3. The effect of waveform angle

In a sinusoidal waveform, a change in angle will alter both the stiffness and damping. Figure 58 shows the effects of varying the maximum angle of the sinusoid for a sample tube made from standard graphite fiber wavy composite with a 7.6 cm wave period. If stiffness is emphasized more than damping, the designer can decrease the maximum angle and dramatically improve the stiffness of the wavy composite. For reference, the stiffness of aluminum would be 68 GPa, and titanium would be 110 GPa. Thus, it is possible to use a 20° - 7.6 cm sinusoidal pattern to create a capable substitute for aluminum with orders of magnitude greater damping. Figure 58 only represents one of the waveforms shown in Figure 56 and Figure 57. Changing the maximum angle and wave period provides the designer with the ability to optimize the structural response for a wide variety of conditions.

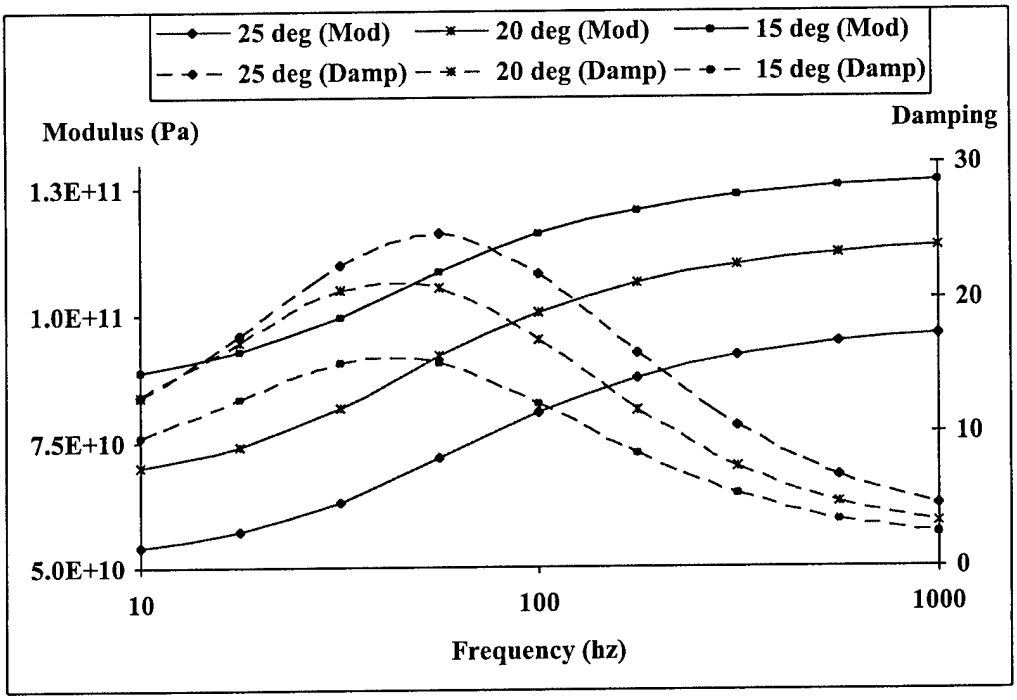

Figure 58: Effects of a change in angle for a sinusoidal waveform of a 7.6 cm wavelength.

Design principle 2: For a given temperature, the maximum angle of the waveform determines the magnitude of damping and stiffness for a given viscoelastic material.

Although not shown, nomograph charts can be used to predict the performance of this material combination at different temperatures as is typically done for viscoelastic materials. The

x-axis represents not only the frequency scale at room temperature but also represents the reduced frequency scale of a frequency-temperature nomograph. To complete the chart as a nomograph, the designer would have to add another frequency scale on the vertical axis and isothermal lines using the WLF or Arrhenius equations (Ferry 1980). Similar charts can be generated for the effects of amplitude-to-wavelength ratio (or maximum angle in the case of a sinusoidal waveform), thickness ratios, in nomograph form. The following illustrates the principle of time-temperature superposition.

6.2.2.4. Temperature shift and time-temperature superposition

Figure 59 shows the frequency shift of the stiffness curve due to changes in temperatures for a given waveform. The principle of polymer frequency-temperature superposition states that a shift in frequency is equivalent to a shift in temperature and is the method by which a master curve or nomograph is obtained (Ferry 1980). This principle is true for wavy composites made with polymer viscoelastic layers.

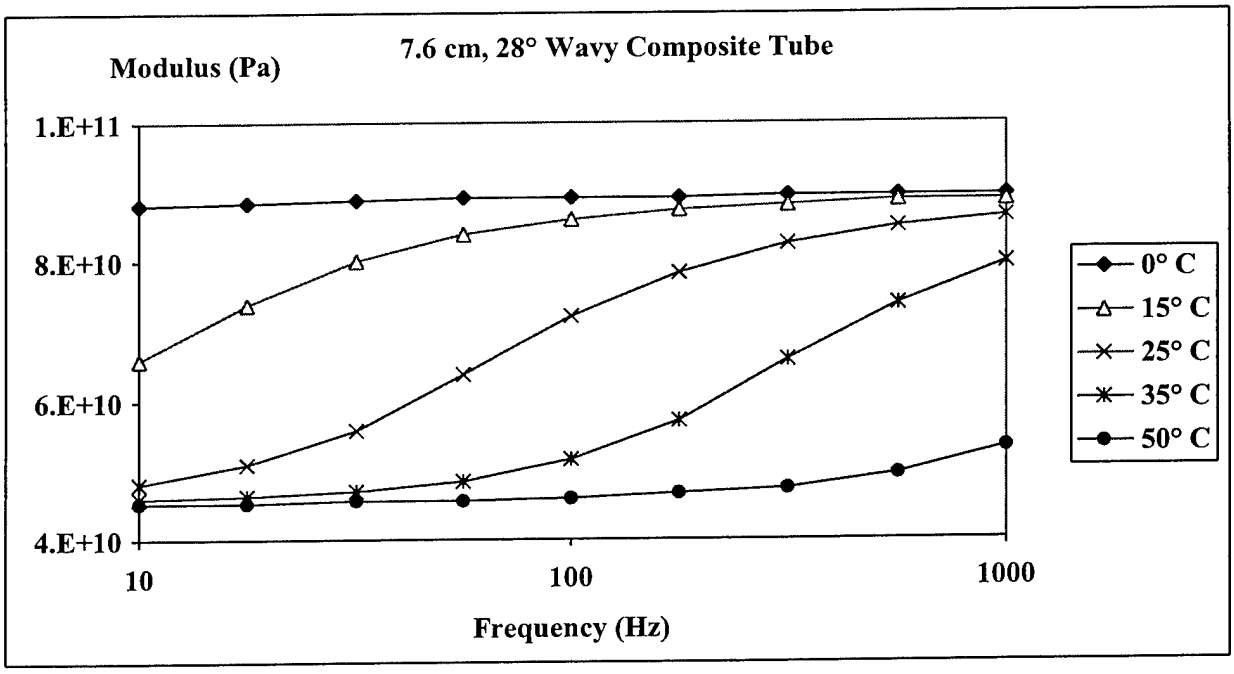

Figure 59: Frequency shift of the stiffness curve due to temperature.

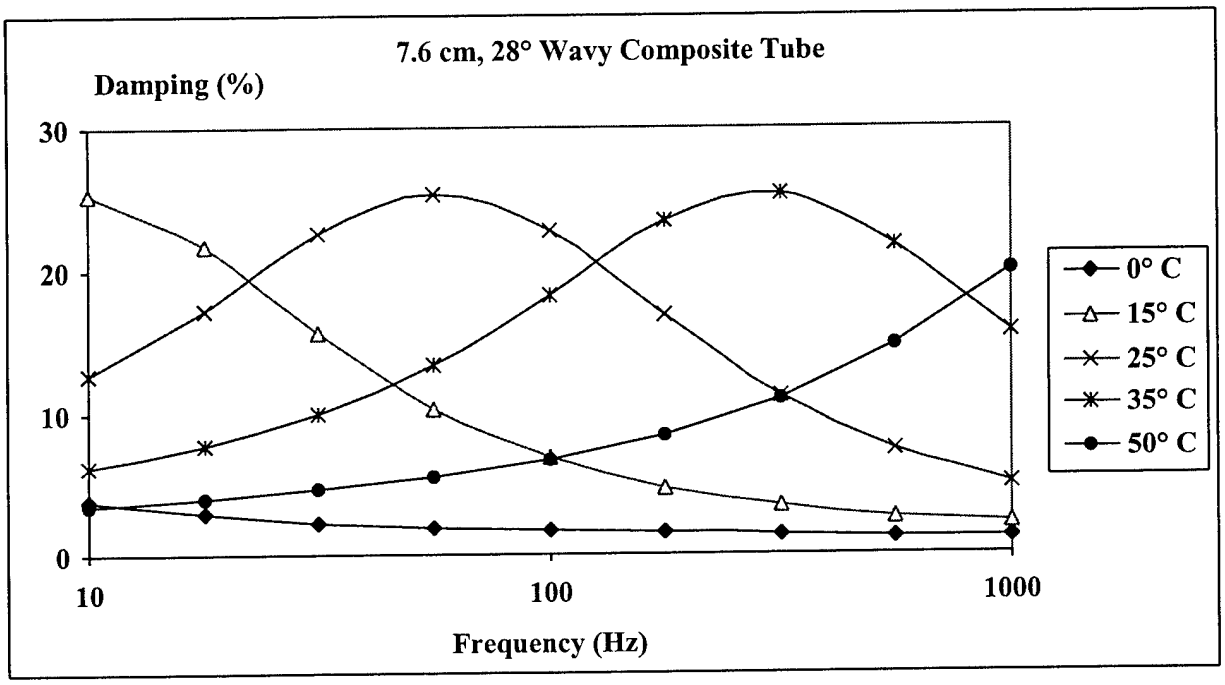

Figure 60: Shift in damping peak due to changes in temperature

Figure 60 illustrates the corresponding shift in the damping curves for the same lay-up. As can be seen, the frequency shift of the damping peak is dramatic for a relatively small shift in temperature for this viscoelastic. The peak value, however, does not change as a function of temperature, only the *frequency* of the damping peak changes. For more detail refer to Chapters 4 and 5.

Design principle 3: For wavy composites, a change in temperature is equivalent to a change in frequency and a master nomograph can be established using the WLF equation.

6.2.2.5. Thickness ratio effects

Changing the thickness of the constraining layer or the viscoelastic layer in a wavy composite has the same effect on stiffness or damping as a minor temperature change, for reasonable thickness ratios. To illustrate this point refer to Figure 61 which shows the effects of changes in the thickness of constraining composite layers or viscoelastic layers on the stiffness of a damped wavy composite laminate composed of two composite facesheets and one viscoelastic layer. The baseline configuration is a wavy laminate with 0.25mm thick composite facesheets with a 7.6 cm, 24 degree sinusoidal waveform, and a 0.2mm thick viscoelastic layer.

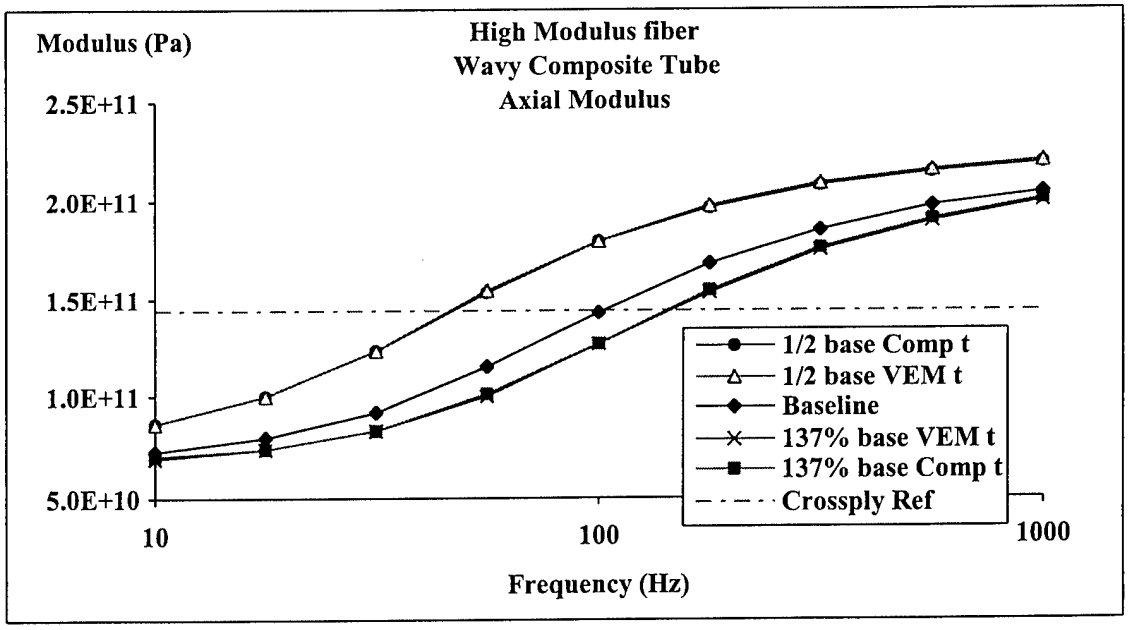

Figure 61: Effects of changing thickness of composite or viscoelastic layers on stiffness.

If the composite facesheets are doubled in thickness, the effect is the same as if the viscoelastic layer was doubled in thickness. Both cause a shift in the frequency of the curve similar to a small temperature shift.

Figure 62 represents the effects of changes in thickness on the frequency of the damping peak of the laminate. Like the stiffness, a change in the thickness of either composite or viscoelastic while holding the other material's thickness constant produces the same result. The effects of changing thickness are additive; changing both VEM and composite thickness will shift the frequency scale even more. Similar to the change in wavelength (Figure 57), as the damping peak moves away from the peak performance of the viscoelastic layer (see Figure 55) the magnitude of the damping peak will diminish slightly.

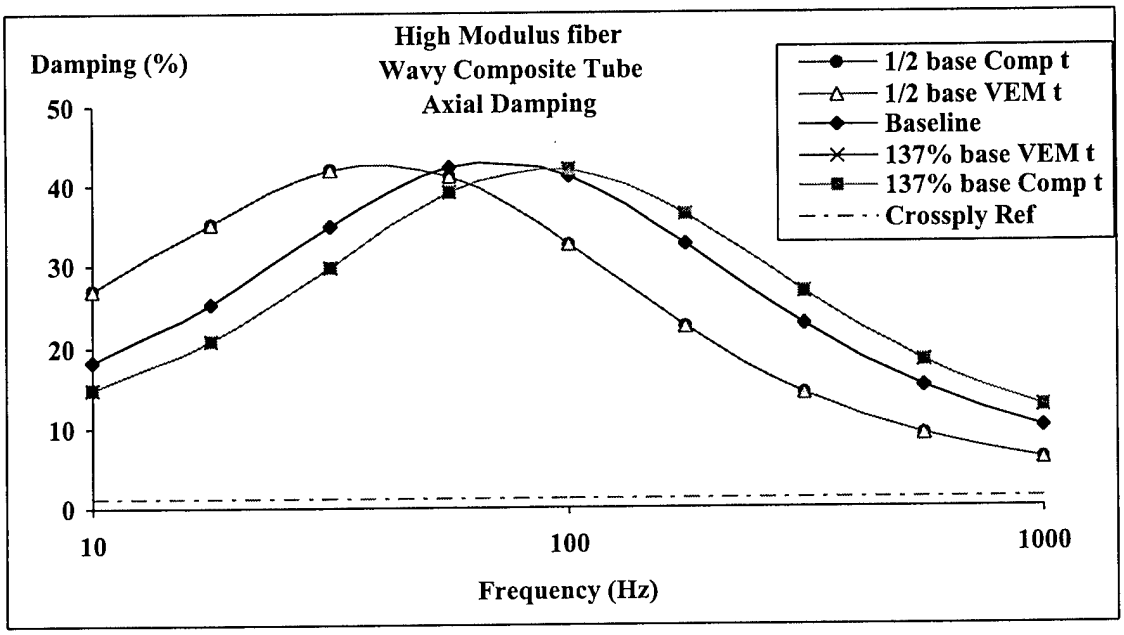

Figure 62: Effects of changing thickness of composite or viscoelastic layers on damping.

It is evident from these figures that thickness ratios have an effect, albeit a minor one, on the frequency of peak damping for a given temperature for reasonable values of thickness. What is meant by reasonable values? Experience to-date has shown that ratios of approximately 1:3 to 3:1 with a baseline thickness of approximately .25 mm give the best overall performance.

Design principle 4: For a given waveform, a change in thickness ratios of viscoelastic or wavy composite will shift the damping and stiffness curves similar to a small change in temperature. Increasing the thickness of either viscoelastic or wavy composite layer shifts the damping peak to a higher frequency; decreasing the thickness of either viscoelastic or wavy composite layers shifts the damping peak to a lower frequency. Effects are additive although not linearly.

6.2.2.6. High modulus fibers and increasing performance in wavy composites

To this point, figures and discussion have centered on examples of wavy composites designed to produce maximum damping performance. If greater emphasis is given to stiffness, there are a number of methods whereby stiffness can be increased with little adverse effect on damping performance. The obvious method of increasing stiffness in a sinusoidal waveform, is to reduce the maximum angle as shown in Figure 58.

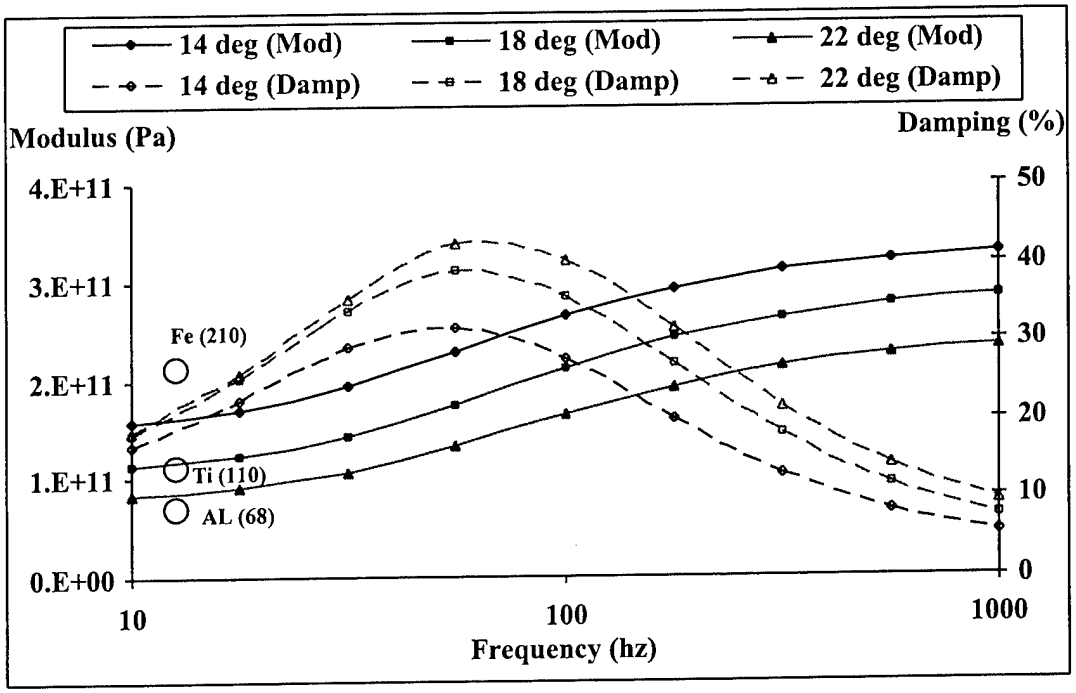

Figure 63: High modulus fiber based wavy composite tube axial modulus and damping performance at different maximum angles, wavelength 7.6 cm

It is also possible to use stiffer fibers in the wavy constraining layers. Figure 63 shows the stiffness and damping performance of three different angles of a 7.6 cm wavelength, using Mitsubishi's K13710 high modulus fiber. Note that stiffness is dramatically increased for little loss in damping. For reference, the stiffness of titanium is approximately 110 GPa, and the stiffness of steel is approximately 210 GPa. When compared to Figure 58 it is immediately obvious that stiffer wavy constraining layers will give both improved damping *and* stiffness. This is shown in Figure 64 where a balance between stiffness and damping is the main design criteria.

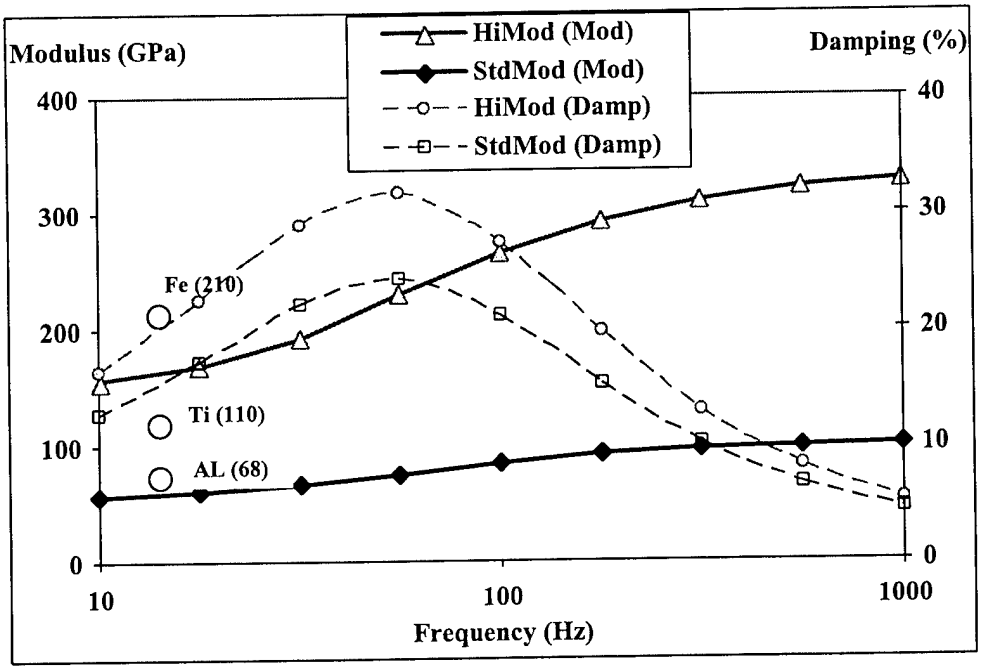

Figure 64: Comparison between high modulus fiber (K13710) and standard carbon fibers.

Design principle 5: The use of higher modulus fibers in the wavy constraining layers will give higher damping and stiffness.

There are other methods of increasing stiffness in wavy composite based structures including the use of conventional composite materials to provide the primary load resisting capability, and use of wavy composite-viscoelastic combinations primarily for damping treatment. Since the wavy composite portion of a mixed composite structure provides significant stiffness in addition to damping, careful design and analysis should be accomplished to optimize the damping, stiffness, and weight.

6.3. CROSSPLY WAVY COMPOSITES

Because of its anisotropy, fiber reinforced composites can be used to tailor the properties of the structure to the expected loads in a very efficient manner. When applied loads on a structure are uncertain or are known but involve many modes (i.e. axial, bending, and torsion for example) careful design and multiple fiber orientations are necessary to prevent failure of the structure. Multiple fiber orientations can give the structure of the composite properties that range from anisotropic to quasi-isotropic to isotropic depending on the materials or laminate structure (Hyer 1997).

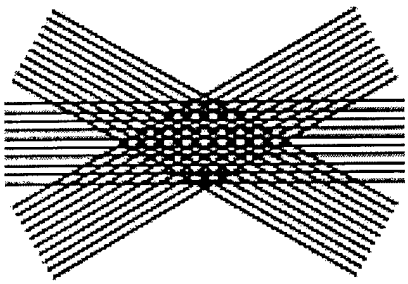

Ply stacking sequence: 0/30/-30

Figure 65: Typical crossply composite structural concept

Crossply lay-ups, as discussed by Reinfelder, et al, and Hyer, typically involve the use of unidirectional pre-preg with fiber orientations designed to maximize the desired structural properties (Figure 1). For example, if a tube is loaded in the longitudinal or axial mode, most if not all of the unidirectional fibers would be oriented in the longitudinal (or 0°) direction for maximum stiffness. Some small percentage of total fibers in the tube may be oriented perpendicular to these fibers for hoop strength, to prevent separation, or to prevent buckling, but such fibers would not resist longitudinal loads efficiently. A tube with all or mostly 0° fibers would be very efficient in resisting longitudinal loads but would not resist any significant torque or bending loads because such loads would be resisted primarily by the shear strength of the matrix and not by fibers.

A better design for resisting torque loads in a tube would be to add additional layers of fibers oriented at angles to the longitudinal axis so that the fibers would spiral around the tube (see Figure 1). Such fibers would provide the primary resistance to torque loads and would provide resistance to shearing loads along the neutral axis during bending similar to a truss like structure.

0° fiber orientation tubes are easy to make by cutting an appropriate length of unidirectional pre-preg from a roll and rolling the composite onto a mandrel. No fibers (for the 0° layers) are cut or interrupted. This is important because loads are resisted best when fibers are not cut. If cut, loads between such fibers are transmitted through the matrix or resin and stiffness and strength can be considerably reduced.

To avoid cutting the fibers (except at the ends of a tube) the angled or off-axis unidirectional pre-preg would have to be spirally wound on the tube. Typically, the unidirectional materials are cut at an angle from a larger sheet and the "off-axis" rectangle of material thus created is rolled on to the tube as is done for the longitudinal fiber plies. This leaves a series of cut fibers that spiral around the tube ending on a discernable seam that runs the length of the tube. This represents a potentially significant weakness in the crossply laminate. If several such layers of opposing "off-axis" plies are used, the normal practice is to offset the ending and beginning of such plies so that the seams of each layer are offset. (Reinfelder, et al, 1998).

In summary, the use of unidirectional fibers to resist loads efficiently can be accomplished but may result in seams and areas of weakness where the continuity of fibers is interrupted.

6.3.1. Wavy crossply structures

Wavy composite can be used to provide equivalent multiple fiber orientations without the disadvantages often apparent with off-axis unidirectional layups. Called "wavy crossply" such structures have the characteristics of ply-stacked composite structures, can be automated, and minimize or eliminate the interruption of fibers.

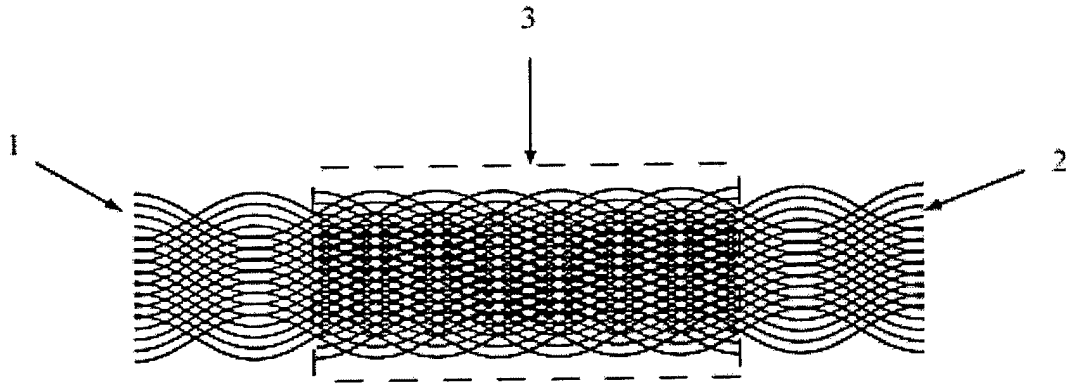

Figure 66: Wavy crossply (3) fabricated from two pairs of wavy composite (1 & 2)

Wavy composite pre-preg can be used to create virtually seamless crossply-like laminates with little or no interruption of fibers. This is simply accomplished by combining two or more wavy composite plies using opposing waveforms (Figure 66, items 1 or 2), or by using combinations of opposing and offset wavy composite waveforms to form the laminate (Figure

66, item 3). Such a laminate displays the properties of both unidirectional and crossply characteristics in that it can efficiently resist both axial and transverse shearing loads.

Finally, there is a finite maximum width to pre-preg (typically 60 inches maximum), which often causes laminators to have to splice and overlap sheets of unidirectional pre-preg together to form large laminae. This is especially true for off-axis unidirectional laminae. This introduces seams, which often represent a significant weakness in the laminate. Wavy composite can be easily spliced together across the width without the need to interrupt the edge fibers. It is possible to create such structures with a minimum of interruption of fiber continuity and without overlapping seams. In fact, wavy crossply tubes have been made that exhibit no discernable seam, have no interruption of fibers (except at the ends of the tubes), and that display classic crossply laminate characteristics.

6.3.2. Detailed description

A single layer of wavy composite has a fiber lay that oscillates between a negative maximum angle and a positive maximum angle in a pre-determined pattern. As a result, the individual laminae will vary in stiffness and displacement characteristics along its length as the angle of the fiber changes. Thus where the angle is 0° relative to the length of the waveform, the laminae will have the characteristics of a 0° unidirectional composite, and where the angle diverges from 0° the laminae will have the characteristics of an off-axis unidirectional laminae. If several opposing wavy composite laminae are joined together in a symmetric lay-up (see Figure 66), the laminate will exhibit quasi-isotropic properties at any point along the length.

Refer to Figure 66. Items 1 and 2 refer to opposing pairs of wavy composite laminae. Where the angle is at a ± maximum, the properties of the laminate will be like a ± unidirectional crossply. These areas where the angles are at a ± maximum will resist in-plane shear loads effectively but will have a lower longitudinal or lengthwise stiffness. Where the angle is at 0° the laminate will have the properties of a 0° unidirectional lay-up (Pratt 1999). These areas (where the angle of the fibers are 0° relative to the longitudinal direction) will not resist shear loads effectively but will have a greater lengthwise stiffness. These localized differences in stiffness can be overcome by combining two pairs of wavy composite laminae into a single laminate as is shown for item 3. The structure of the wavy laminate enclosed by item 3 is termed "wavy crossply laminate."

Through the depth of the laminate, for one pair of opposing wavy laminae, the angle will be at a ± maximum but the second pair of opposing wavy laminae will have a fiber angle that is at 0° or nearly 0° relative to the general direction of the laminate. This gives the laminate an equivalent unidirectional lay-up of four total layers where two of the layers are unidirectional plies with a ± fiber orientation, and the other two layers were equivalent to two 0° unidirectional laminae. The unidirectional version of a crossply laminate cannot be easily automated; wavy crossply laminate can be automated.

To further illustrate the capability of wavy crossply laminates, the following table documents the equivalent axial and shear modulus of several different configurations of wavy crossply laminates. A typical carbon fiber-resin combination was used to represent the material properties of both unidirectional and wavy composites. Table 9 shows the configuration of each laminate next to the words "unidirectional", or "wavy crossply", to define each example. The laminate configuration is defined by the angle of the plies relative to the longitudinal direction of the sample tube used to model the lay-up.

Table 9: Performance comparisons of wavy and conventional crossply laminates

Laminate	Configuration	Axial modulus	Shear modulus
1. Unidirectional	0°	142.2 GPa	5.2 GPa
2. Unidirectional	+30°/-30°	51.4 GPa	29.2 GPa
3. Unidirectional	0°/+30°/-30°	84.3 GPa	21.5 GPa
4. Wavy crossply	± 30° wavy (one pair) (Figure 2, item 1 or 2)	82.4 GPa	12.6 GPa
5. Wavy crossply	± 45° wavy (two pair) with quarter waveform offset between pairs (Figure 2, item 3)	53.9 GPa	27.5 GPa
6. Wavy crossply	± 30° wavy (two pair) with quarter waveform offset between pairs (Figure 2, item 3)	88.6 GPa	20.0 GPa

For example, "0°" means all fibers are oriented at zero degrees to the reference, or run longitudinally in the tube. The relative axial stiffness of the laminate is given in the column labeled "Axial modulus." This represents the smeared axial material properties of the lay-up. Axial modulus represents the relative ability of the laminate to resist tension or compression loads, and even bending loads if the neutral axis shear forces are ignored. The "Shear modulus" column represents the ability of the laminate to resist torsion or shear loads.

Laminate #1 is a unidirectional fiber composite lay-up that shows the 0 degree properties of the fiber reinforce composite used to model all subsequent lay-ups. Laminate #2 shows the properties of a conventional ± 30 degree unidirectional composite crossply lay-up. Note the

equivalent axial modulus of laminate #2 is considerably reduced from that of laminate #1, but the equivalent shear modulus is greatly improved over the shear modulus of laminate #1. This is a classic example of how crossply composites lose axial modulus rapidly as the angle of the fiber diverges from zero degrees, but their ability to resist shear loads improves.

If more axial stiffness is required, a unidirectional 0 degree ply can be added. The results of this combination are shown as laminate #3 in Table 9. The axial modulus is improved by 64% relative to laminate #2 but the shear modulus is reduced 26%.

Wavy composite can be used to create wavy crossply laminates equivalent to the unidirectional crossply laminates discussed above. Wavy crossply laminate #5 is equivalent in both axial and shear modulus to unidirectional crossply laminate #2. Likewise, wavy crossply laminate #6 is equivalent in both axial and shear modulus to unidirectional crossply laminate #3. Both wavy crossply laminates are significantly easier to fabricate, do not cut fibers (and therefore do not show any seam), and can be readily automated. The same cannot be said for the two unidirectional crossply laminates.

The range of possible uses of the example wavy crossply lay-ups shown in Table 9, is potentially limitless. Applications include automotive, aerospace, and marine drive shafts, composite wing structures of all types, panels, composite I-beams, channels, and virtually an endless combination of possibilities. Composite arrow shafts and golf club shafts would likewise benefit from greatly reduced labor costs in construction.

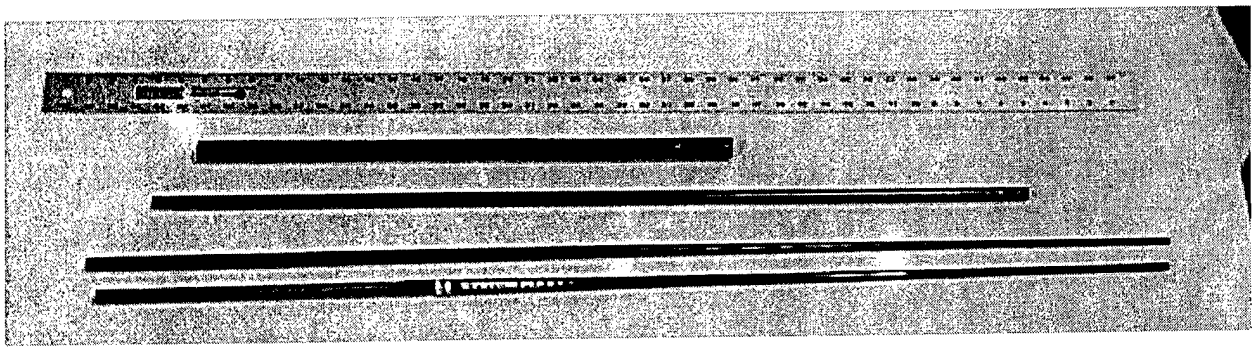

Figure 67: Several examples of wavy crossply tubular structures.

One such application is shown in Figure 67. A 48-inch ruler is shown above for reference. The top tube is a damped wavy tube that was built to test the axial properties of one combination of wavy composite and viscoelastic material. It has a length of approximately 61 cm, and a ID of 2.22 cm. The second tube from the top is a 1.25 cm diameter tube made with

four layers of wavy composite in a "wavy crossply" configuration, and two layers each of viscoelastic and opposing wavy composite for damping. The third tube is a tapered golf club shaft made the same way as the second tube only on a tapered mandrel. It is shown next to a conventional composite golf club shaft for reference.

6.4. ADVANCED WAVY COMPOSITE DESIGNS

This section discusses advanced topics in wavy composite design that have been accomplished and that improve the strength and stiffness practical structures.

One of the concerns of the use of the basic concept for wavy composite is the strength of the laminate. While extensive testing of the possible failure modes for a damped wavy laminate has not been accomplished, some previous work has been accomplished on a related subject (Wright 1994). The most obvious failure mode for loads in line with the general direction of the waveform would be matrix failure along the lay of the fiber at the location of maximum fiber angle. This failure mode can be addressed very easily by addition of unidirectional cross-plies as shown in Figure 68.

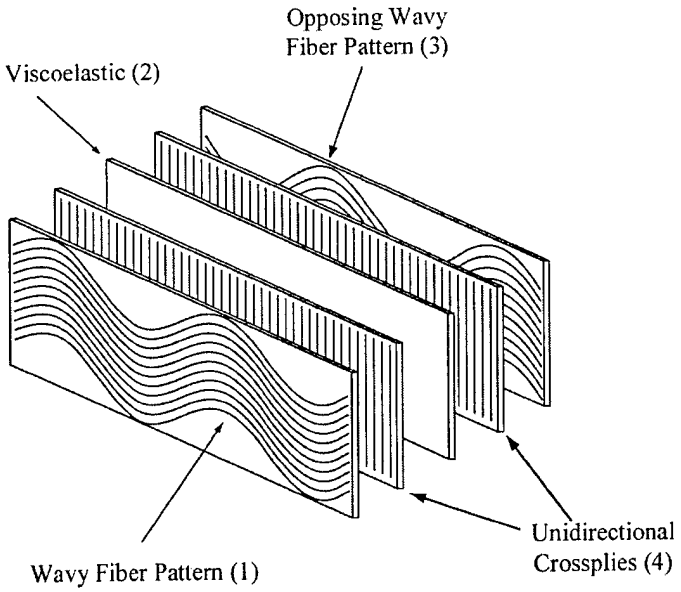

Figure 68: Damped wavy laminate with unidirectional crossplies

Analysis, verified by testing, indicates that damping is not adversely affected by the cross-ply and can actually be enhanced for a 1:10 ratio of cross-ply to wavy laminate. In general, the use of crossplies enhances strength enough that its use as a general construction method is recommended for most applications.

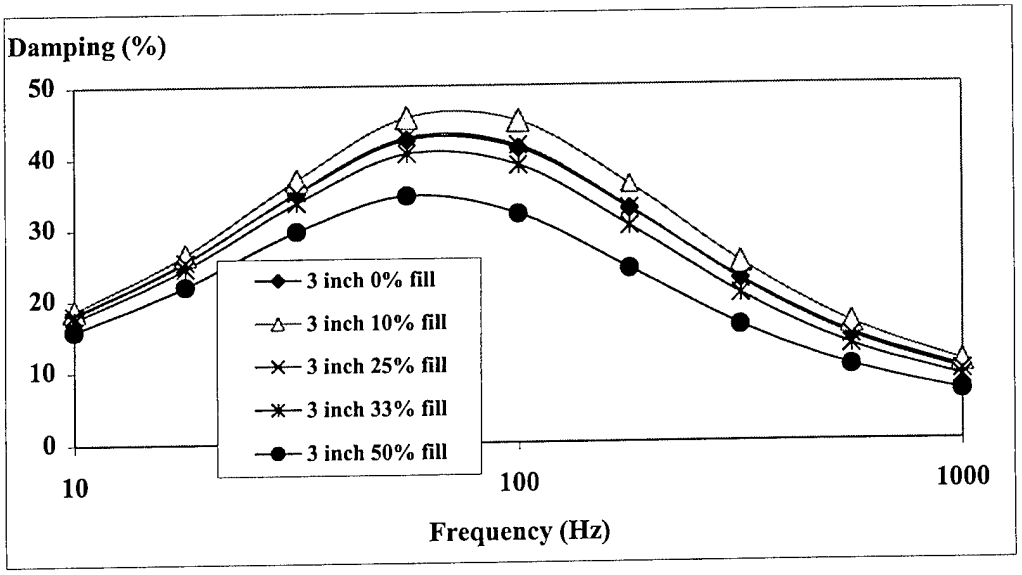

Figure 69: Damping vs. percent fill (cross plies)

Note that both Figure 69 and Figure 70 show significant improvement in damping and stiffness respectively. In fact, analysis of this high modulus fiber-based layup shows that addition of up to 25% crossply fibers in the laminate is equal to a straight wavy composite with no unidirectional crossplies.

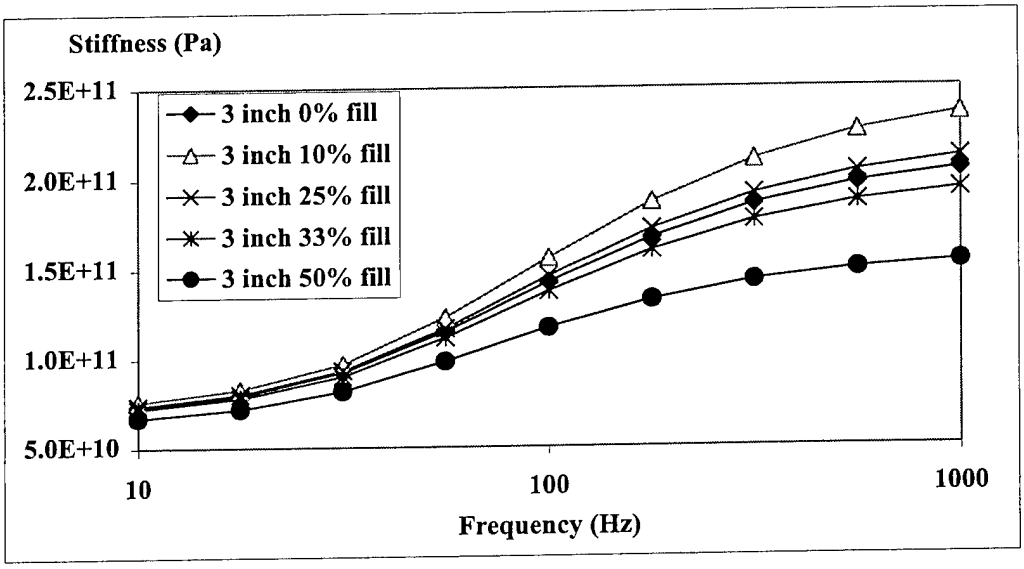

Figure 70: Stiffness vs. percent fill (cross plies)

A typical laminate would consist of three plies of wavy composite with one crossply (90 degrees) of unidirectional composite. This would provide maximum stiffness and strength to the laminate.

Figure 71 shows a modified version of the crossply reinforced laminate of Figure 68 that has been used to improve torsional or twisting flexural stiffness. Narrow flat foam cored lay-ups such as skis can experience significant twist along the length of the structure because the viscoelastic layer prevents transference of twisting loads between adjacent wavy layers.

By removing viscoelastic periodically along the length of the laminate as shown in Figure 71, the adjacent wavy composite layers will be "welded" together and will greatly enhance resistance to twisting. If the viscoelastic "patches" are placed at the locations of maximum fiber angle, damping is not adversely affected. This method has been successfully applied to test tubes and skis. Other applications being considered are floor beams for aircraft and drive shafts.

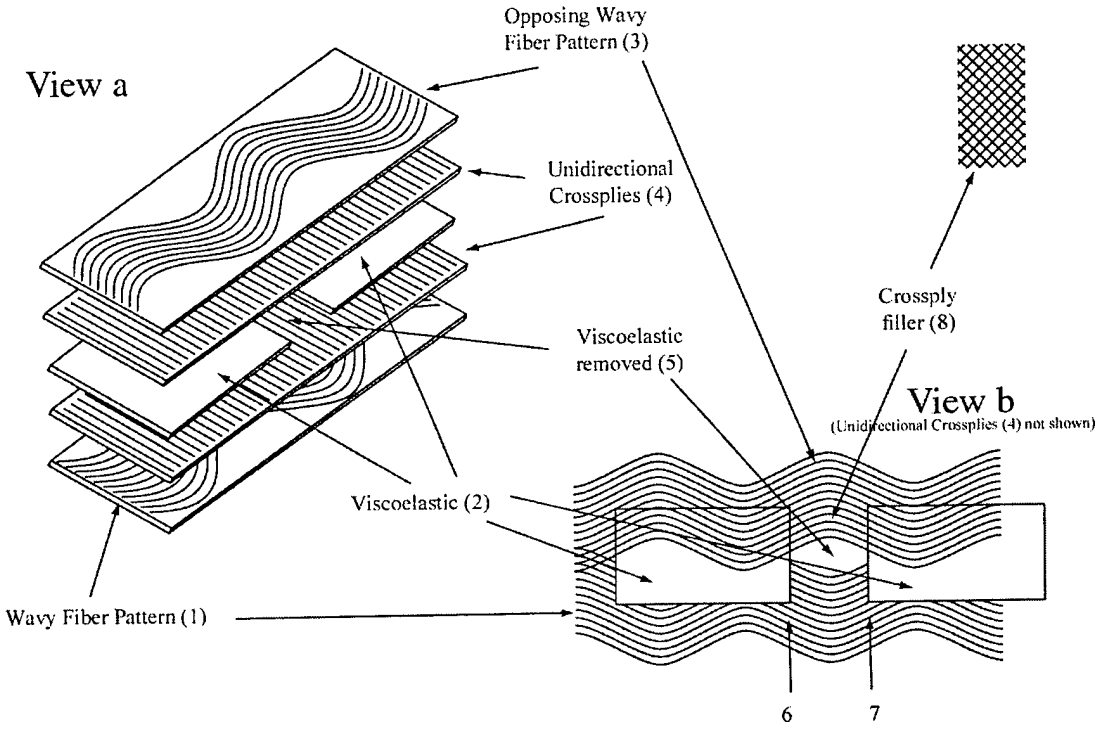

Figure 71: Damped wavy laminate with targeted VEM layers

6.5. DESIGN CONSIDERATIONS

The number one consideration for designing with this new material is the performance of the viscoelastic layer. Since the composite-viscoelastic combination takes on the characteristics of the viscoelastic layer, the performance limitations, if any, can be attributed to the viscoelastic. The ideal viscoelastic would be very broadband, have good stiffness, and be insensitive to

temperature shifts. If such a viscoelastic material exists, the creation of a highly damped, broadband wavy composite would only require the selection of the best waveform and angle for the desired stiffness and damping.

For example, there is a very capable adhesive that is used in the manufacture of brake linings and pads that has broadband viscoelastic properties. Computer studies with our FEA code showed that the performance would be very broadband if a short waveform was selected since this waveform would exhibit peak damping at higher frequencies and maintain the high damping for a significant range of lower frequencies. Unfortunately, the viscoelastic is made with a crosslinked compound that continues to crosslink at the cure temperatures for the composite and which resulted in a narrowing of the damping performance. After this crosslinking the damping performance of the viscoelastic layer was reduced to the same level or lower level of other viscoelastics. The advantage was that this particular viscoelastic can be used at high temperatures (260 to 300 degrees Celsius) but the broadband properties were lost. With development, it may be possible to enhance the broadband properties in the future.

6.5.1. Operational temperature range

The number one consideration for the use of this material is therefore the operational temperature range of the application. Viscoelastic materials transition from a glass-like material at low temperatures (or high frequency) to a rubbery material at high temperatures (or low frequencies). This will limit the practical range of uses for a given material combination. An example of these temporary limitations would occur in the use of this material in the skins of aircraft. At altitude, the aircraft skin and structure can be subjected to very low temperatures that would cause some viscoelastic materials to transition to a glass-like state. There are adhesives that are still pliable at low temperature and such should be explored for use as viscoelastic layers but most viscoelastic materials used to date have glass transition temperatures within about 5 degrees Celsius of each other and exhibit viscoelasticity over a three-decade frequency range.

6.5.2. Frequency range and important modes

The second most important consideration for use of this material is the operational frequency range, which in turn is determined by the important vibratory modes of the structure. It should be remembered that viscoelastic materials, and thus wavy composites, are temperature and frequency dependent and that a shift in frequency is equivalent to a shift in temperature.

Therefore, the considerations given for the temperature range of operation apply to the frequency range of operation.

6.6. AEROSPACE STRUCTURAL CONCEPTS

The objective of this section is to illustrate the likely impact on the dynamics of lightweight highly damped wavy composite based structures designed for use in space. Three applications are illustrated and discussed to show the advantages of this new material.

6.6.1. Dynamically stiff space based lasers (STAR WARS)

Wavy composite damping had its origin in the Star Wars programs of the late 1980's. The application was a space-based laser satellite mounted on a composite truss structure. In order to focus enough energy on an incoming missile from a geo-synchronous orbit, the structure had to be *dynamically* stiff so that perturbations of the structure by on-board pumps, and other equipment were not amplified (see Figure 51). The use of wavy composite for construction of the truss members was proposed and prototypes built (using cut-segmented chevron patterns), but were never tested (Olcott 1992).

The concept is still a very sound one. Using high modulus fibers as the wavy composite constraining layers damping as high as 50% could be expected in the structure (using off-the-shelf materials) without the added weight of active control actuators, sensors, controllers, and their attendant reliability issues. Instead it is possible that this new wavy "smart" material alone could provide the necessary *dynamic rigidity* for the effective operation of a space-based anti-missile defense. Even if some "active" control was necessary for "fine tuning" the dynamic properties of the satellite structure, high inherent damping would make the active control solution significantly more stable, robust, and simpler (von Flotow and Mercadal 1995).

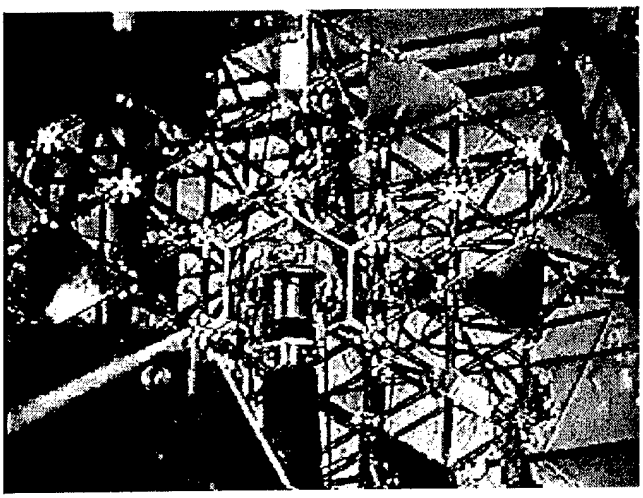

Figure 72: Space-based laser anti-missile concept which inspired the wavy composite concept

There is another significant benefit from high inherent damping that was discussed in Section 6.1.2. involving settling time. Sensing incoming missiles becomes extremely difficult when the sensors and the satellite's structure are vibrating after a course change. The low inherent damping of unidirectional high modulus composites, especially in a space environment, means that any perturbation of a satellite due to an attitude change will cause the satellite to vibrate for a considerable time. Additionally, appendages such as antennas, solar arrays, etc. will tend to exacerbate the dynamic stability problems of the satellite as they vibrate at their natural frequencies. To solve these varied and diverse vibration problems with active control would be difficult and expensive, especially considering that a robust passive solution is readily available. As was pointed out in Section 6.1.2. improving damping is a much more efficient way to improve the settling time of a structure.

6.6.2. Launch shrouds and payload containers

Wavy composite can be used to provide acoustic protection to a payload either as part of a launch shroud or as a payload container. The problem occurs during launching of the payload and its flight through the atmosphere. Low frequency rumble and structural borne vibrations from the amplified motor fluctuations can damage or destroy sensitive guidance control systems or payloads. It is assumed that the majority of acoustic excitations are caused by non-diffuse, acoustic standing waves, and mechanically excited vibrations of the launch vehicle that couple efficiently to the air surrounding the payload. In this case, added stiffness *and* damping are appropriate solution methods for attenuating the sound pressures on the payload (Norton 1996).

If the sound field is diffuse, generally, only added mass will cause an increase in transmission loss (Norton 1996). A typical example of a diffuse sound field and a mass based solution to transmission loss is the concrete barriers typically seen next to interstate highways that run through suburban areas. In this case, the mass of the concrete barrier represents an appropriate solution.

Added mass is *not* an appropriate solution for the typical launching environment where vibrations from dynamic modes of the vehicle ("pogo effect"), reflected sound waves from the rocket motors, and mechanically excited panel resonance, all combine to cause extremely high (170 dB) sound pressures on the payload. In this case, added damping and stiffness are the appropriate solutions for increased acoustic protection of the payload. Additionally, the extremes of vibration, shock, and environmental conditions require an integrated dynamic solution. With these assumptions in mind, the following explanation will motivate the proposed dynamic solution based on stiffness and damping.

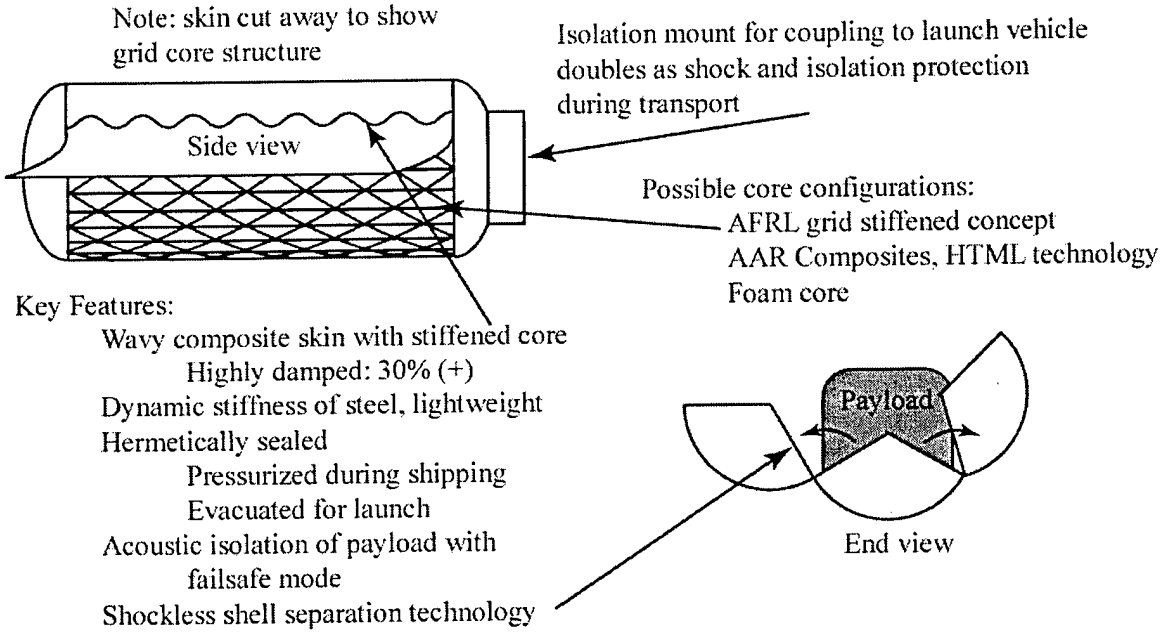

Figure 73: Payload container concept

The payload container concept (Figure 73) would be a dynamically stiff structure that would be sealed and evacuated for launching. Since sound doesn't travel in a vacuum, this concept would provide acoustic isolation from both mechanically excited and acoustic standing waves. With the evacuated chamber providing acoustic isolation, the payload would still be

subject to vibrations caused by the rocket fluctuations and rumble transmitted through the skin of the container through the payload attaching points. Here too, the high inherent damping of the structure of the container would reduce vibrations to levels where they would no longer be a concern.

If a sealed container is not desired, or a vacuum during launch is not practical or is lost, the wavy composite skin would provide a fail safe mode where the stiffness and damping of the container would provide a minimum 50 dB transmission loss. Wavy composite materials and designs can provide both the necessary stiffness and damping to accomplish these goals.

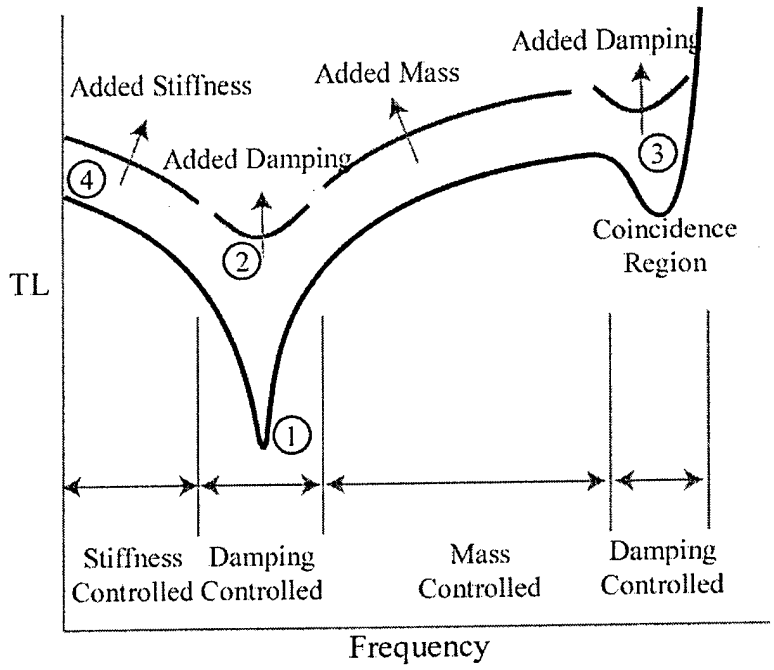

Figure 74: Characteristic transmission loss of a panel (Norton 1996).

Dynamic stiffness of the structure of the shell is the key to optimal acoustic protection. For low frequency excitations typical of launch environments (due to rocket fluctuations and rumble), the acoustic performance of the shell will be determined by the low frequency stiffness and damping properties of the first few bending modes of the shell. If the first bending mode occurs above the driving frequency of the rocket fluctuations or exhaust rumble, transmission loss in the shell will be controlled by the stiffness. However, if the first bending mode frequency occurs close to the driving frequency of the rocket fluctuations or exhaust rumble, transmission loss in the panel will be controlled only by the damping of the panel. This is shown in Figure 74

where the dip in transmission loss (point 1) is caused by the lack of damping in the panel at the first bending mode.

Adding damping to the panel makes a dramatic improvement (point 2) in the low frequency acoustic performance as shown in Figure 74. With the damping available through the use of high modulus wavy composites, it is possible to increase performance in this area by more than 20 dB. This is shown in the FEA analysis accomplished by Patterned Fiber Composites, Inc.'s analysis code.

Adding stiffness will increase the low frequency performance as shown in Figure 74 (point 4) but may not represent the optimal solution. If, for example, the stiffness controlled region is already providing the required 50 dB reduction in acoustic levels, increasing *damping* will have a tendency to flatten the acoustic transmission loss curve and provide a more uniform transmission loss performance. Thus it is the judicious use of damping *and* stiffness that will provide an optimal design.

Finally, high structural damping in the construction of the payload container provides benefits that make other technologies more effective. Damping provides the necessary high dynamic impedance for payloads, containers, and airframes, to enable isolation mount technology to effectively isolate the payload or guidance systems. Without the improvements that damping offers, softmounts can actually be stiffer than the structure they are attached to which negates any benefit that may be derived from isolation mounts (von Flotow and Mercadal 1995).

A variant of the payload container is the damped, launch shroud fairing concept shown in Figure 75. All the advantages discussed for the payload container apply to the launch shroud and will not be repeated here.

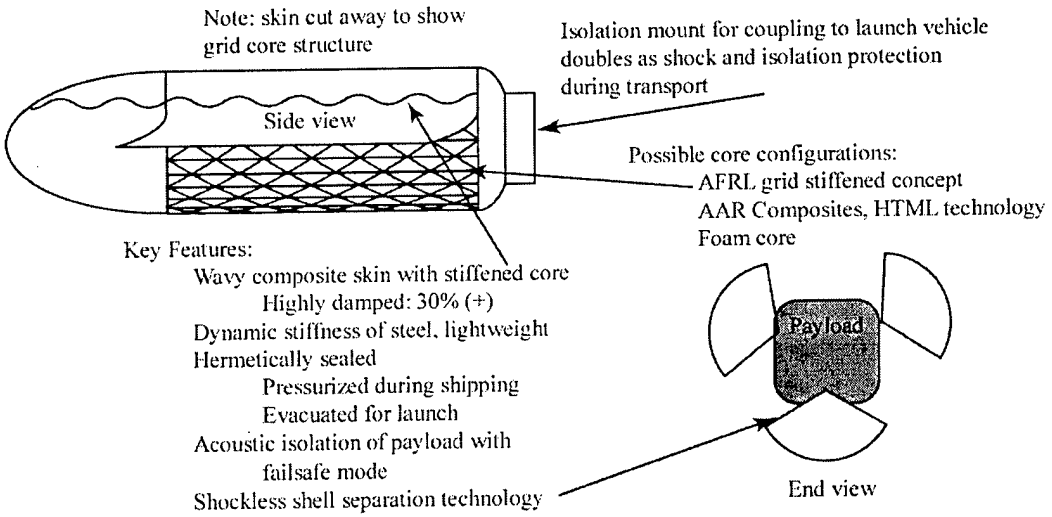

Figure 75: Launch shroud concept

It should be noted that the advantages of damping discussed in conjunction with the acoustic loss analysis shown in Figure 74 applies for several modes of vibration, not just the first bending mode. Most panels will have at least five modes that will affect acoustics, especially in the audible range. Figure 74 only shows the first mode, the higher modes would show similar advantages for increased damping and the effects would overlap. The end result would be a very robust design that would increase acoustic attenuation across a relatively broad band of interest.

6.6.3. Missile bodies and dynamic stiffness

Figure 51 is repeated here as Figure 76 for convenience and illustrates what happens to the dynamics of any structure when the frequency of the driving force is close to the natural resonance. At very low frequencies (in this example 100-300 Hz) there is a one-for-one relationship between the driving amplitude (input side) and the free response of the output. As the driving frequency of the input approaches the natural resonance of the structure, the ratio of output to input is amplified until at resonance the output of the free end reaches its maximum (in this case an input of ± 1 is amplified 144 times). The damped wavy panel will limit amplification to 6 times the input.

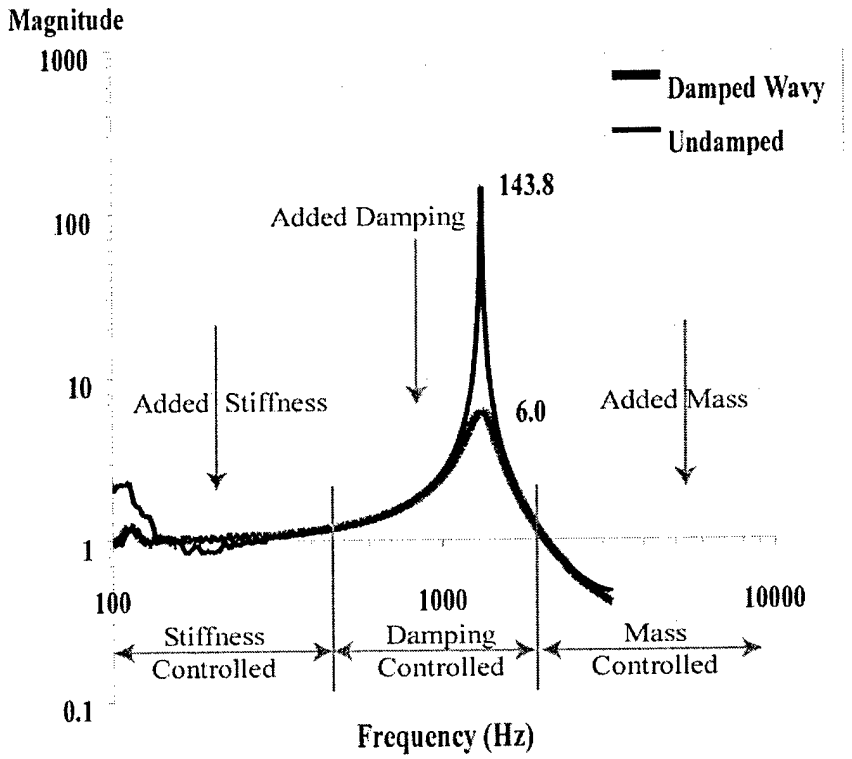

Figure 76: Actual vibration magnification or "Pogo effect" in wavy damped vs. undamped tubes excited in the axial mode.

This is known as the "pogo effect", an expression that was coined by the aerospace community to describe how unacceptable g-forces were showing up in the payload of rockets during launch. It happened on the Apollo 6 mission, and was a constant problem with the Titan rocket. Extrapolated to airframes in general, the limitation on vibration amplification that comes from high inherent damping, provides protection to sensitive avionics and improves accuracy of on-board weapon systems.

6.7. SUMMARY

The most efficient solution to a dynamic structural problem is to use a material that provides high damping.

- Damping limits amplification of vibrations, stress, and strain at resonance
- Damping dramatically improves settling time of free vibrating structures
- Damping improves transmission loss in panels

In addition to preventing catastrophic failure of airframes from amplified vibrations as discussed in the missile example (pogo effect), the use of damped wavy composites in airframes of all types has additional advantages. Since damping limits the amplification of vibrations at resonance, it also limits the amplification of stress and strain in the airframe. Unchecked by damping, resonance in airframes can cause dangerously high stress and strain levels that can either accelerate fatigue or in extreme cases, can cause catastrophic failure.

Half of all launch failures in recent years have been attributed to excessive noise and vibration in the launch vehicle that damaged or destroyed either the payload or the guidance system. Again, while changing mass or stiffness can often provide an acceptable solution to a single frequency dynamic problem but damping can provide a more efficient, robust, and broadband solution for the structure.

The lack of inherent damping in conventional composites means that space-based structures will tend to vibrated for long periods and will adversely affect the accuracy of sensors and weapon systems. While adding stiffness or reducing mass can improve settling time, this approach is most often impractical if not impossible to achieve. To get the same performance out of an undamped composite as can be obtained from high modulus wavy composites, the designer would have to increase stiffness or decrease mass by a minimum of 600 times to a maximum of 6000^{+} times depending on what criteria is used. Obviously, damping is a much more efficient way of providing a stable structure.

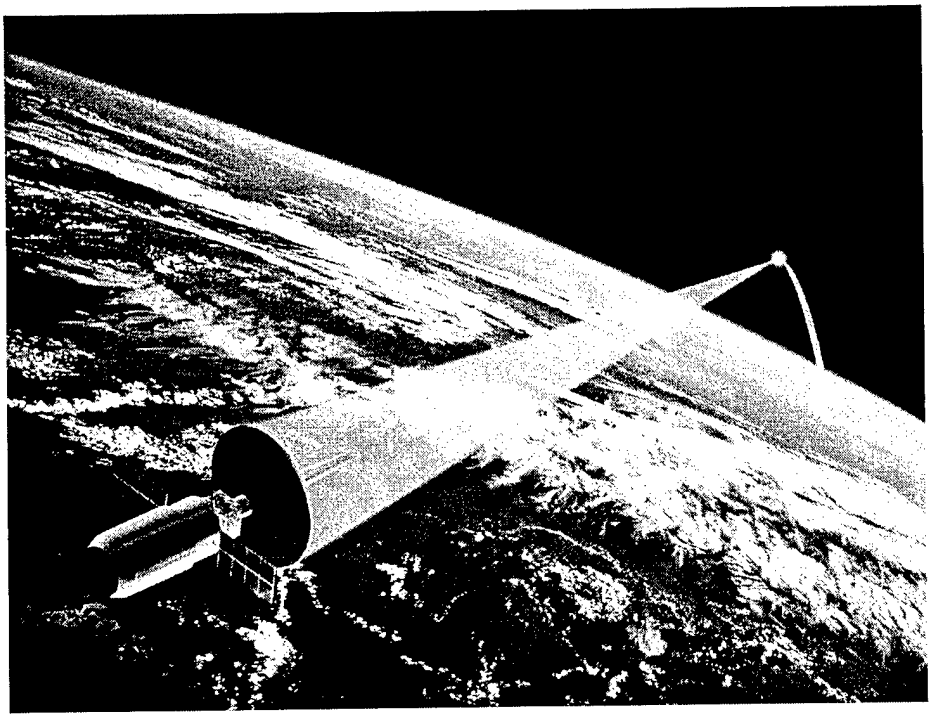

Figure 77: Space-based laser anti-missile system (SBL-IFX), a candidate for wavy composite

Wavy composite is unique and unparalleled in performance in that it exhibits both high damping and stiffness; no other material can do what this material can do. It is now possible to create a laminate that exceeds the stiffness of steel, with thousands of times the damping and a fraction of the weight. It is a new material paradigm that requires rethinking the structural designs of the past. We are only limited by our imagination.

CHAPTER 7: CONCLUSIONS

7.1. OBJECTIVES:

Wavy composite is a new material that exhibits both high stiffness and damping. If high modulus fibers are used in the production of the wavy composite, it is possible to attain the stiffness of steel, thousands of times the damping, with the lightweight advantages of graphite-based composite. Prior to this contract, wavy composite had never been modeled accurately, tested comprehensively, or adequately characterized, and there was no capability to produce commercial grade wavy composite. This pioneering work has focused on creating and characterizing this new material system.

Specifically, the objectives of this Phase II work were to

1) Develop a wavy composite pre-preg manufacturing capability,
2) Develop a Finite Element Analysis code that would accurately predict the performance of wavy composite,
3) Test and characterize wavy composite damping and correlate results to the FEA code,
4) Design and build a launch adapter.

All of these objectives with the exception of item 4 have been accomplished, as outlined in detail in this report. Item 4 was not accomplished due to funding constraints imposed by the program office, though the ability to accomplish this and many other practical designs exists. The results are summarized below.

7.2. ACCOMPLISHMENTS

The accomplishments of the first three objectives listed above and their implications are covered in this section.

7.2.1. Production:

A second-generation wavy pre-preg machine was built during the first year of the contract. The machine is capable of producing 25 kilotons of wavy composite annually

and has successfully produced waveforms from 152 mm to as small as 25 mm in length with angles from 0 to ±35 degrees.

7.2.2. Wavy Composite Testing:

The axial test stand developed as part of this contract has been shown to be an effective tool in characterizing the performance of stiff, highly damped composites. Investigations into all of the possible sources of error have shown that the test stand is accurate and robust.

Time-temperature superposition has been applied to create master stiffness and damping curves over a very broad frequency range. Wavy composite takes on the properties of the viscoelastic, and the viscoelastic curve fit constants appear to be a reliable approximation that can be used to shift test data and form master nomograms. Further testing at very low frequencies or on a larger body of data will determine the time-temperature superposition shift constant more accurately.

Axial test results have been presented for basic sandwich lay-ups with waveforms between 2.5 cm (1.0 in.) and 15 cm (6.0 in.), angles between 22 and 30 degrees and various thickness ratios. About 100 total tubes were built, tested, and characterized. Two replications were performed on each test specimen. There was very little scatter in the stiffness and damping results for replicated tubes.

Methods for testing in bending and in torsion have revealed that the material behaves similarly in bending and torsion, though further research will be necessary to make these methods as robust and reliable as the axial test.

7.2.3. Finite Element Modeling and Model Correlation:

A discrete laminate FEA model was necessary to analyze wavy composites, because inter-laminar shear strains drive wavy composite damping. Patterned Fiber Composites Inc.'s finite element model created as part of this contract overcomes the problems in commercial codes. Aspect ratios as high as 1:1000 have been successfully analyzed, greatly reducing analysis time as the number of elements needed to model composite shell structures is reduced by many orders of magnitude. Nonlinear brick-16 elements allow accurate modeling of sinusoidally varying composite properties. In a

comparison with PATRAN using the ABACUS analysis engine, Patterned Fiber Composites' analysis code was hundreds of times faster and produced more accurate results.

Comparisons with test data have shown that the finite element code accurately models changes in waveform, max angle, and layer thickness. Though the test data shows some scatter, the FEA code has been shown to be accurate to 5% when predicting stiffness in tubes tested in the axial mode. The damping results are even more reliable, typically accurate within 2%, though the material appears to deviate from ideal performance when the viscoelastic thickness falls below 0.15 mm (0.006 in.)

7.2.4. Design Expertise and Experience:

The tools developed for modeling and testing wavy composites have been used to develop an understanding of the principles of designing damped wavy composite structures. The most efficient solution to a dynamic structural problem is to use a material that provides high damping.

- Damping limits amplification of vibrations, stress, and strain at resonance
- Damping dramatically improves settling time of free vibrating structures
- Damping improves transmission loss in panels

In addition to preventing catastrophic failure of aerospace structures from amplified vibrations, the use of damped wavy composites in aerospace structures of all types has additional advantages. Since damping limits the amplification of vibrations at resonance, it also limits the amplification of stress and strain in the structure. Unchecked by damping, resonance in aerospace structures can cause dangerously high stress and strain levels that can either accelerate fatigue or in extreme cases, can cause catastrophic failure.

Half of all launch failures in recent years have been attributed to excessive noise and vibration in the launch vehicle that damaged or destroyed either the payload or the guidance system. Again, while changing mass or stiffness can often provide an acceptable solution to a single frequency dynamic problem, added damping represents a more efficient, robust, and broadband solution for the structure.

The lack of inherent damping in conventional composites means that space-based structures will tend to vibrate for long periods of time. This adversely affects the accuracy of sensors and weapon systems. While adding stiffness or reducing mass can improve settling time, this approach is most often impractical if not impossible to achieve. To get the same performance out of an undamped composite as can be obtained from high modulus wavy composites, the designer would have to increase stiffness or decrease mass by 600 to 6000^{+} times. Obviously, damping is a much more efficient way of providing a stable structure.

Wavy composite is unique and unparalleled in performance in that it exhibits both high damping and stiffness; no other material can do what this material can do. It is now possible to create a laminate that exceeds the stiffness of steel, with thousands of times the damping and a fraction of the weight. It is a new material paradigm that requires rethinking the structural designs of the past. We are only limited by our imagination.

CHAPTER 8: RECOMMENDATIONS

8.1. RECOMMENDED FUTURE RESEARCH

Our number one recommendation is to use the material. While there is room for improvement in materials, testing and computer analysis, this new material system has already shown unprecedented performance improvements over existing technologies. The fact that analysis shows the ability to dramatically improve performance further, by steps as simple as using stiffer fibers, provides a bonus advantage and motivation for continued research.

There is inertia in the engineering community that leaders must overcome. Engineers are conservative, non-risk takers by nature. Because of this it typically takes decades for a new material to find acceptance in all but the most benign applications. The history of composites is a prime example.

No new material is without its "glitches" and struggles. The same has been the case with wavy composite. It's as easy to make a bad wavy composite design as it is to make a bad conventional composite design. However when both designs are executed with reasonable accuracy, the wavy composite performance far exceeds the dynamic performance of conventional materials. There is no peer.

Has this research solved all of the issues? No, but it has advanced the state of the art to the extent that real, practical structures and components can be built and concepts tested. With a little research in materials, modeling, testing, and qualification, this material can be ready for even the most extreme applications. The only ingredient required to realize this goal is the will to carry it forward.

8.1.1. Use the material

This new material concept was invented by NASA for space applications and should be used there. Space is the new frontier, high ground and "key terrain" for the United States. The Space Based Laser – Integrated Flight Experiment (SBL-IFX) has been chosen for development of the US's anti-missile defense. Damping or the lack thereof has been cited as one of the key technology needs for success of the program. This material can reduce settling times and vibrations in the structure by 99% or better with the right selection of materials. Thus the use of this material in the very application for which it was invented is our first recommendation.

There are a host of other applications in aerospace, civil infrastructure, marine, and sports (to name only a few) that can benefit significantly from the damping, stiffness, and lightweight advantages offered by this new material. The point is use it.

8.1.2. Material research

There is room for improvement in the materials used. This effort only explored the use of this material with standard modulus fibers (34 msi – 234 GPa) and sports resin systems. It is fully expected that other fibers and resin systems will perform in a predictable manner provided material compatibility issues are addressed.

The use of high modulus fibers should be explored. Both damping and stiffness will increase. It may even be possible to come close to critical damping in structures with the right combination of materials. What would critical damping do for the structure of a laser satellite? The answer is obvious: zero settling time, stability, and many other advantages yet to be discovered.

We have used only four different viscoelastic materials (VEM), all provided by Avery-Dennison. All have a relatively narrow band of temperature and frequency where damping and stiffness are optimal. Since it has been proven that wavy composite – VEM structures mirror the characteristics of the viscoelastic, improvements to the VEM will improve the performance of the viscoelastic. A broadband viscoelastic is needed. Other requirements include VEM's for cold and very hot applications. They may exist, but they haven't been tried.

Aerospace and civil infrastructure material qualification is a must before this material can be used for the purpose for which it was invented. Until that time, no engineer will work with it except in basic research applications.

8.1.3. Testing of torsion, bending, acoustic, strength, and fatigue

The torsional performance of this material should be investigated for application in drive shafts for helicopters, automobiles and general machinery. A torsional test algorithm has already been developed and finite element modeling capability exists. A better, more precisely machined test setup is required.

Investigations have shown that performance of the material in the first bending mode is similar to axial performance, though other bending modes seem to show the damping peak

shifted to higher frequencies. Further research should be performed to correlate axial, bending and torsional results. Bending tests on tubes, panels or other structural elements may confirm that the material performance in other bending modes is even better than predicted on the axial material properties nomogram.

Because of structural borne and induced vibrations, noise is of concern in every aerospace application. Engineers now have a new weapon for attacking acoustic problems, especially low frequency problems where traditional sound deadening materials do not perform well. Finite Element modeling predicts that damped composite panels could yield a 20 to 30 dB improvement in transmission loss. Adding damping to structural members such as the airframe, aircraft skins, or turbine engine mounts will help to reduce acoustic emissions at their source. Wavy composite will pave the way for a quieter future.

As mentioned in Chapter 4, the frequency at which low frequency stiffness and damping performance falls off is highly sensitive to error. A simple low frequency axial test at a single frequency would serve as an anchor so that the time-temperature superposition shift constant would be known with high accuracy. Stiffness and damping would then be known with very high accuracy at any practical frequency or temperature.

No investigations into ultimate strength or fatigue were performed as a part of this study, though developments such as 90°-fill fiber and segmented viscoelastic have shown outstanding performance. Adequate tests could be performed on existing tensile and fatigue equipment. This would produce greater confidence in the material and pave the way for use in aerospace.

8.1.4. Finite Element Analysis code improvements

Improvements for the FEA code should include development of geometry and mesh generator program, finding a better solution method, and better definition of the wavy composite material properties.

Development of a geometry and meshing program would improve the utility of the FEA program.

Further research and testing should be done to find an efficient solution method for the FEA program.

Current methods of waveform definition are very restrictive. Waveforms can only be defined by position along the global x-direction. This limits the complexity of the model to an element "1" parametric direction that is collinear with the global x-direction. Future improvements should allow waveform definitions to follow the contours of complex shell geometries.

8.2. SUMMARY

This new material was invented for "Star Wars". The following is quoted from the 2000 National Space & Missile Materials Symposium introduction:

> **"Revolutionary materials technology is critical and will take a generation or more to achieve. Materials are the enablers for next generation, affordable and safe reusable launch systems, advanced spacecraft, and payloads...."**

This research proves that one of the next generation materials "...for next generation, affordable and safe reusable launch systems, advanced spacecraft, and payloads..." is available for immediate use.

REFERENCES

Adams, R. D., Fox, M. A. O., Flood, R. J. L., Friend, R. J., and Hewitt, R. L. (1969). "The Dynamic Properties of Unidirectional Carbon and Glass Fiber Reinforced Plastics in Torsion and Flexure." *Journal of Composite Materials*, 3, 594-603.

Bicos, A. S., Johnson, C., and Davis, L. P. (1997). "Need for and Benefit of Launch Vibration Isolation." *Proceedings of SPIE - International Society for Opitical Engineering*, 3045, 14-19.

Dimarogonas, A. (1995). *Vibration for Engineers*, Prentice-Hall.

Dolgin, B. P. (1990). "Composite Passive Damping Struts for Large Precision Structures." US Patent No. 5,203,435, NASA, USA.

Ferry, J. D. (1980). *Viscoelastic Properties of Polymers*, John Wiley & Sons.

Lazan, B. J. (1968). *Damping of Materials and Members in Structural Mechanics*, Pergamon Press, London, England.

Nielsen, L. F., Wismer, N. J., and Gade, S. (2000). "An Improved Method for Estimating the Dynamic Properties of Materials." Journal of Sound and Vibration, 20-24.

Norton, M. P. (1996). *Fundamentals of Noise and Vibration Analysis for Engineers*, Cambridge University Press.

Olcott, D. (1992). "Improved Damping in Composite Structures Through Stress Coupling, Co-Cured Damping Layers, and Segmented Stiffness Layers," Doctoral Dissertation, Brigham Young University, Provo, Utah.

Pratt, W. F. (1999). "Patterned Fiber Composites, Process, Characterization, and Damping Performance," Doctoral Dissertation, Brigham Young University, Provo, Utah.

Pratt, W. F., Sommerfeldt, S., and Allen, M. (2001). "Testing and Characterization of Wavy Composites." SAMPE 2001, SAMPE, Long Beach, CA.

Sperling, L. H. "Sound and Vibration Damping in Polymers." *Science and Engineering at the 197th National Meeting of the American Chemical Society*, Dallas, TX, 5-22.

von Flotow, A., and Mercadal, M. (1995). "Measurement of Noise and Vibration Transmitted into Aircraft Cabins." *Sound and Vibration*, 29(10), 16-19.

Wright, C. D. (1994). "Improved Strength Properties of Damped Composite Structures," Masters Thesis, Brigham Young University.

Zapfe, J. A. (1995). "Prediction of Damping in Laminated Beams Using a Discrete Layer Finite Element Model and an Iterative Full Domain Smeared Laminate Model," Doctoral Dissertation, Pennsylvania State University, State College, PA.

Zapfe, J. A., and Lesieutre, G. A. "Iterative Calculation of the Transverse Shear Distribution in Laminated Composite Beams." *American Institute of Aeronautics and Astronautics*, 3117-3125.

APPENDIX A: ADDITIONAL TEST DATA AND FEA PREDICTIONS

The following charts show results compared to FEA predictions for other 30° max angle tubes.

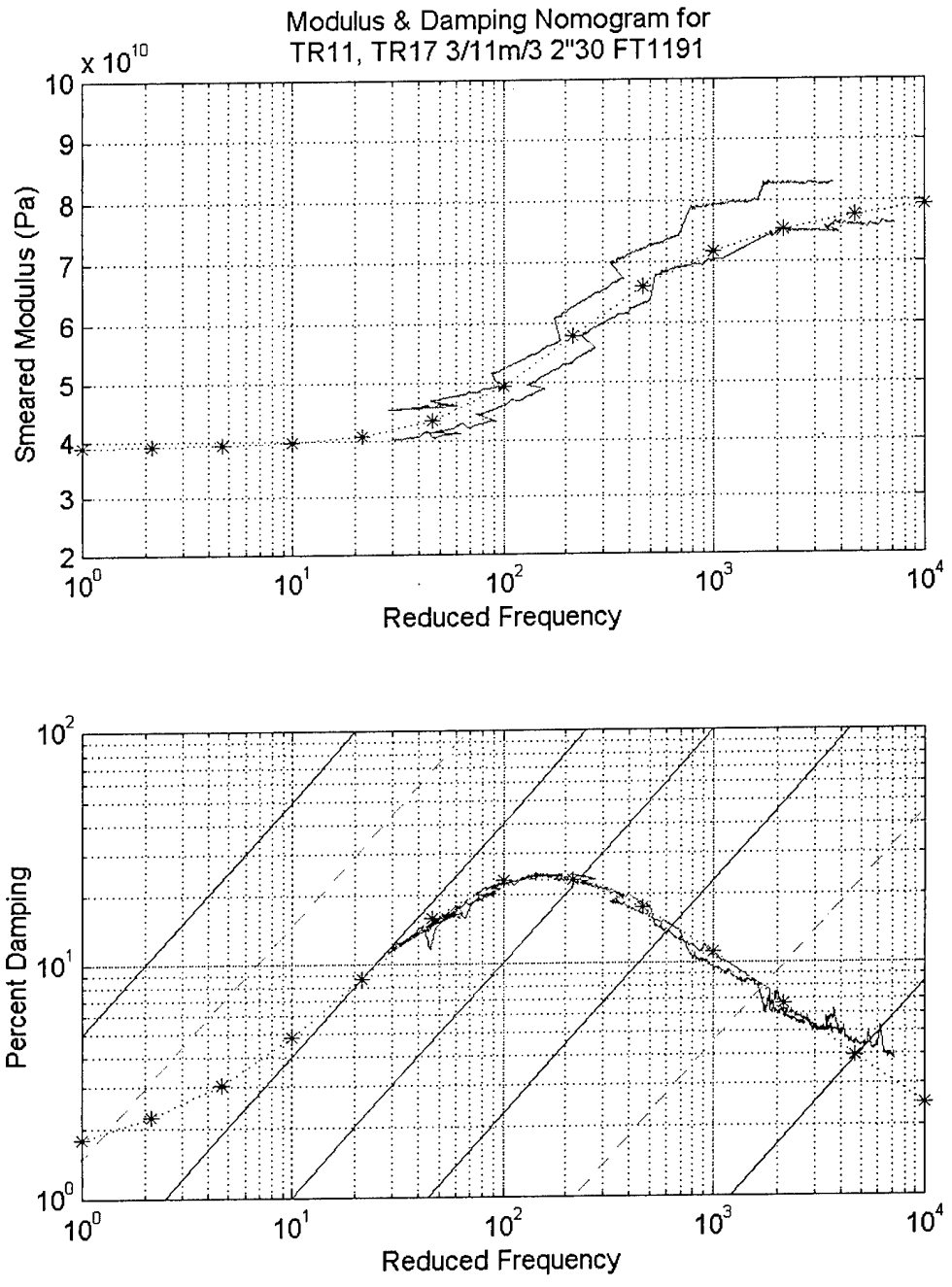

Figure 78: Test Data vs. FEA prediction for 5.0 cm (2.0 in.) 30° +3/11m/-3 tubes

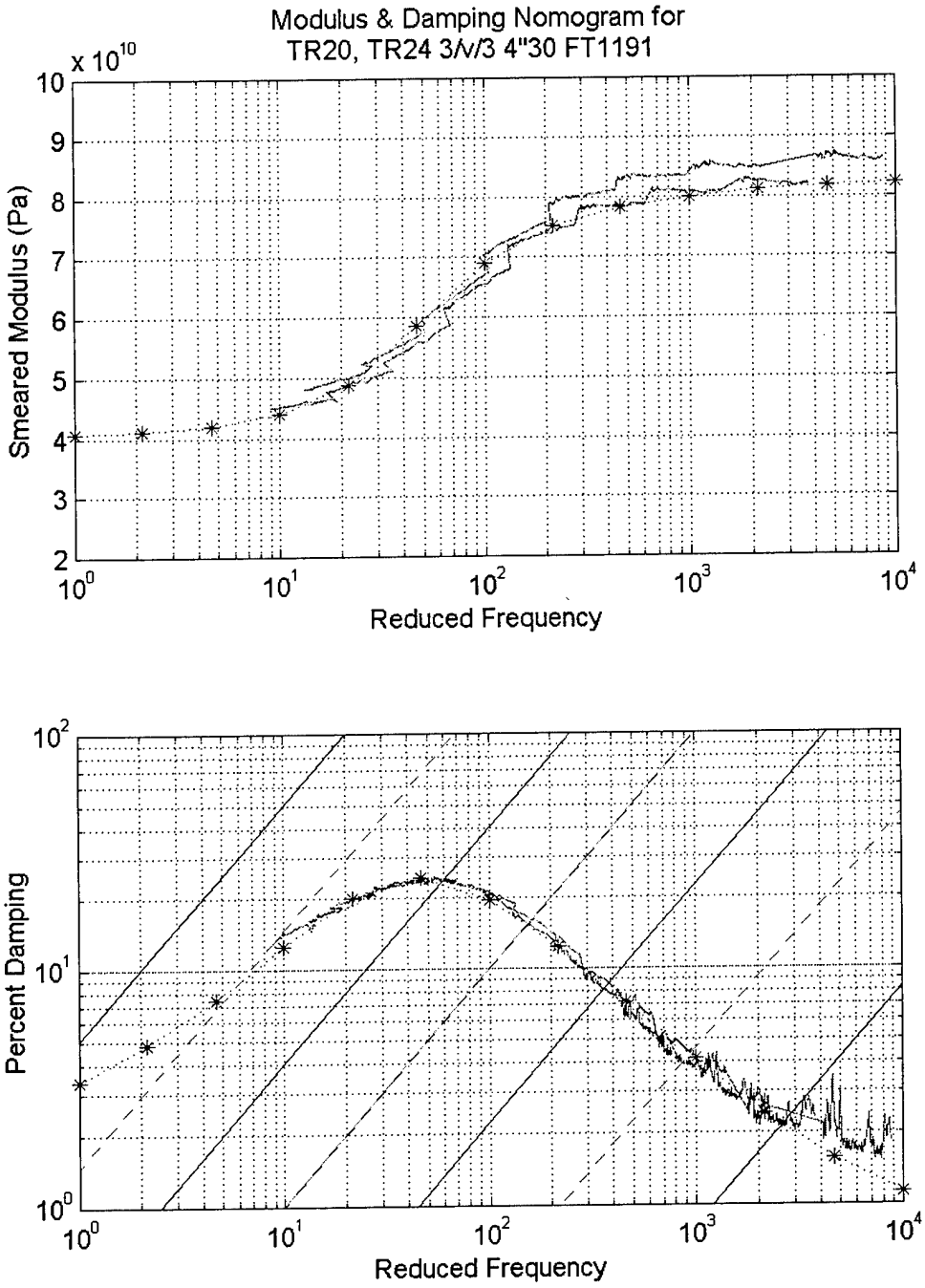

Figure 79: Test Data vs. FEA prediction for 10.0 cm (4.0 in.) 30° +3/11m/-3 tubes

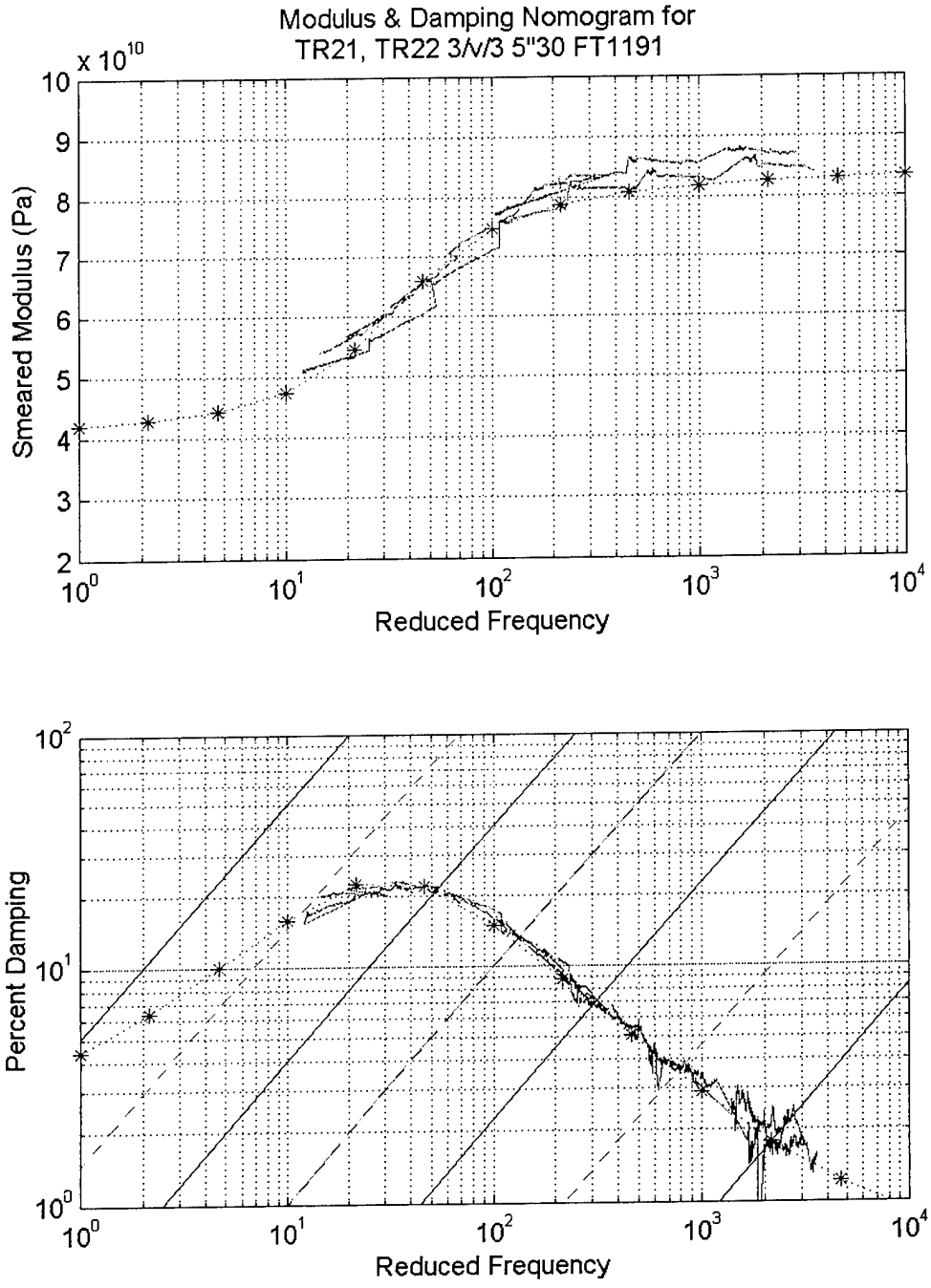

Figure 80: Test Data vs. FEA prediction for 12.5 cm (5.0 in.) 30° +3/11m/-3 tubes

The following are test results compared to FEA predictions for other 22° (max angle) tubes.

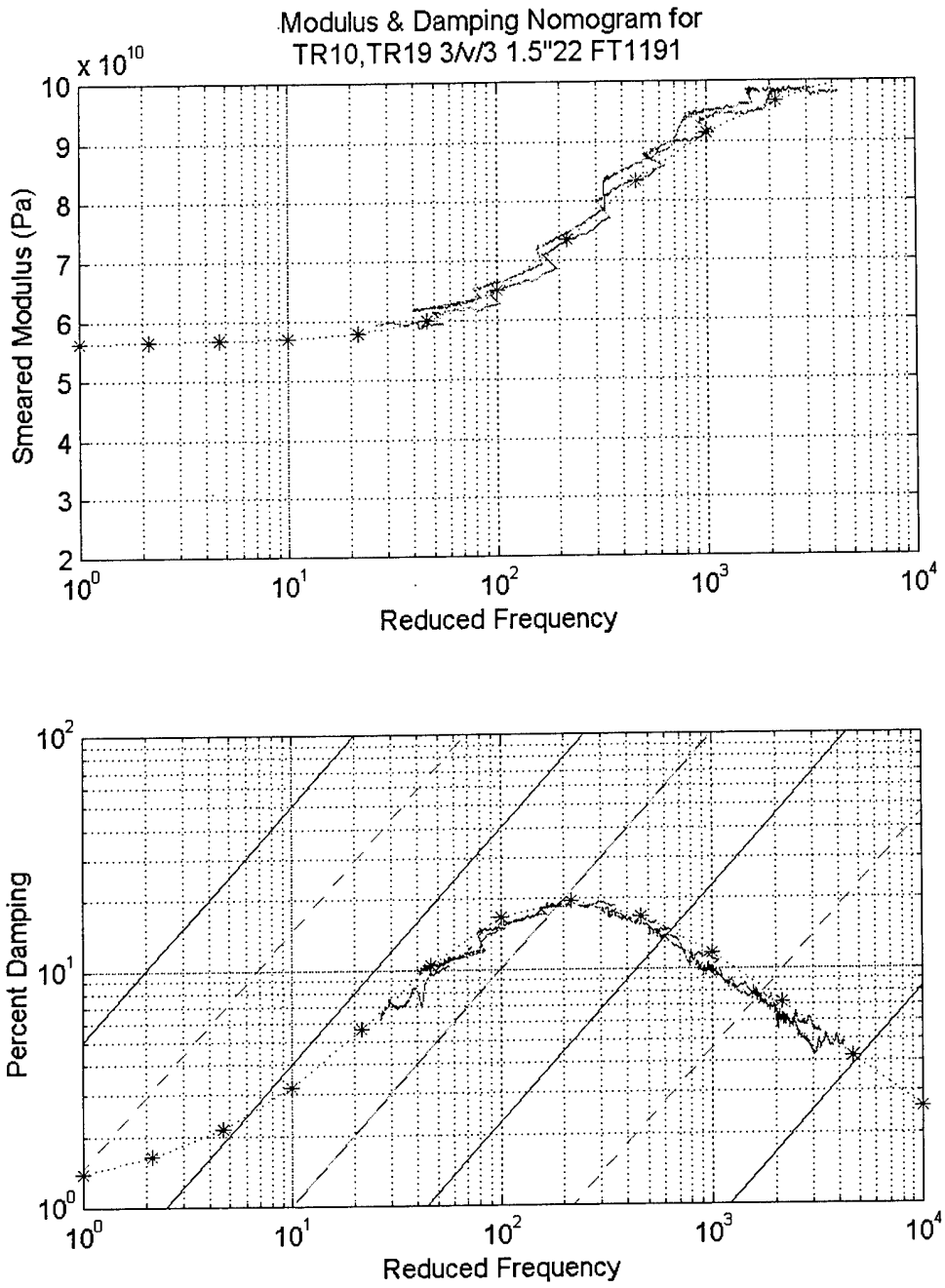

Figure 81: Test Data vs. FEA prediction for 3.75 cm (1.5 in.) 22° +3/11m/-3 tubes

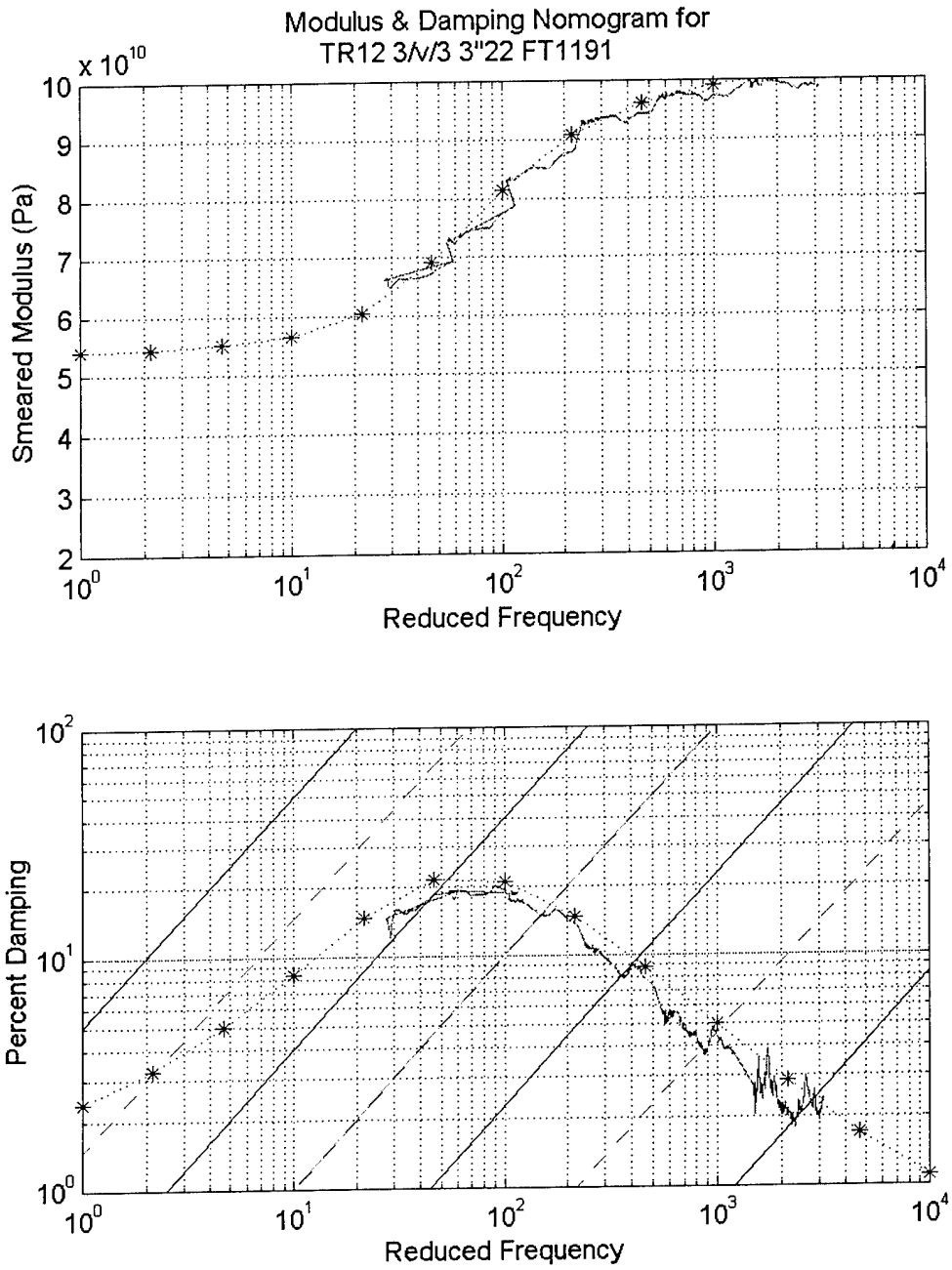

Figure 82: Test Data vs. FEA prediction for a 7.5 cm (3.0 in.) 22° +3/11m/-3 tube

DISTRIBUTION LIST

DTIC/OCP 8725 John J. Kingman Rd, Suite 0944 Ft Belvoir, VA 22060-6218	1 cy
AFSAA/SAMI 1570 Air Force Pentagon Washington, DC 20330-1570	1 cy
AFRL/VSIL Kirtland AFB, NM 87117-5776	2 cys
AFRL/VSIH Kirtland AFB, NM 87117-5776	1 cy
Pattern Fiber Composites, Inc. 923 West 500 North Lindon, UT 84042	1 cy
Official Record Copy AFRL/VSSV/Tang-Tat Ng	5 cys